1986

Composite service life prediction via fiber bundle testing-evaluation of testing equipment and data acquisition system.

Petridis, Dimitrios M.

NAVAL POSTGRADUATE SCHOOL
Monterey, California

THESIS

COMPOSITE SERVICE LIFE PREDICTION
VIA FIBER BUNDLE TESTING-
EVALUATION OF TESTING EQUIPMENT
AND DATA ACQUISITION SYSTEM

by

Dimitrios M. Petridis

December 1986

Thesis Advisor : Edward M. Wu

Approved for public release; distribution is unlimited

SECURITY CLASSIFICATION OF THIS PAGE

REPORT DOCUMENTATION PAGE

a REPORT SECURITY CLASSIFICATION UNCLASSIFIED	1b RESTRICTIVE MARKINGS
2a SECURITY CLASSIFICATION AUTHORITY	3 DISTRIBUTION / AVAILABILITY OF REPORT Approved for public release; distribution is unlimited.
2b DECLASSIFICATION / DOWNGRADING SCHEDULE	
4 PERFORMING ORGANIZATION REPORT NUMBER(S)	5 MONITORING ORGANIZATION REPORT NUMBER(S)
6a NAME OF PERFORMING ORGANIZATION Naval Postgraduate School	6b OFFICE SYMBOL (If applicable) 67
7a NAME OF MONITORING ORGANIZATION Naval Postgraduate School	
6c ADDRESS (City, State, and ZIP Code) Monterey, California 93943-5000	7b ADDRESS (City, State, and ZIP Code) Monterey, California 93943-5000
8a NAME OF FUNDING / SPONSORING ORGANIZATION	8b OFFICE SYMBOL (If applicable)
9 PROCUREMENT INSTRUMENT IDENTIFICATION NUMBER	
8c ADDRESS (City, State, and ZIP Code)	10 SOURCE OF FUNDING NUMBERS

PROGRAM ELEMENT NO	PROJECT NO	TASK NO	WORK UNIT ACCESSION NO

11 TITLE (Include Security Classification)
COMPOSITE SERVICE LIFE PREDICTION VIA FIBER BUNDLE TESTING-EVALUATION OF TESTING EQUIPMENT AND DATA ACQUISITION SYSTEM

12 PERSONAL AUTHOR(S) Petridis Dimitrios M.

13a TYPE OF REPORT	13b TIME COVERED	14 DATE OF REPORT (Year Month Day)	15 PAGE COUNT
Master's Thesis	FROM _____ TO _____	1986 December	177

16 SUPPLEMENTARY NOTATION

17 COSATI CODES			18 SUBJECT TERMS (Continue on reverse if necessary and identify by block number)
FIELD	GROUP	SUB-GROUP	Fiber, filament, bundle, service life prediction, composite, Weibull model, response speed, data acquisition rate.

19 ABSTRACT (Continue on reverse if necessary and identify by block number)

The objective of this thesis is to investigate the problem of the safe service life prediction of graphite composite structures such as pressure vessels used in the pilot ejection seats, rocket motor cases and space shuttle energy storage compartments. The basic data required for life prediction is the stress- rupture life, i.e., the composite life under constant load and it has to be recognized that extensive testing over long periods of time is required to produce statistically meaningful data. The contribution of this investigation is focused on identifying the characterization methodology for efficient data generation (to minimize cost and time), the appropriate theoretical models for correlation of the data (to translate data to applications) and in evaluating the limitations of the available testing (lower bound response speed) and data acquisition equipment (upper bound recording rate) thereby enhancing future experimental planning and testing.

20 DISTRIBUTION / AVAILABILITY OF ABSTRACT	21 ABSTRACT SECURITY CLASSIFICATION
☒ UNCLASSIFIED/UNLIMITED ☐ SAME AS RPT ☐ OTIC USERS	unclassified

22a NAME OF RESPONSIBLE INDIVIDUAL	22b TELEPHONE (Include Area Code)	22c OFFICE SYMBOL
Edward M. Wu	408- 646 3459	67 Wt

DD FORM 1473, 84 MAR 83 APR edition may be used until exhausted
All other editions are obsolete

SECURITY CLASSIFICATION OF THIS PAGE

Approved for public release; distribution is unlimited.

Composite Service Life Prediction via Fiber Bundle Testing - Evaluation of Testing Equipment and Data Acquisition System

by

Dimitrios M. Petridis
Major, Hellenic Air Force
B.S., Hellenic Air Force Academy, 1974
B.S., University of Patras Greece, 1982

Submitted in partial fulfillment of the
requirements for the degree of

MASTER OF SCIENCE IN AERONAUTICAL ENGINEERING

from the
NAVAL POSTGRADUATE SCHOOL
December 1986

ABSTRACT

The objective of this thesis is to investigate the problem of the ***safe service life prediction*** of graphite composite structures such as pressure vessels used in the pilot ejection seats, rocket motor cases and space shuttle energy storage compartments.

The basic data required for life prediction is the stress rupture life, i.e., the composite life under constant load and it has to be recognized that ***extensive*** testing over ***long*** periods of time is required to produce statistically meaningful data. The contribution of this investigation is focused on identifying the characterization methodology for efficient data generation (to minimize cost and time), the appropriate theoretical models for correlation of the data (to translate data to applications) and in evaluating the limitations of the available testing (lower bound response speed) and data acquisition equipment (upper bound recording rate) thereby enhancing future experimental planning and testing.

TABLE OF CONTENTS

LIST OF TABLES

LIST OF FIGURES

TABLE OF SYMBOLS

α_i (i=s,w)	:	Typical Weibull shape parameter for strong and /or weak sample fiber bundles
α	:	Positive constant (exponent) of the Weibull shape function
α_0	:	Positive constant of the Weibull shape function corresponding to a characteristic fiber filament length δ_0
β_i (i=s,w)	:	Typical Weibull scale parameter for strong and /or weak sample fiber bundles
β	:	Positive constant of the Weibull shape function
γ	:	Positive constant of the Power-Law Breakdown Rule
δ	:	Ineffective length of the overload region
δ_0	:	Characteristic fiber filament length
f_i	:	i^{th} fiber filament of a composite bundle
FCDF or F*	:	Failure's Cummulative Density Function (*Probability of Failure*)
F_w	:	Probability of Failure in Weibull coordinates
G_n	:	Probability of Failure of a stochastically selected microbundle, composed of n filaments

$H_{m,n}$: Probability of Failure of a *composite* fiber bundle composed of m microbundles of n filaments each

$^*H_{m,n}$: Approximation to $H_{m,n}$

I_s : Specification Current

I_{lc} : Current through the Load Cells

K_i (i=r,R) : Load Concentration Factor corresponding to i consecutive fiber filaments immediately adjacent to a sound fiber filament counting on both sides ($r < R$)

k^* : Critical crack size

k : Boltzmann's constant

$\kappa[x]$: Power-Law Breakdown Rule function

l : Gauge length or physical displacement of the tensile testing equipment moving cross-head

l_i(i=u,m,l) : Life of a weak sample fiber bundle for the upper, median and lower tails

L_i(i=u,m,l) : Life of a strong sample fiber bundle for the upper, median and lower tails

m : Number of microbundles of a *composite* fiber bundle

n : Number of fiber filaments per *composite* fiber bundle

P_i : i^{th} load level

P_{si} : Strength of the i^{th} fiber filament

P_{si}^{NF} : Load that would have been achieved at the end of the loading sequence up to the P_{si} level under the condition that No Failures had occured

P_{wi} : Load level that results in the failure(s) of the i^{th} fiber filament(s)

p : Tensile load per fiber filament in a *composite* bundle

p_j $(j=1,\delta)$: Strength scale parameter for *single* fiber filaments at gauge or unit length

$^*p_j$: Median strength for *single* fiber filaments

p_c : Strength scale parameter for *composite* fiber bundles

$^*p_c$: Median strength for *composite* fiber bundles

Q_i : i^{th} constant positive stress level

RCDF : Reliability Cummulative Distribution Function

$(RCDF)_S$: RCDF of the fiber filaments that *survived* the loading sequence

$(RCDF)_{NF}$: RCDF of the whole fiber bundle under the condition that No Failures of fiber filaments occured during the loading sequence

R : Resistance of the Load Cells and/or the LVDTs

R_{tot} : Total resistance of a Load Cells' and /or a LVDTs' set

ρ : Positive constant (exponent) of the Power-Law Breakdown Rule

$S_i (i=u,m,l)$: Strength of a strong sample fiber bundle for the upper, median and lower tails

$s_i (i=u,m,l)$: Strength of a weak sample fiber bundle for the upper, median and lower tails

$\sigma_i(t)$: i^{th} time dependent level of stress

t_o : Short finite period of time of the order of a few minutes

t_i $(i=a,b,c,d)$: Time to median failure of the model fiber bundle under the creep-rupture load P_i

t_j $(j=1,\delta)$: Life scale parameter for *single* fiber filaments at gauge or unit length

$^*t_j$: Median time to failure for *single* fiber filaments

t_c : Life scale parameter for *composite* fiber bundles

$^*t_c$: Median time to failure for *composite* fiber bundles

T : Absolute temperature

U_0 : Potential Energy in the case of chain scission

v : Moving cross-head speed of the tensile testing equipment

V_S : Power supply specification voltage

V_S^{REC} : Recommended excitation voltage of a Load Cells' and/or a LVDTs' set

$Vi_{lc}(i=1,2)$: i^{th} Load Cell set excitation voltage

W : Function dependent on the load concentration factor [K_r] and on the probability of failure of fiber filaments of length δ under the tensile load p, [$F^*_{\delta}(p)$], used to describe the probability of failure of composite fiber bundles[$H_{m,n}(p)$] composed of large numbers [n] of fiber filaments

$\psi(x)$. Weibull Shape function

ACKNOWLEDGEMENTS

First of all, to the Hellenic Air Force, for the unique opportunity that I was offered to further expand my professionalism by pursuing the degree M.Sc. in Aeronautical Engineering, for the partial fulfilment of which this thesis was created.

Next, to Mr. Jim Nageotte of the Advanced Composites Laboratory, for his helpful technical advices, the design and implementation of the LVDTs' mounting provisions, the fabrication of the distribution boards and the equipment troubleshooting without which the overall experimental set-up could have not been made possible.

Also to the outstanding machine shop work of Mr. Glen Middleton which led to the precise simulation of the graphite fiber testing experiment.

Finally, my most sincere thanks to my thesis advisor Dr. Edward M. Wu for his striving efforts to gain one more individual who believes in the following philosophy fundamentals as quoted below:

The principle goal of education is to create men who are capable of doing new things, not simply repeating what other generations have done. .....Jean Piaget

The ultimate goal of the educational system is to shift to the individual the burden of pursuing his own education......John Gardner

Do not give them any more straw to make bricks with as your custom has been ; let them go and find the straw for themselves.....Exodus 5

Give me a fish and I will eat today. Teach me how to fish and I will eat for the rest of my life......ancient Chinese proverb

His creativity, patience and encouragement have made this work a worthwhile and memorable learning experience. It has been both a pleasure and a priviledge to have worked under his direction.

I. INTRODUCTION

A. BACKGROUND

Although composites have been employed ever since materials were first used, such as the naturally occuring wood or the man-made mud bricks reinforced by straws and have been widely used in the recent 50 years in the building industry (reinforced concrete), the high technology of the composites has evolved in the aerospace industry only in the last 25 years. The first strength critical application for modern composites were filament-wound pressure vessels using glass fibers.

What has highly motivated the effort of composites development has been the goal to come up with a combination of properties not achievable by any of the constituent materials acting alone. Thus a solid could be fabricated from elemental materials which by themselves could not satisfy particular design requirements such as strength and/or stiffness to weight ratios the use of which is of cruisial importance in the aerospace industry. Another highly motivating aspect was the very high reliability of the composites due to the micro-redundancy which comes as a

result of the fiber-matrix load sharing that in fact diffuses the local fiber failure sites. And it was this materials redundancy that finally proved that composites were a superior application for monocoque structures such as pressure vessels and rocket motor cases.

According to Tsai [Ref. 1] the results of this effort in the field of the Aerospace Industry came sequentially in the form of various fuselage components as well as some primary control surfaces of several first class fighters such as:

1. The boron/epoxy fuselage section and horizontal tail of the General Dynamics F-111.

2. The graphite/epoxy fuselage components for the Northrop F-5 made also by General Dynamics.

3. The limited use of the boron/epoxy material system in the rudder of the Mc Donnell-Douglas F-4 which has accounted for a 35% weight reduction compared to its Alluminum counterpart.

4. The boron/epoxy horizontal stabilizer of the Grumann F-14.

5. The composite stabilator of the Mc Donnell-Douglas F-15.

6. The graphite/epoxy horizontal and vertical stabilizers of the General Dynamics F-16.

On the other hand in the commercial aerospace industry Boeing was the first manufacturer to utilize about 2 tons of composite materials in the

floor beams and all the control surfaces of the 767 airliner while the Beach Aircraft's Starship 1 all-composite aircraft is scheduled to start its flight test program before the end of 1986.

Apart from the U.S manufacturers extensive use of composites has also been used in the Dassault-Breguet's Rafale, the Israel Aircraft Industries' Lavi and the all-composite fin box of the Airbus Industrie A310-300, an impressive structure in its simplicity, also described by Tsai [Ref. 1].

In parallel to the manufacturing milestones that had to be resolved once the goals for composite compoments were set, the reliability problems had to be resolved as well. Among them was the problem of safe life prediction of the composite components and its relation with the composite strength. The significance of solving this problem for the aerospace industry becomes more obvious when one focuses on the construction of space and/or missile applications where repetition for experimental purposes is either impossible or limited to numbers often less than 3 due to obvious economic constraints. Consequently one has to realize that other methods have to be established, methods such as statistical inference and other mathematical techniques which will enable the engineers to estimate

accurately the service life of the composite component or system under evaluation, based on a limited number of experiments which is acceptable from the cost and time standpoints.

From physical experiences and mathematical modeling, it is known that the average macroscopic strength of composites depends strongly on the number of micro-fiber failure sites and the strength of specific composites depends on the clustering of the fiber failure sites. As a result, information on the statistical characteristics of fiber filament strength is the base for estimating the reliability of the macro-strength composite structures. Specifically the statistical lower tail distribution of the filament strength and filament life are required. The characterization of the lower tail behaviour requires testing of large number (thousands) of samples. In the case of strength characterization, large number of samples is a matter of economics whereas in the case life characterization, this is a matter of economics and time. Aside the cost constraints which are always obvious, the reason that time constraints are more than equally serious in this case, is that experimental testing of fiber filaments could last indefinitely without providing adequate data. This inherent uncertainty in life characterization can only be overcome by accelerating testing

methodologies. In this investigation, fiber bundle testing is chosen to increase the number of samples. However, fiber filament testing is still required to serve as a validating tool on the fiber bundle testing results. Higher stress levels are used to accelerate the life testing in order to assure that failure data will be observed within the existing time constraints. Under stress-life acceleration circumstances the service life prediction could be made possible at a given confidence level utilizing the appropriate statistical methods, given that the fiber bundles under testing had already been able to withstand either a prescribed load level without any failures, or a higher load level experiencing a known number of filament failures per bundle. The results of this investigation are relevant to man-safe applications as in composite pressure vessels used in the pilot's ejection seats, the liquid oxygen tank in the jet aircrafts, the space shuttle tanks for energy storage, or the composite rocket motor cradel of the guidance system of various missiles, where mostly graphite fibers are used, as well as the broad class of composite applications where the structure is subjected to sustained tensile loading.

The problem of accurately determining the life of one of current high strength graphite fiber (Hercules AS4) has already been started at the N.P.S

by Lt.Fred D.Carozzo and the results of his thesis [Ref. 2] identified three major milestones that have to be eliminated in order to make this characterization methodology operational:

1. To avoid the stalling of the tensile testing equipment during the loading sequence, because stalling appears almost exactly as an increase in broken fibers in a bundle and hence can produce false interpetation.

2. To explain why the creep data recorded during the creep-rupture phase of the experiment do not agree with the expected physics of the problem.

3. To increase the recording rate of the data acquisition system used, because it is a known fact that much more fibers per bundle must have failed during the loading sequence than what has already been recorded. The number of fibers per bundle within the bundle which failed during the loading sequence is needed to calulate the conditional probablity for the AS4 fiber bundle service life.

B. GOALS

The objective of this research which is associated with the reliability characterization methodology is to obtain strength-life data for graphite fibers. The final target is to present these data in such a way that " Given a stress level one could predict the probability of safe service life

for a known confidence level and vise versa (that is, given the anticipated service life of a composite application specify the stress level that should not be exceeded during service in order to achieve the given safe-life limit within a prescribed confidence level) ". With this ultimate goal in mind, what this thesis is desired to contribute to is four fold:

1. To present a general lay out of the methodology that is to be used as a guideline to reach the ultimate goal of obtaining strength-life data.

2. To evaluate what is the minimum loading speed that the existing testing equipment can be operated with, so that no stall will occur during the loading sequence of the fiber bundles in order to avoid interruptions and to identify the load dependency of the minimum speed.

3. To give a reasonable explanation on why the creep data recorded during the creep-rupture phase of the experiment do not agree with the expected physics of the problem.

4. To study the limitations of the existing data acquisition system and propose solutions to increase the recording rate of data points during the short time loading sequence.

Consequently the projected end-use for the information generated by this investigation can be specifically tailored to the applications of the Hercules AS4 graphite fiber bundles and hence the upper load level

boundaries for specific applications can therefore be established such that the predetermined service life of the composite component under evaluation could be safely achieved.

II. APPROACH TO THE PROBLEM

A. GENERAL

It is intuitively obvious that due to the minute transverse dimensions of the composites fibers, huge numbers of fiber bundles have to be used in the construction of a composite structure, regardless of its absolute dimensions. It is also evident that the type of constituents to be used in a composite structure ought to have been experimentally tested in advance and demonstrated that they comply with the desired standards and/or specifications concerning their strength and service life prior to the beginning of the manufacturing process. This means that there has to exist a pilot model design fabricated under known parameters prior to the commencment of the manufacturing process. Furthermore, since the constituent materials used for the model evidently differ in essence from those the actual manufacturing will start from (even though they have been fabricated from the same material compositions and according to the same procedures) there is a need to assure the reliability of the production line components. The answer to production reliability can only be given in terms

of confidence levels and under agreed upon conditions between the Procuring Activity and the Manufacturer. It is also likely to assume that within the production the fiber bundles will not have the same strength or the same life. Heuristicallly, it is assumed that " ***high strength is associated with long life whereas low strength with short life respectively*** ". Under the above circumstances, provided it is possible to identify the strongest and the weakest fiber bundles by quality control methods, **Figure 1** could serve as a good starting point for understanding how strength and life of the same fibers could be related, under the proviso that these relations have to be determined as accurately as possible later on. Rosen [Ref. 3] and Phoenix & Wu [Ref. 4] show that both the strength (at $t = t_0$ where t_0 is a very short finite period of time), and the life of the fiber bundles at various levels of strength follow the Weibull distribution which is usually described by means of a shape parameter (α_i) and a scale parameter (β_i).

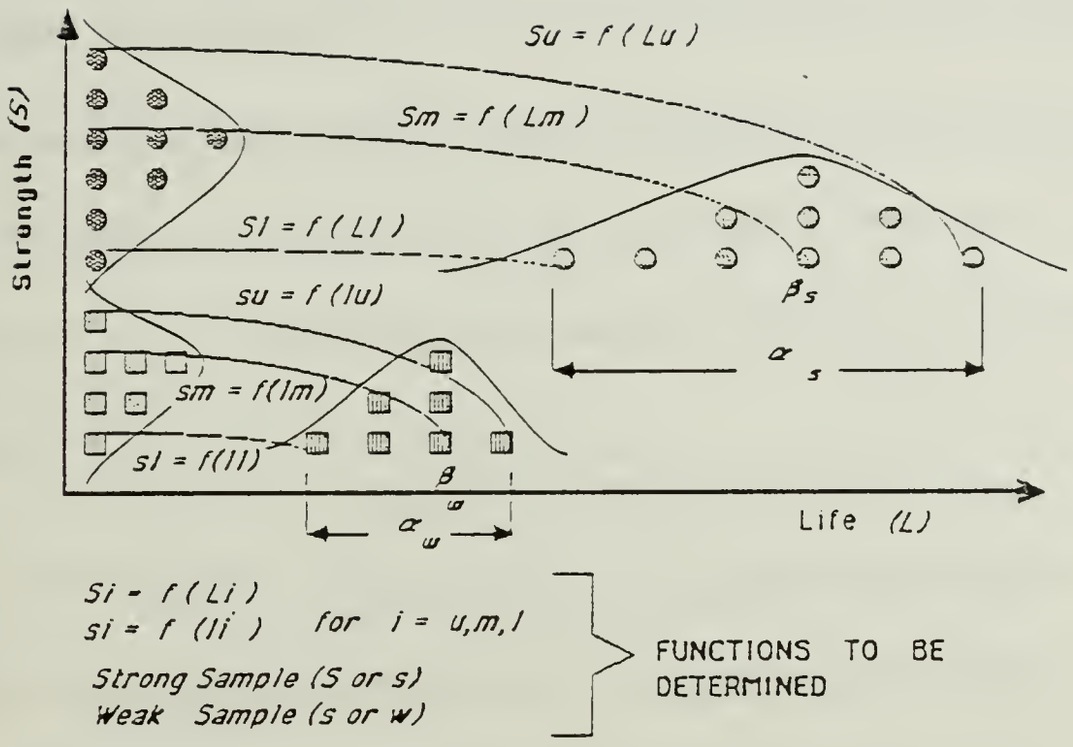

Weibull distribution parameters

α i = scale parameter

β i = shape parameter

Figure 1. Weibull Strength to Weibull Life correspondence of strong and weak fiber bundles composed of 10 fiber filaments.

B. BASIC LINE OF METHODOLOGY

Without any loss of generality one can now follow the thought experiment described below for a fiber bundle composed of ten (10) filament fibers identified from now on as f_i for i=1,2,3,...,10. One can also assign the intrinsic strengths of these filament fibers to be (with the implicit assumption that the numerical values of the strength random variable follow the Weibull distribution) as follows:

1. One filament (assume f_1) of strength P_{s1} = 10 lbs.
2. One filament (assume f_2) of strength P_{s2} = 12 lbs.
3. Two filaments (assume f_3 and f_4) of strength P_{s3} = 14 lbs.
4. Three filaments (assume f_5, f_6 and f_7) of strength P_{s4} = 16 lbs.
5. Two filaments (assume f_8 and f_9) of strength P_{s5} = 18 lbs.
6. One filament (assume f_{10}) of strength P_{s6} = 20 lbs.

If one desires to estimate the strength of this bundle, one can load the bundle to different strength levels (P1, P2, P3, etc.) and observe the survival of the filaments. There will be strength levels below which even the weakest fiber of the ten in the bundle can safely withstand. For a

continuous increase in stress level there exists be a load level (P_{w1}) at which the weakest fiber will finally fail and, under the same thought process, there must be another load level at which the next weaker fiber in the bundle will fail (P_{w2}), and so on, until all the fibers in the bundle will fail and hence one will be able to observe the failure of the entire bundle. Having already postulated that the fiber's strength in the bundle follows the Weibull model distribution, one can plot the probability of failure for this bundle at $t = t_0$, as presented in **Figure 2**. At this point it has to be noted that the finite time t_0 is only of the order of a few minutes and therefore negligible if compared with the anticipated duration of the service life and therefore, with the experiment to follow for the life testing.

A very important observation to be noted is that the fibers in the bundle are automatically ranked with respect to their strength, which means that the weaker fibers in the bundle fail first whereas the stronger fibers fail last, or at a higher load level. The significance of this observation is what actually explains the big advantage of the fiber bundle testing versus the single filament fiber testing and can become more

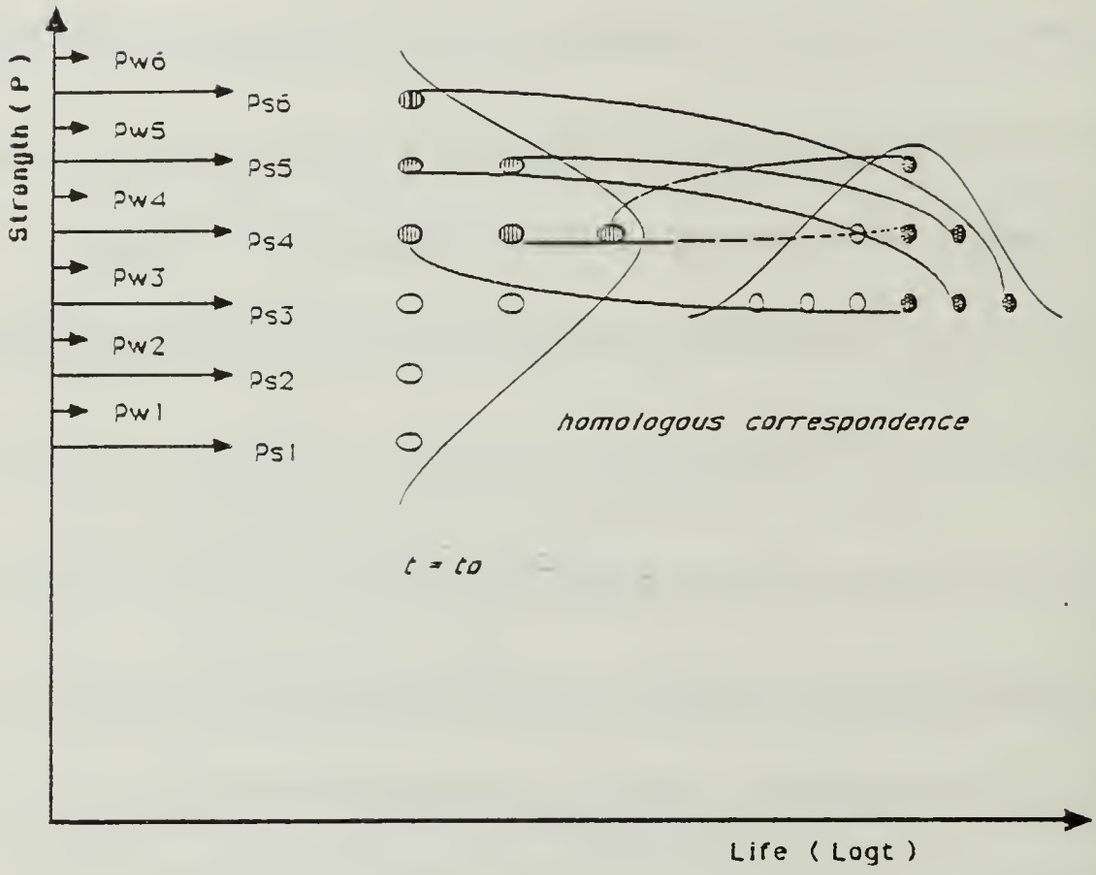

Figure 2. Homologous correspondence of Weibull Strength at t = to to Weibull Life distribution for a fiber bundle composed of 10 fiber filaments.

obvious if one thinks of bundles composed of 3000 up to 10000 filaments (as it is usually the case). The expediency is that the lower tail will always be the first to be observed. As it has already been stated earlier, if the applied load level does not exceed for example, the (P_{w1}) level, then no failures will occur until t_0. However if one were to leave the bundle loaded at a load level ($P_{s1} < P_{w1}$), some failures could be observed after a long period of time. And it is reasonable to think that under this load P_{s1} after a long period of time the weaker fiber will fail first, the next weaker fibers will fail later, and so on, until all the fibers in the bundle will have failed, when it would also be possible for someone to observe the failure of the entire bundle. Assuming again a Weibull distribution model for the life of the fibers bundle as per Phoenix & Wu [Ref. 4] one can plot the probability of failure of this very bundle in time or in other words in life, given that no failures have occured during the loading sequence until t_0 *

---

* How this plot could be obtained will be explained later in the Detailed Method of Solution.

Usually due to very long period of time which may have to elapse until the first failures could be observed it is customary to start thinking in Log (t) coordinates as far as the abscissa is concerned and this is the way the figures will be presented during this thought experiment.

But the situation described so far is merely the simplest, and therefore the thought experiment has to be carried through in a more realistic way. Such a real world application could be one in which the load level (P_{w2}) and this load level could have been maintained to be constant in time corresponding to a stress level say (Q_2).

Under these circumstances what should happen could be described as follows:

1. During the loading sequence until t_0 the fibers f_1 ($P_{w2} > P_{w1}$) and f_2 ($P_{w2} > P_{s2}$) will fail, whereas the remaining ($f_3 - f_{10}$) will survive.

2. During the time that the constant load P_{w2} is maintained, the rest of the failures have to occur in such a way that the filament fibers f_3 and f_4 will fail earlier, to be followed by the failures of filament fibers f_5, f_6 and f_7, the failures of f_8 and f_9 and finally the failure of the last one f_{10} which completes the failure of entire bundle.

In this simplest case where no failures had occured during the loading sequence (due to the low magnitude of the applied load) one was able to infer about the life of the fiber bundle in terms of the Weibull model based on the magnitude of the load level the fiber bundle was able to withstand without failure. Direct statistical inference was possible because no failures had occured during the loading sequence. However in the real world applications there are always finite number of failures during the loading sequence and therefore one has to be able to determine the number of these failures and their respective failure stresses in order to be able to use the same technique and infer about life. In other words life inference is possible only on the basis of the *conditional probability* that failures did not occur during the loading sequence. And in order to evaluate this condition one has to know the exact number of the fiber filaments that have failed during the loading sequence, so that the magnitude of the load level that would have been achieved if no failures had occured can be used as before. This requires an accurate data acquisition system that has to be used in order to be capable to record the possible failures during the loading sequence.

Although the sequence of failures described so far is what is anticipated in accordance with intuition, (i.e whatever strength of the fiber filaments was not consumed in testing during the loading sequence, can be used for longer life endurance under a homologous strength-life relationship), this might not be the case and therefore one has to find out experimentally whether this one to one correspondence exists between failures at $t = t_0$ and failures in time ($t = t_i$ for i = a,b,c,d) for every arbitrary selected load level or in other words whether the above mentioned relationship of strength and life is homologous or stochastic (see Figure 2).

On the other hand, another major constraint is the fact that for all practical purposes it is not possible nor necessary to wait until the failure of the last filament fiber because this might occur much later than the structural lifetime. This is the reason why the engineers only have to wait until the first few failures occur and then terminate the experiments on purpose. The background of such a descision lies on the fact that the engineering interest is in the early failures of the structure under evaluation which justifies a safe service life. In terms of the thought experiment described so far if one assumes that the P_{w2} load level would

be achieved during the loading sequence at $t = t_0$, and hence fiber filaments f_1 and f_2 would have failed and furthermore the load level P_{w2} can be managed to be reached in time, one should have to wait at least until the first few failures (namely those of fiber filaments f_3 and f_4) will occur when the experiment can be terminated. If the same thought experiment is carried out several times reaching higher load levels in every loading sequence and infered life is plotted every time as a Weibull distribution based on the load level that would have been achieved if no failures had happened during the loading sequence, a curve resembling the familiar S-N fatigue curve will arise as shown in **Figure 3**.

The significance of coming up with a graph such as that of Figure 3 for a real word application as the widely used graphite fiber AS-4 is more than obvious, apart from the fact that serves as a basis for the so called *Proof-Test* with the intent of determining definitively both the strength and the life of the same specimen simoultaneously.

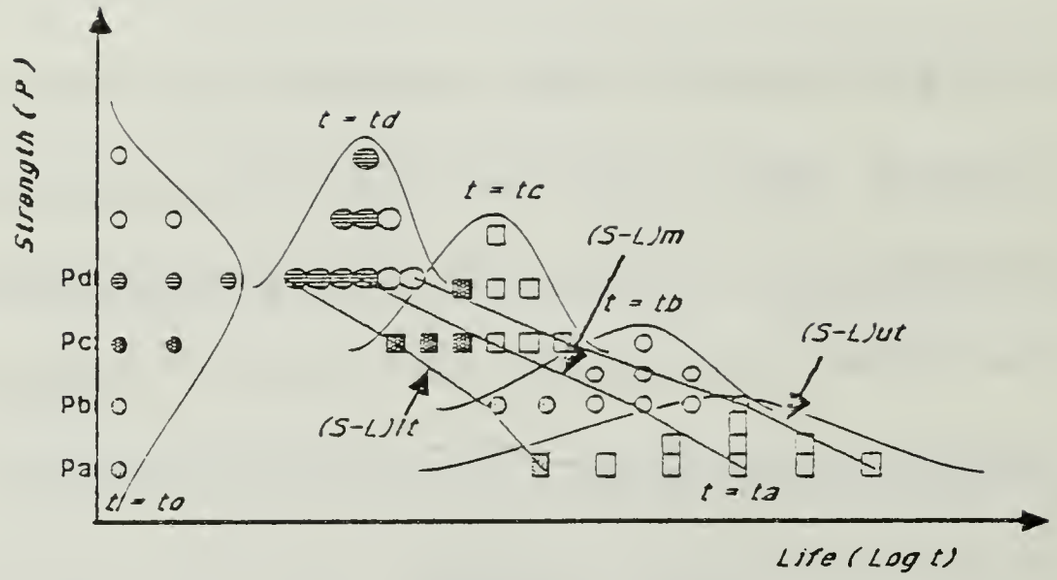

Figure 3. Weibull Life distributions for four identical fiber bundles composed of 10 fiber filaments achieved as a result of different load levels reached at the end of the loading sequences.

C. DETAILED METHOD OF SOLUTION

What remained to be clarified is the method of representing the probability of failure of the fiber bundle in time, given that no failures have occured during the loading sequence ($0 < t < t_0$) where t_0 is a short period of time of the order of several minutes.

To demonstrate how this can be done and also get more insight in the process of approach to the overall problem we will continue with the thought experiment considering four (4) identical fiber bundles like the one which has already been described. If one starts loading them up to four (4) different load levels namely P_{s1} = 10 lbs, P_{s2} = 12 lbs, P_{s3} = 14 lbs and P_{s4} = 16 lbs and then maintain these four load levels in time the following pictures can then be presented for each one of these fiber bundles:

1. *CASE A*: 10 filament bundle under P_{s1}=10 lbs tensile load

Since P_{s1} is the strength of the weakest fiber filament in the bundle, obviously no failures will occur during the loading sequence. However, after some period of time failures will start occuring as time increases, giving the picture shown in **Figure 4-1a**. Observing carefully the

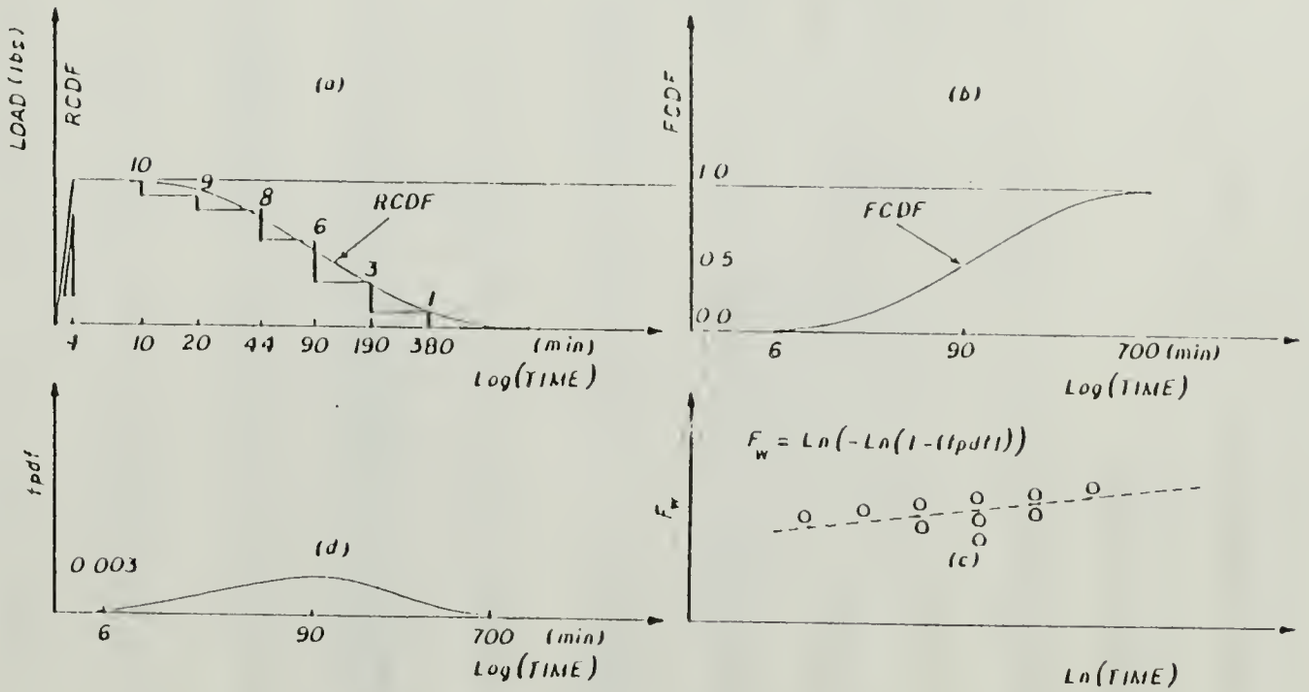

Figure 4-1 : Weibull life distribution for the model fiber bundle of 10 filaments under the Creep-Rupture load of 10 lbs.

steps of this curve it will not be difficult for one to understand that each one of these steps stands for certain failures of fiber filaments in the bundle. And the way this stepped curve is plotted shows that the fiber filaments of the same strength fail simoultaneously. Smoothening the stepped curve obtained, it is not difficult for one to observe that the new smoothened curve stands for the Reliability Cummulative Distribution Function (RCDF) of the fiber bundle under evaluation. And since the Failure Cummulative Distribution Function (FCDF) is always related to the (RCDF) by the relationship:

$$(FCDF) = 1-(RCDF) \tag{II.1}$$

it is evident that FCDF for this bundle can be obtained by plotting the complement image of the RCDF with respect to the vertical (load) axis as shown in **Figure 4-1b**. It has to be noted at his point that this picture is usually presented in the so called Weibull coordinates due to several reasons such as the following:

a. The Weibull model is used to simulate both the strength and the life of the fiber bundles ([Ref. 3] and [Ref. 4]).

b. When Weibull coordinates are used for life the abscisa is presented in Log (t) which is consistent with what has been already stated on the same aspect.

c. In Weibull coordinates the FCDF represents itself as a straight line instead of a sinusoidal shaped curve as when physical coordinates are used.

Therefore it is customary to present the picture of Figure 4-1b in the Weibull coordinates form as shown in **Figure 4-1c**. Taking now into account that no failures have occured during the loading sequence, one can now plot the failures' probability density function **(fpdf)** using the relationship:

(II.2) $$\textbf{(fpdf) - [d(FCDF)/dt]}$$

This failures' probability density function for this first fiber bundle denoted by **fpdf** is finally being presented in **Figure 4-1d**.

2. *CASE B*: 10 filament bundle under P_{S2} =12 lbs tensile load

Since P_{S2} is the strength level that is higher from only one fiber filament strength, it is reasonable one to anticipate one failure to occur during the loading sequence and if this load level is maintained in

time some more failures will start occuring until the whole fiber bundle will fail giving a picture as the one shown in Figure 4-2a. The only difference between this case and the previous one is that the stepped curve obtained this time stands for the Reliability Cummulative Distribution Function of the fiber filaments that *survived* the load level achieved at the end of the loading sequence $(RCDF)_S$. In order for one to be able to use the same technique as in the previous case to come up with the failures' probability density function it is first necessary to evaluate the load level that would have been achieved during the loading sequence under the condition that no failures had occured. This load level can be easily avaluated given that the number of the fiber filaments that have failed during the load sequence is known. If one then denotes this load level by P_S^{NF} it is clear that:

$$(P_{Si}^{NF}/P_{Si}) = (100/\%\ \text{of survived filaments}) \qquad (II.3)$$

$$\text{for} \quad i = 1,2,3,\ldots,10$$

Hence for the case under evaluation (i = 2), where P_{S2} = 12 lbs and the

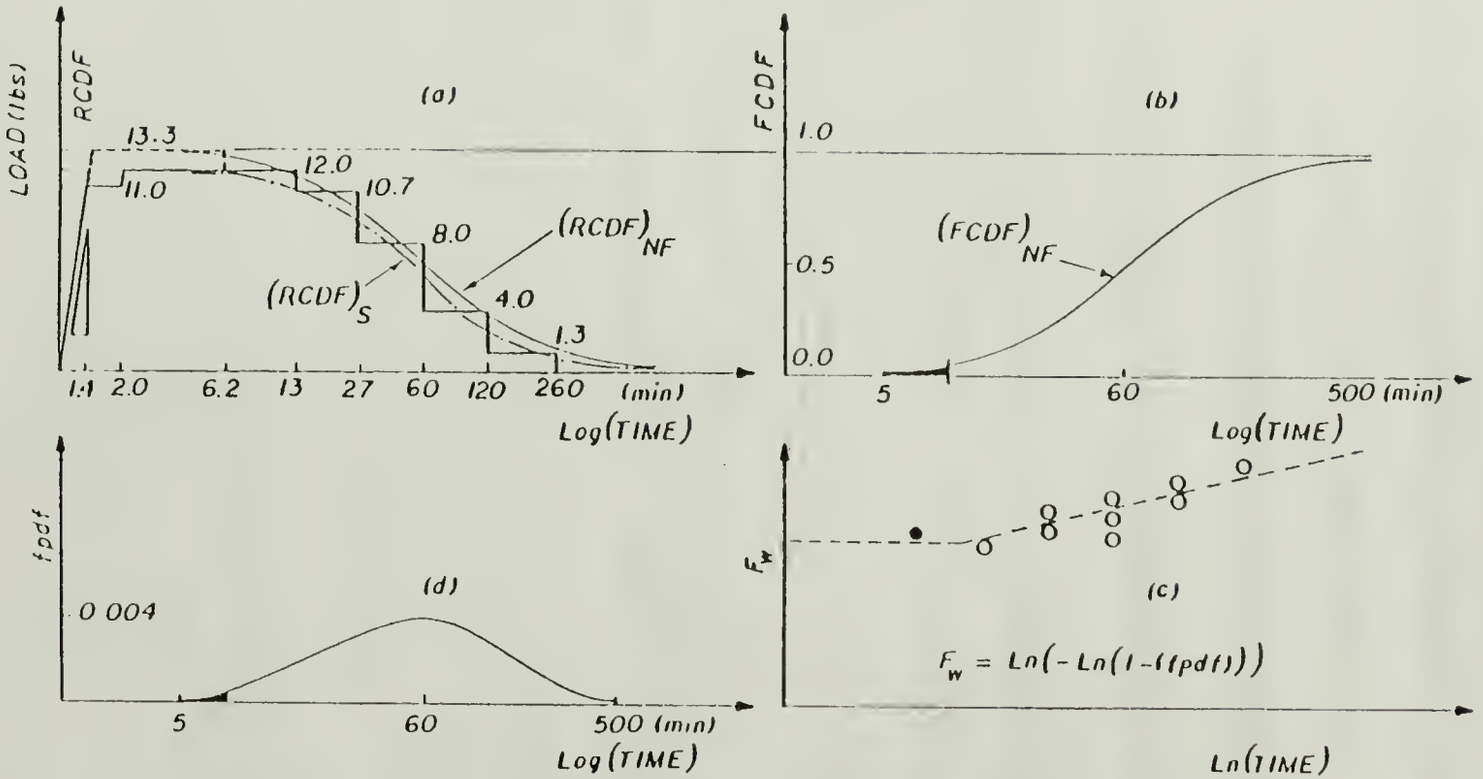

Figure 4-2 : Welbull life distribution for the model fiber bundle of 10 filaments under the Creep-Rupture load of 12 lbs.

percentage of the survived fiber filaments is 0.90 (one failure out of ten) one can easily find that P_{S2}^{NF} = 13.3 lbs. Then the upper left portion of the existing stepped curve can be extrapolated to the left to account for the $(RCDF)_{NF}$ that is the Reliability Cummulative Distribution Function under the condition that no failures had occured during the loading sequence. Using the same reasoning as before one can now obtain the FCDF for both the survived fiber filaments in this case $(FCDF)_S$ and for the fiber bunble under the condition that no failures had occured during the loading sequence $(FCDF)_{NF}$. Of course what is actually important for this case is only the latter that can be evaluated by equation (II.1). This result is presented in **Figure 4-2b** in physical and in **Figure 4-2c** in Weibull coordinates. Finally one can plot the **fpdf** for this case using equation (II.2) as presented in **Figure 4-2d**.

3. *CASE C*: 10 filament bundle under P_{S3}=14 lbs tensile load

This case is exactly similar to what has already been described with the exception of the load or stress level that would have been achieved at the end of the loading sequence if no failures had occured

(p^{NF}_{s3} = 17.5 lbs). Therefore the whole procedure is outlined only schematically as shown in Figures 4-3a , 4-3b , 4-3c and 4-3d

4. *CASE D*: 10 filament bundle under P_{s4}= 16 lbs tensile load

Again due to the fact that no conceptual differences exist no matter what is the creep-rupture load level the procedure is outlined only schematically (p^{NF}_{s4} = 26.7 lbs), as shown in Figures 4-4a, 4-4b, 4-4c and 4-4d.

5. *Results*

If one now takes the results of Figures 4-1d, 4-2d, 4-3d and 4-4d and plots them with respect to the corresponding load levels achieved at the end of each loading sequence, the picture shown in Figure 5 can be obtained in which the Strength-Life curves for the extreme lower tail $(S\text{-}L)_{lt}$, the median $(S\text{-}L)_m$, and the extreme upper tail $(S\text{-}L)_{ut}$ of the Weibull model distribution are plotted. A close observation of this figure can lead to the following worthy of comment thoughts:

a. Given that one can produce accurately several points on the S-L curves the exact determination of the life distribution is possible at any desired strength (stress) level is only a matter of the availability of equipment if time is not a problem.

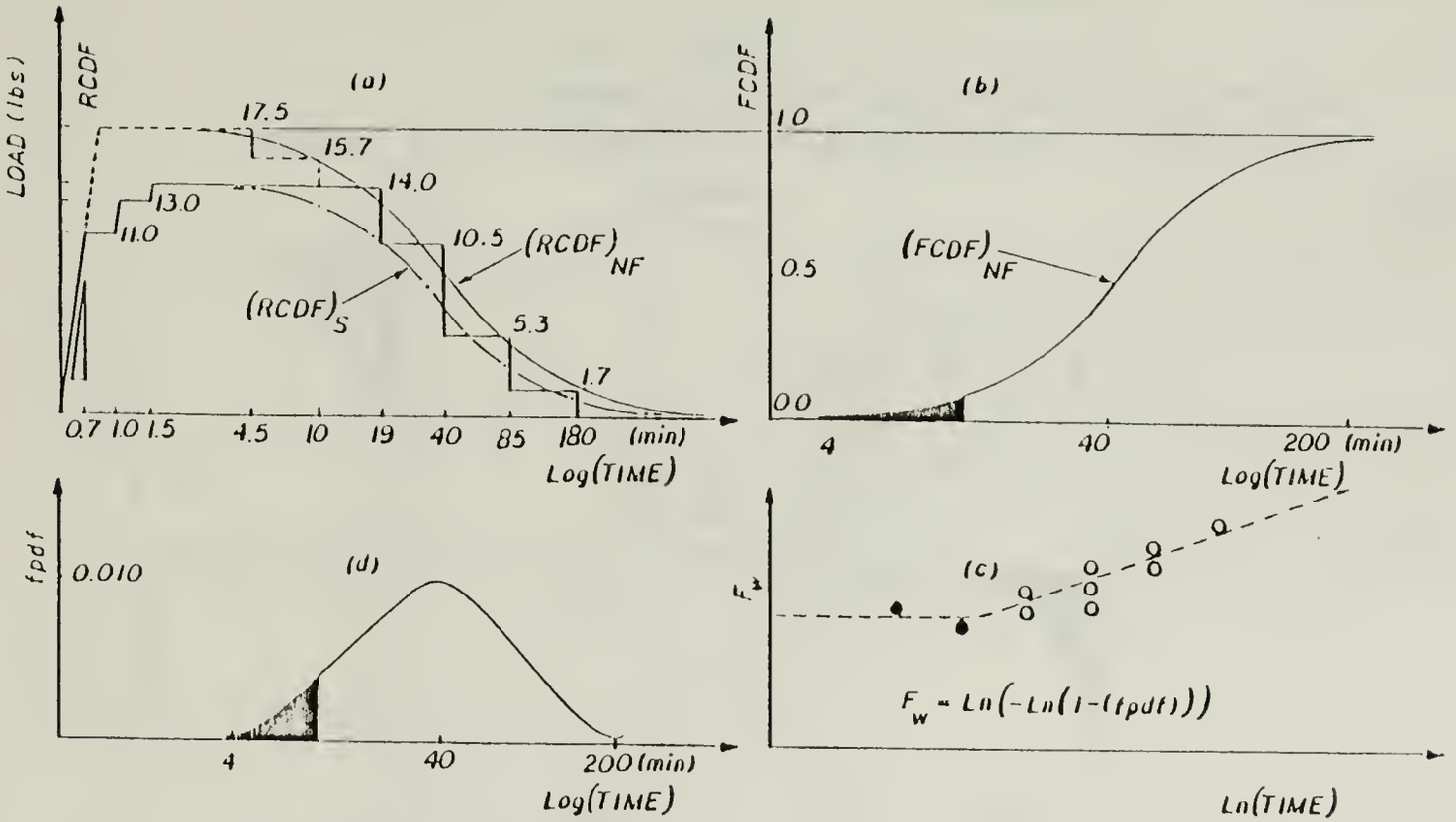

Figure 4-3 : Weibull life distribution for the model fiber bundle of 10 filaments under the Creep-Rupture load of 14 lbs.

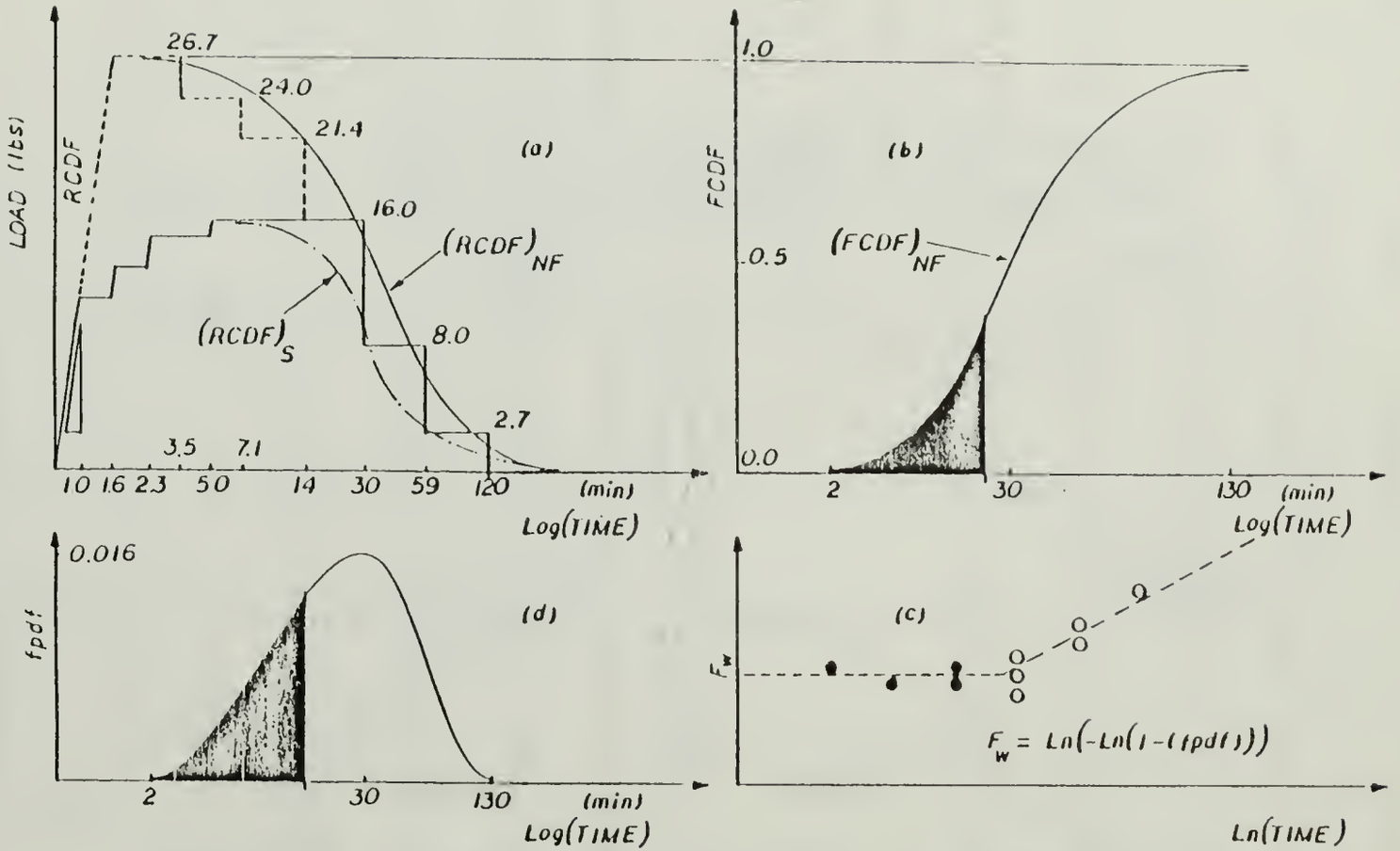

Figure 4-4 : Weibull life distribution for the model fiber bundle of 10 filaments under the Creep-Rupture load of 16 lbs.

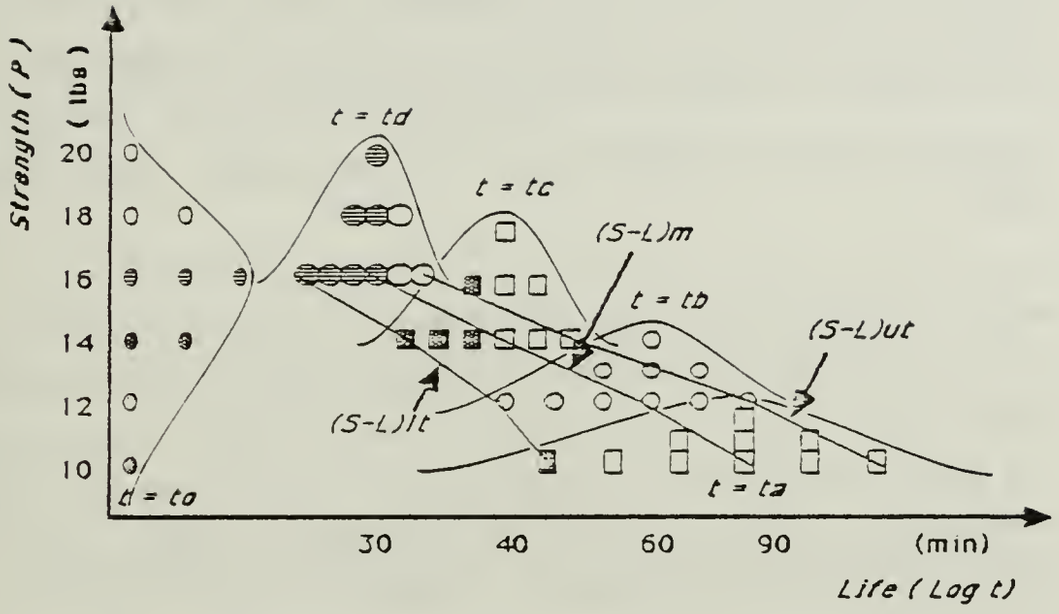

Figure 5. Strength - Life curves for the extreme lower tail (S-L)lt median (S-L)m and upper tail (S-L)ut, based on the results of four experiments of identical fiber bundles composed of 10 fiber filaments under different Creep-Rupture loads.

b. The higher the number of fiber filaments in the bundles the higner the confidence level of the results to be obtained, or in otherwords the more certain the Weibull curves will be and with the less spread (i.e., smaller coefficient of variation).

c. The Weibull curves are obtained on the basis that one can produce an accurate curve FCDF under the condition that no failures had occured during the loading sequence. The accuracy of the plot mainly depends on the exact evaluation of the fiber filaments that had failed during the loading sequence and on the assumption that every fiber is carrying the same amount of load, assuming that internal friction is absent known as the "*equal load-sharing rule*".

d. What is of great practical importance is the exact determination of the extreme lower tail of the Weibull distributions for various load (stress) levels because this is the key factor for evaluating the safe service life of any application. Another very serious point in discussing the significance of the extreme lower tail is the fact that the time coordinate is given in Log (t) and therefore a small error of 0.01 order of magnitude in Log (t) is translated in more than 0.1 order of magnitude error in useful service life which in any case is typically unacceptable. It is not difficult to observe that the exact determination of the extreme lower tail is based on how accurately one can determine the load that could have been achieved if no failures had happened during the loading sequence. Therefore one can understand that it is of cruisial importance to obtain exact data points with no irrelevant indications during the loading sequence and in order to accomplish this task two aspects have to be thoroughly examined:

   1. How to avoid the irrelevant indications when evaluating the data points recorded during the loading sequence.

2. How to record as many failure data points as possible to increase the precision of the final results.

D. STATISTICAL MODEL OF FAILURE

The failure of a bundle composed of brittle fibers such as carbon and glass in a flexible matrix under tensile loads, is a complex statistical process involving the scattered failure of fibers at imperfection sites and hence the overloading of the adjacent fibers at these sites, as well as the propagation of the neighboring fiber failures to a critical size according to Rosen [Ref. 6].

The mathematical model for the failure process was first presented by Rosen [Ref. 6] and is described in detail by Phoenix [Ref. 7].However for purposes of completeness and in order to gain some insight in the features of the bundle failure a review of the simplest case is presented herein.

According to this model the composite material is considered to be composed of repeating representative elements, the bundles, which are actually the focus of this work. Each bundle can conceptually be viewed as a close planar (or three dimensional) arrangement of n parallel fiber

filaments that form a tube as shown in **Figure 6**, which is loaded in tension. This tube structure is in turn conceptually partitioned into a series of **m** short sections that are called microbundles. Furtermore the length δ of these short sections is called the ***ineffective length*** after Rosen [Ref 6] and actually represents the length of the overload region of the neighboring fiber filaments to a fiber failure site. In other words the composite consists of bundles each one of which has a length equal to $m\delta$ and a volume of $nm\delta$. When a moderate tensile load per fiber **p** is applied to a bundle, fiber filaments fail randomly at sites where the strength is less than **p** and typically these random failures are spatially quite far appart. At the location of these failures sites the corresponding fiber filaments can not carry any load and therefore an overload of magnitude $K_r p$ takes place on each neighboring fiber filament, where $K_r > 1$ is defined as the ***load concentation factor*** and **r** represents the number of consecutive failed fiber filaments immediately adjacent to a sound fiber filament counting on both sides. For this very simple case that is being described here K_r is assumed to be:

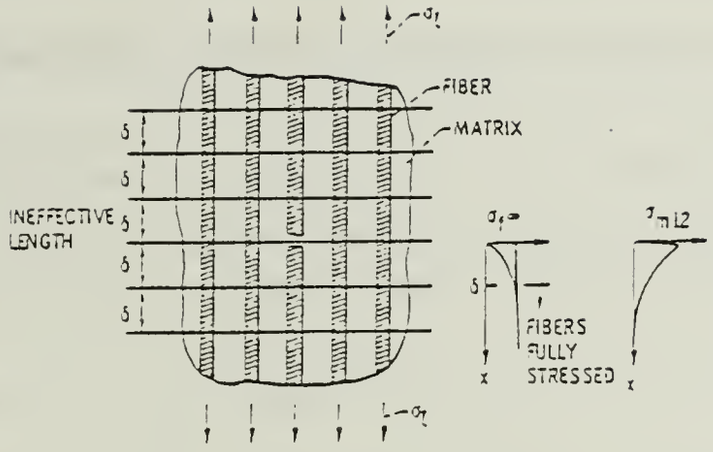

σ_l : tensile longitudinal stress
σ_{foo} : longitudinal fiber filament stress
$\sigma_{m\,12}$: transverse in plane matrix shear stress
x : longitudinal direction

Figure 6a. Statistical Tensile Failure Model after Rosen, W.B. [Ref. 6]

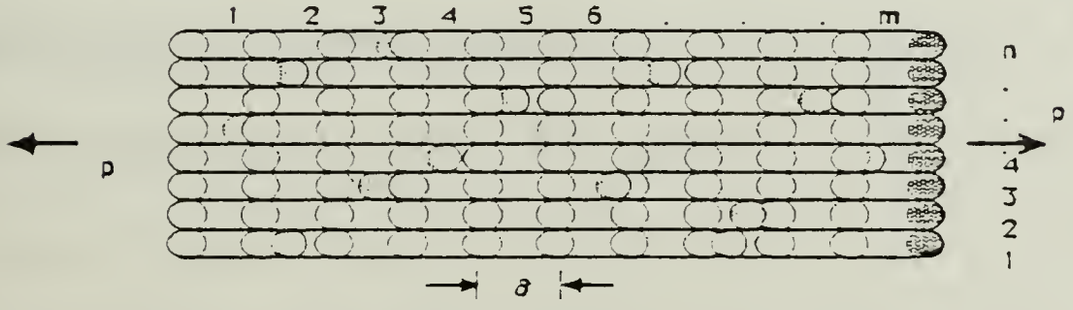

δ : Ineffective Length of fiber filaments
p : Load per fiber filament
n : Number of fiber filaments
m : Number of fiber microbundles
○ : Failure sites of fiber filaments

Figure 6 b. Bundle of fiber filaments in a matrix in the form of a planar tape. The bundle is composed of m microbundles in series each with n fiber filaments. Failure sites are localized within microbundles.

(II.4) $$K_r = 1+r/2 \quad \text{for} \quad r = 1,2,3,...$$

The length of this overload region which has already been defined as δ is typically of the order of a few fiber filament diameters and both K_r and δ depend on the fiber and the matrix material properties which can be estimated by elasticity or numerical analysis. Under the increased load $K_r p$ additional failures will appear to the close neighboring fibers, which in turn will be subjected to a higher overload say $K_R p$ ($K_R p > K_r p > 1$). This process continues until all the failure occurences form a front of a critical size k^*. If this critical size is exceeded a catastrophic crack propagates throughout the bundle leading to the failure of the entire composite structure.

In order to tailor this model to the thought experiment already described two cases of stress history of the composite are of interest.

The first one is a constant stress history expressed as :

(II.5) $$\sigma_1(t) = Q \qquad \text{for} \quad t \geq 0$$

where Q is the constant positive stress level. This constant stress history is often referred to in the literature as *stress - rupture* or *creep - rupture*. Application of this type of stress history is schematically illustrated at Figure 4-1a.

The second one is a linearly increasing stress history expressed as:

(II.6) $$\sigma_2(t) = Rt \qquad \text{for} \quad t \geq 0$$

where R is a positive rate of stress increase. This type of stress history is assumed to account for the early failures of the fiber bundles that will take place during the loading sequence and it is often described as *short - term strength*. Application of this stress history can be viewed by looking at Figures 4-2a, 4-3a and 4-4a. The FCDF for the failure time of a single fiber filament of length δ is given by Phoenix and Wu [Ref. 4] after Coleman [Ref. 8] by the following relationship:

(II.7) $$F(t;\sigma) = 1-\exp[-\nu[\int_0^t \kappa(\sigma(s))ds]] \quad , \quad \text{for} \quad t \geq 0$$

where $\sigma(t)$, $t \geq 0$ is the stress history,

$\kappa(x) = \gamma x^{\rho}$, $x \geq 0$ is the *power-law breakdown rule*

ρ as well as γ are positive constants,

$\psi(x) = \alpha x^{\beta}$, $x \geq 0$ is the Weibull shape function to compensate for the commonly observed Weibull behavior of the fibers and α as well as β are again positive constants.

Experimental evidence [Ref. 4], suggests that $10 < \rho < 80$ and also that $1/4 < \beta < 4$ for a wide range of fibers. It has also to be noted that α is proportional to the fiber-element length, or $\alpha = \alpha_0 \delta$ for a constant α_0 corresponding to the characteristic fiber length δ_0. Considering δ to be the characteristic length, since it is natural to the composite long single fiber filaments of length $l >> \delta$ will have α taken as $m\alpha$ where $m = l/\delta$. The theoretical justification of this fiber model is discussed by Phoenix [Ref. 7] in terms of the kinetic failure of idealized molecular crystals of the form found in stiff polymeric filaments such as Kevlar. More specifically the key parameter ρ involves an approximation to the

potential function for chain scission and is shown to follow the relationship:

(II 8) $$\rho = U_0/kT$$

where T is the absolute temperature,

k is Boltzmann's constant,

U_0 is expressed in units of activation energy but in the case of chain scission is only about 40 % of the energy of the bond rupture whereas the other parameters α , β and γ vary with temperature in very complex ways.

Based on the model and the stress histories of interest described so far the behavior of single fiber filaments and fiber composites will be presented from both the sthrength and life standpoints together with the basic assumptions that are inherent to every case and finally some summarizing results will also be presented to serve as a means of gaining the necessary insight for the experimentally anticipated results according to Phoenix and Wu [Ref. 4] and Phoenix [Ref. 5].

1. Behavior of single fiber filaments

a. *Short-term Strength*

The fiber filament strength is known to be closely approximated by the Weibull distribution which under the linearly increasing stress history [Eq.(II.6)] can be written in terms of the (FCDF) = F* as follows:

$$F^*(p) = 1-\exp[-p/p_1(R)]^{\beta(\rho+1)} \quad , \text{for } p \geq 0 \tag{II.9}$$

with a shape parameter $\beta(\rho+1)$ and a scale parameter equal to:

$$p_1(R) = m^{-1/[\beta(\rho+1)]} p_\delta(R) \tag{II.9a}$$

where $p_\delta[R] = \alpha^{-1/[\beta(\rho+1)]} [(1+\rho)/\gamma]^{1/(\rho+1)} R^{1/(\rho+1)}$ is the scale parameter for unit fiber length δ and R is the loading rate. Finally the median fiber strength can be shown to be equal to:

(II.9b) $$p^*_1(R) = p_1(R)[\ln(2)]^{1/[\beta(\rho+1)]}$$

Unfortunately the accuracy of Eq.(II.9) in modelling the true FCDF can only be demonstrated for the lower tail of $F^*(p)$ that is for $p<<p_1$ and this is because strengths associated with the middle and upper tail are not typically observed at laboratory gauge length l (of the order of several centimeters). However this does not constitute a serious problem since the results show that the knowledge of the middle and upper tails are not important in the characterization of composite strength. As it has already been explained what is really of practical importance is the accurate determination of the extreme lower tail.

b. *Stress-Rupture*

A single fiber filament of length $l = m\delta$ under the constant stress history described by Eq.(II.8) has a lifetime which can be described by the following formula after the appropriate reduction of Eq.(II.7):

(II.10) $$F(t) = 1-\exp\{-[t/t_1(Q)]^{\beta}\} \quad , \quad \text{for } t\geq 0$$

with shape parameter β and scale parameter given by the formula:

(II.10a) $$t_1(Q) = m^{-1/\beta}\, t_\delta(Q)$$

where $t_d(Q) = Q^{-\rho}/(\gamma \alpha^{1/\beta})$ is the scale parameter for unit fiber filament length δ. For the constant stress level Q the median time-to-failure can be evaluated as:

(II.10b) $$t^*_1(Q) = t_1(Q)[\ln(2)]^{1/\beta}$$

If the median strength is known at the stress rate R, and one wishes to calculate the median time to failure at the stress level Q, the equivalent median lifetime can be evaluated by substituting Q in Eq.(II.10a) with $p^*_1(R)$ of Eq. (II.9b) equal to:

(II.10c) $$t^*_1(R,\rho) = p^*_1(R)/[R(\rho+1)]$$

2. Behavior of composite fiber bundles

a. *Short-term Strength*

One can now consider a single microbundle and define as $G_n(p)$ for $p \geq 0$ the (FCDF) of its strength or in other words the probability of failure of a stochastically selected microbundle under a nominal load per fiber filament equal to p. Similarly one can also define $H_{m,n}(p)$ for $p \geq 0$ the FCDF for the strength of a bundle consisting of fiber filaments in a matrix. Since the necessary and sufficient condition for the survival of the bundle is the survival of each one of the m microbundles, the probability of survival for the whole bundle under the load p can be written as $[1-G_n(p)]^m$. Therefore the probability of failure of this bundle under the load np, amounts to the so called ***weakest link rule*** and can be presented as follows:

$$H_{m,n}(p) = 1-[1-G_n(p)]^m \quad , \quad \text{for } p \geq 0 \tag{II.11}$$

Another basic assumption that has to be stated here is the fact that each one of the surviving fiber filaments carries the same

amount of load a statement which amounts for the ***equal-load sharing rule*** after Rosen [Ref. 6]. The first ones to obtain accurate results for this kind of a model were Harlow & Phoenix [Refs. 9 &10] but only for small number of fiber filaments per bundle (i.e., $n<14$). Later the same authors [Refs. 11 & 12] developed a powerful recursion analysis for treatment of larger bundles. According to this analysis the FCDF of the bundle strength can be quite succesfully approximated by using the weakest link rule as follows:

$$H_{m,n}(p) = 1-[1-W(p)]^{mn} \quad , \quad \text{for } p \geq 0 \tag{11.12}$$

where $W(p)$ is a very complicated function depending on the load concentration factor K_r and the FCDF of the fiber filaments of length δ under the tensile load p. The first one to develop a tractable approximation for $W(p)$ was Smith [Ref. 13] who showed by means of asymptotic analysis for ***large*** n (i.e $mn = 10^6$) that Eq. (11.12) can take the following form if one also replaces the constant stress history Q (described

in this case by the constant load p) by the linearly increasing stress history Rt :

(II.13) $$ {}^{*}H_{m,n}(p) \approx 1-\exp\{-[p/p_C(R)]^{k^*\beta(\rho+1)}\} \quad , \text{ for } p \geq 0 $$

with shape parameter $k^*\beta(\rho+1)$ and scale parameter given by the formula:

(II.13a) $$ p_C(R) = (mn)^{-1/[k^*\beta(\rho+1)]}\, p_\delta(R)(d_{k^*})^{1/(\rho+1)} $$

where k^* represents the critical failure sequence size and mathematically is the integer solving the equation :

(II.13b) $$ 1/r(k+1) < \beta\rho/\ln(mn) < 1/r(k) $$

where the function $r(k)$ is defined by the following equation :

(II.13c) $$ r(k) = \ln({}_{k-1}K^k) - \ln\Big({}_{i=1}\prod^{k} K_{i-1}\Big) \quad \text{and} $$

$$d_k=\Gamma(\beta+1)^{-1/\beta}\Gamma(k\beta+1)^{1/(k\beta)}2^{(1-k)/(k\beta)}\prod_{j=1}^{k}(k_j-1)^{-\rho/k}$$

for $k = 1,2,3,...$ (II.13d)

As before the median strength can be given by the equation:

(II.14) $$p^*_c(R) = p_c(R)[\ln(2)]^{1/[k^*\beta(\rho+1)]}$$

b. *Composite Stress-Rupture*

Similarly the FCDF for the lifetime of the composite material under the constant stress history described by Eq.(II.5) has a Weibull approximation of the form:

(II.15) $$^*H_{m,n}(t) \approx 1-\exp[-[t/t_c(Q)]^{k^*\beta}, \text{ for } t\geq 0$$

with shape parameter $k^*\beta$ and scale parameter given by the equation:

(II.16) $$t_c(Q) = (mn)^{-1/(k^*\beta)}(d_{k^*})t_\delta(Q)$$

where d_{k^*} has already been defined by Eq.(II.13d) for $k^* = k$ and $t_\delta(Q)$ is

defined in the same way as for the Eq.(II.10a). The median lifetime of the model composite can therefore be given by the following expression:

$$t^*_c(Q) = t_c(Q)[\ln(2)]^{1/(k^*\beta)} \qquad (II.17)$$

Using the reasoning given in the analysis of the fiber filament behaviour if the median strength $p^*_c(R)$ is known for the stress rate R the median lifetime under the stress level $Q = p^*_c(R)$ can be evaluated as:

$$t^*_c(R,\rho) = p^*_c(R)/[R(\rho+1)] \qquad (II.18)$$

It has to be noted that the Weibull approximations (II.13) and (II.15) are only valid when $\beta\rho$ is *large*, say greater than 6, as well as, that the best Weibull fit to $H_{m,n}(t)$ may produce a value of k^* which is not an integer usually when the solution for k yields almost an equality on either side of Eq.(II.13b).

Summarizing the important characteristics of the model described one has to note that:

1. Comparisons of the median lifetime and strength of a single fiber filament and a fiber composite are actually meaningless.

2. The variability in strength and lifetime for a composite is much less than that for a single fiber filament primarily due to the critical crack size.

3. The size effect is a lot milder for the composite relative to that of the fiber for the strength and drastically lower for the lifetime again primarily due to the critical crack size.

III. THE CONTRIBUTION TO THE SOLUTION

In accordance with the approach stated in the Introduction the required methodology appropiate to be used as a quide line in order to achieve the ultimate objective of obtaining strength-life data been presented in the of the problem approach section.

For the equipment used by Carozzo [Ref. 2 : Fig. 3.4] shown in **Figure 7** and from his evaluation of its performance (summarized in Figures B.1 and B.2a of his thesis ([Ref. 2]) shown in **Figures 8a** and **8b** one can observe that although the desired target was the acquisition of data in hundredths of seconds (i.e 6000 data/min) the results suggested that a rate of only 3-4 data/min was achievable. In an effort to acquire more data during the loading phase, the testing traverse speed was lowered to the minimum. This slowest speed setting of the INSTRON testing equipment (at13 grams/sec) caused the drive motor of the INSTRON to stall erratically [Ref. 2 : pp. 29-30]. In addition, during the the creep rupture phase of the experiment the time dependence of creep was physically observed by the upward movement of the moving cross - head of the INSTRON. However

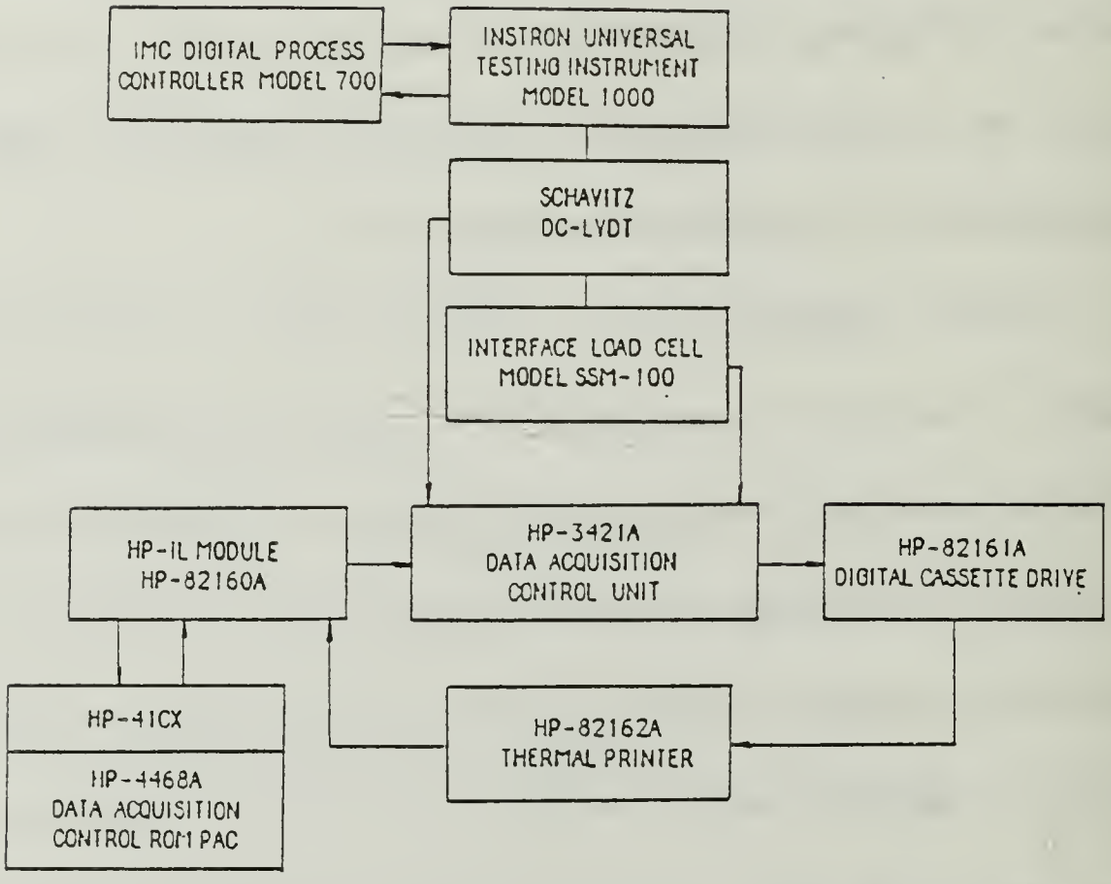

Figure 7 : Block Diagram of the initial Experimental Set-Up after Carozzo [Ref. 2].

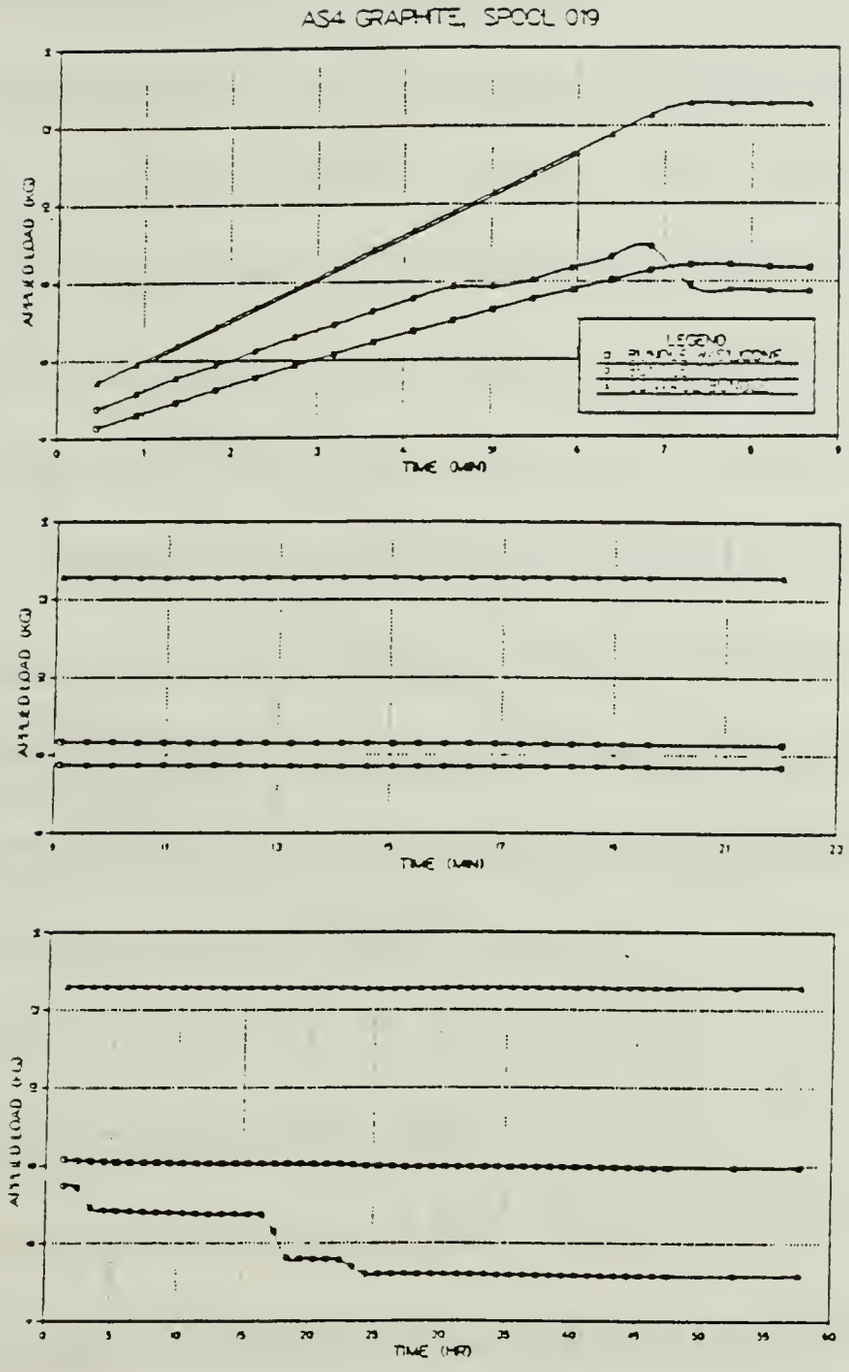

Figure 8a : Load - Time curves for Test #1 after Carozzo [Ref. 2].

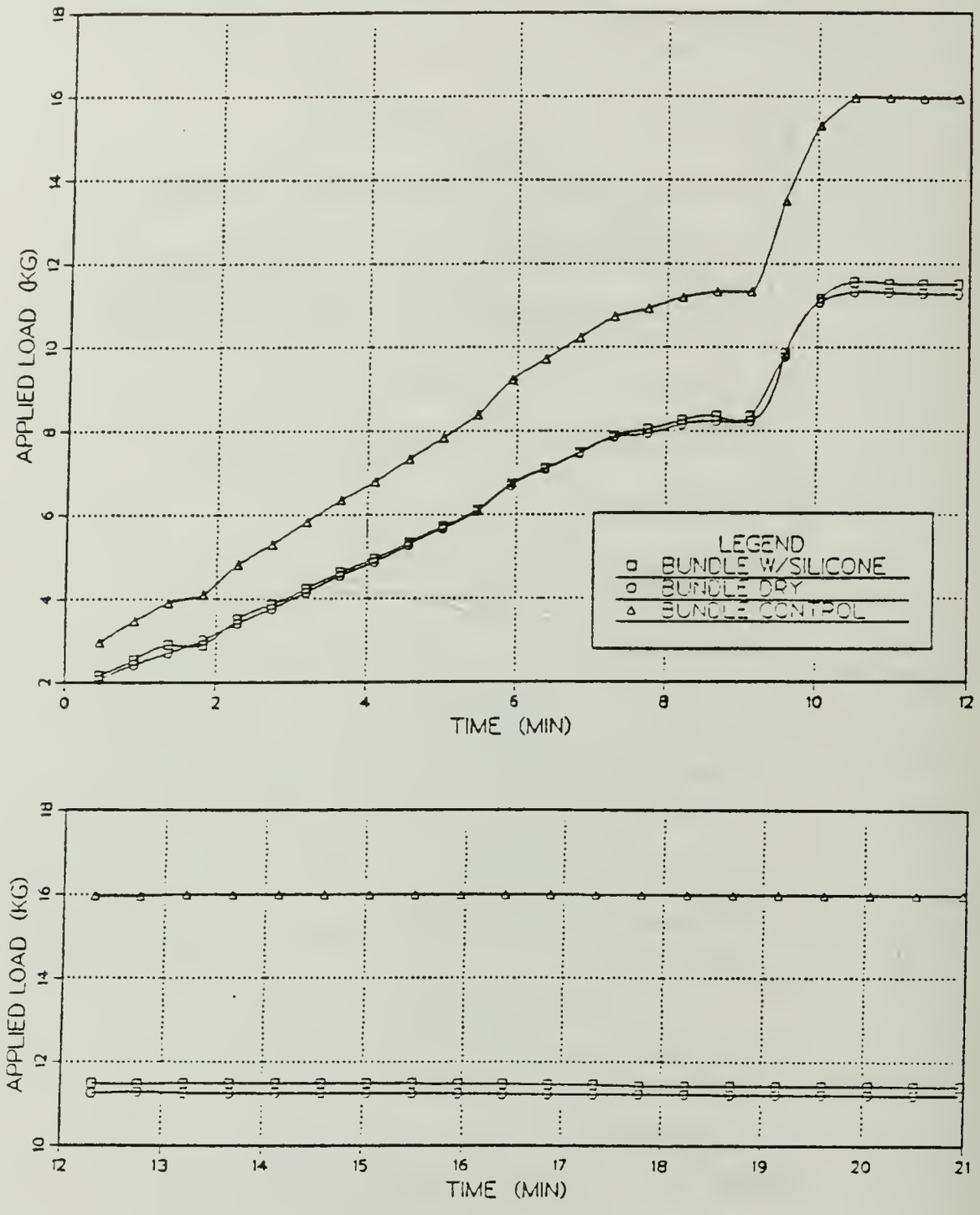

Figure 8b : Load - Time curves for Test #2 after Carozzo [Ref. 2].

the data recorded to support this observation were considered completely unreliable in that it showed that the cross-head moved up and down which is equivalent to an entropy decrease ([Ref. 2 : p. 31]). These observations were what actually gave rise to the other goals of this work which are to evaluate the limitations of the testing equipment available and propose procedures that will serve in eliminating them (i.e explaining why the creep-rupture data were unreliable, avoiding the stall , by-pass the problem of inadequate accuracy of the extension measurements etc.), as well as to find out how more data could be acquired at least during the loading sequence for the reasons that have already been explained in the detailed analysis of the approach to the overall problem.

A. TESTING EQUIPMENT LIMITATIONS

The implementation of the INSTRON model 1000 Universal Testing Equipment requires at least the description of it's operating principles prior to investigating it's inherent limitations.

1. Operating Principles

The INSTRON 1000 is an 120 ± 10V AC single phase 50-60Hz motor belt driven testing device capable of tensile and compressive

testing, extension measurements and the testing machine has been modified to perform creep monitoring if necessary. The load measurements are achieved by means of a combined Load Transducer (LT)/ Linear Variable Differential Transformer (LVDT) system, installed within the moving cross-head. The traverse crosshead measurement is achieved by a Shaft Encoder (SE) and the creep monitoring by means of a Digital Processor/Controller (DP/C) that can compensate for the cross-head adjustments relative to a predetermined load variation. The creep dispacement was specifically recorded by an additional LVDT that was mounted on the fixed cross-head of the INSTRON 1000. The operating principle of the LVDT is that of a transformer composed of a housing of the transformer coil and a core. The insertion of a ferrous rod-core alteres the electro-magnetic coupling thereby causing a change in the output voltage. Therefore by controlling the core insertion and measuring the output voltage one can evaluate a relationship that will allow for converting output voltage to displacement and vice versa. A detailed description of the major units, subsystems and enhancement features of the testing equipment and their primary functions is presented in Section I of Appendix A.

2. Determination of INSTRON 1000 Limitations by Simulation

The strength of the fiber bundles to be tested is of the 50 lbs order of magnitude and the maximum utilization of INSTRON 1000 under the existing provisions set-up involves testing of nine (9) bundles simoultaneously (including the control bundle). Hence the load level of interest is of the 450 lbs order of magnitude, an estimate that dictates for the use of only the 1000 lbs **LT** during the simulation. Given also that the graphite fiber bundles ought to be tested in tension, because the area of interest is ultimately the broad class of composite applications where the structure is subjected to sustained tensile loading, as well as that the graphite fiber bundles are expensive to use them for purposes other than the actual experiment a simulation process is obviously necessary. During this simulation experiment, the above mentioned load level (450 lbs) will have to be easily achieved and/or overcome a good number of times so that several conclusions could be drawn as far as the limitations of the equipment are concerned.

The objectives, the theoretical model, the design of a simple mechanical set-up that had to be used with the INSTRON 1000 during the

simulation and the detailed procedure of this aside task are presented in Section II of Appendix A.

3. Stability of the **LVDT**

The background for checking the stability of the **LVDT** lies on the fact, that although the cross-head of the INSTRON must have moved during the creep-rupture phase, no reasonable output had been recorded accordingly and the output (displacement) was measured by means of an **LVDT** which was externally mounted on the INSTRON 1000.

The background, the objectives, the set up used and the detailed procedure of this separate aside task are presented in Section III of Appendix A.

B. DATA ACQUISITION SYSTEM LIMITATIONS

One of the major problems associated with the graphite bundle life testing as presented by Carozzo [Ref. 2 : Fig. B1 & B2a] (Figures 8a and 8b) is the slow data aquisition rate that was achieved during the loading sequence (0.04 readings/sec) was substantially less than the manufacturer's specification of about 2 readings/sec [Ref. 15 : p. 32]. For completeness and future reference purposes the experimental set-up used by Carozzo during

the initial run of the experiment is presented in **Figure 9.** A survey of the available literature on this subject revealed that the reading rates can be influenced by many factors.

1. Signal environment factors

The most significant factors in this area are the line related factors (the smaller the loop the better , 60 Hz line frequency gives about 17% faster reading rates), [Ref. 15 : pp. 30,34] & [Ref. 16 : p. 42], the broadband noise (the larger the loop, the more the noise contrbutions from the various accesories in the loop), [Ref. 15 :p. 30] & [Ref. 16 : p. 42] and the thermal gradients (negligible in this case due to the relatively constant temperature of the lab environment), [Ref. 15 : p. 30].

2. Desired accuracy

At 3.5 digits of resolution (N3) the ability of the voltmeter to acurately measure DC voltages in the presence of AC voltages at power line frequencies is expressed by the Normal Mode Rejection (NMR), [Ref. 15 : pp. 30, 43], which in this case is 0 db NMR. The smaller the number of digits of resolution the smaller the "Integration Time" which obviously determines the reading rate and hence for (N3) the reading rate is ***faster***. Similarly at

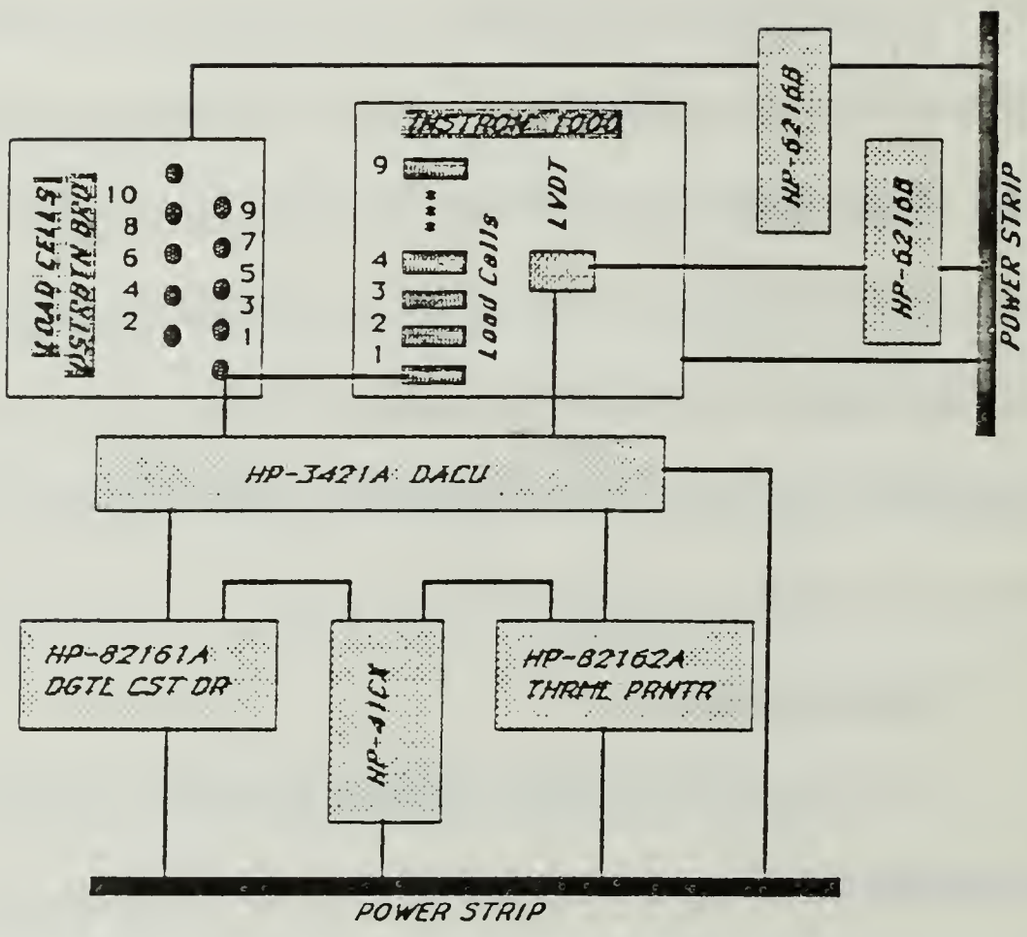

Figure 9 : Block diagram of the experimental set - up used during the initial run of the experiment involving one INSTRON 1000 machine.

N4 (59 db NMR) an ***intermediate*** reading rate is achieved and finally at N5 (80 db NMR) the reding rate is ***slow***.

3. Type of measurement

a. Resistance measurements [Ref.15 :pp. 30-32].

(1) At 30 Mohm (200 msec settling time) the recording rate is 1.5 readings/sec.

(2) At 3 Mohm (20 msec settling time) the recording rate is 2.1 readings/sec .

b. Voltage measurements.

(1) The DC readings are 5 to 50 times faster than the AC ones [Ref. 15 : p. 32].

(2) Positive voltage measurements increase the reading rate. Possible problems can be raised by the **LVDT**s whose outputs can be negative dependent on their null point with respect to the measurements under evaluation.

(3) AUTOZERO is a function that allows the operator to enable or disable the internal zero correction of the voltmeter of the HP-3421A. The default condition is ON (used by the set-up of Figure 9) but turning AUTOZERO OFF could substantially increasthe reading rate but with a tradeoff of long term stability and accuracy [Ref. 15 : p. 41]. However no problems of this sort are of interest during the relatively short period of the loading sequence which is of the order of a few minutes (see Figures 8a and 8b).

4. Inherent to the HP-3421A features

Calibration has to be performed after the installation of the one 44462A / 10 channel Multiplexer (option 020) but it is of interest only when absolute values are necessary; however this is not this case.

AUTORANGING is a function meaning that signals with a wide dynamic range such as switching from channel to channel to take readings are made more quickly by utilizing it [Ref. 15 : p. 44]. But this function is made primarily for taking readings in the N4 mode and not in the N5 mode which has to be used due to the HP-41CX involvement(see Figure 9).

When operating with the HEWLETT PACKARD-INTERFACE LOOP (**HP-IL**) most 3421A commands will " Hold - Up " the computer until all readings have been taken. These problems are known as information transfer ones. Recording time by the HP-41CX when the order of magnitude of the 3421A capacity is about 2 readings / sec and the target is to take say 100 readings using one 44462A 10 channel multiplexer assembly 50 seconds are required for the 100 readings. The computer will not be able to perform any operation during the 50 seconds while the 3421A is taking the measurements.

The 3421A commands that do not hold-up the computer are the so called **advanced commands** of digital monitoring (MN, MH and ML) the totalize function (TOT) and the digital trigger (DT) commands. However if any of the digital monitor modes (MN ,MH ,ML or DT) are in effect in the 3421A any communication through the **HP-IL** will cause the mode to be aborted. In other words if the 3421A is waiting for a digital trigger and the computer or another instrument in the loop sends any commands or data through the interface, the 3421A will abort the digital monitor and will no longer respond.

On the other hand, according to Carozzo [Ref. 2 : p.25] the basic data logger software program provided by the the HP-44468A Data Acquisition Control Pac was modified to permit the recording of time in hundredths of seconds and edited to reduce the number of data registers uscd. However recording time in hundredths of seconds is 50 times faster the maximum capacity of the HP-3421A DACU (2 readings/second). In addition to this the system timing is greatly dependent on the nature of the set-up itself and especially on whether the printer or tape cassette (or both) are used the number and type of measurement sequences, User Functions as well as the number of channels in each sequence [Ref. 16 :p. 42].

Several contacts with system engineers of Hewlett-Packard revealed that the reading rates of the HP-3421A manual for the case of the experiment under evaluation, (ZIF1-2.19/13.18/22.22) [Ref. 15 : p. 32] refer only to the unit itself and if this unit is interfaced with the HP-41 calculator they reduce to 1.0/1.0/2.0 whereas no data were available in case the printer and the cassette drive are within the loop. Their suggestion with respect to the very slow data acquisition rate was to definitely take out of the loop the printer and the cassette drive and also try to use AUTOZERO OFF and AUTORANGING, or switch to another system as the HP-85 desk top computer or the neuer HP-71 which provide the opportunity of using the advanced commands that allow for better programming flexibility (i.e. use of AUTOZERO and AUTORANGING functions and as less digits of resolution as possible according to the requirements of the experiment) and also by-pass the problem of storing and printing data by using their own modules without contributing to a larger interface loop. Under the above circumstances (interfacing the HP-3421A DACU with the HP-85 and using the advanced commands) according to the HEWLETT-PACKARD engineers the recording rates of the HP-3421A DACU as presented in the Operating, Programming and Configuration Manual [Ref. 15 : p. 32] reduce to 3/9/11

respectively depending on the number of digits of resolution required which is substantially higher to what already has been achieved.

The points of contact with HEWLETT-PACKARD as well as the official correspondence made with the customers division, by which the company was asked to confirm by letter the information released by phone and suggest possible solutions of improvement is presented in Appendix B.

C. OVERALL EXPERIMENTAL SET-UP

To come up with the overall experimental set-up several caclulations had to be made concerning the optimum, yet safe number of pieces of equipment that ought to be used. These calculations are presented in Appendix C and dictated the utilization of one (1) power supply HP-6216B for every set of nine (9) Load Cells (per INSTRON 1000) as well as an extra power supply HP-6216B for the **LVDT**s that would be externally mounted to the INSTRON machines for the recording of the creep-rupture displacement.

The basic steps that were followed for the overall experimental set-up which is presented in a diagram form by **Figures 10a** and **10b**, are also given in Appendix C under the title " Implementation of the Overall Experimental Set-Up ".

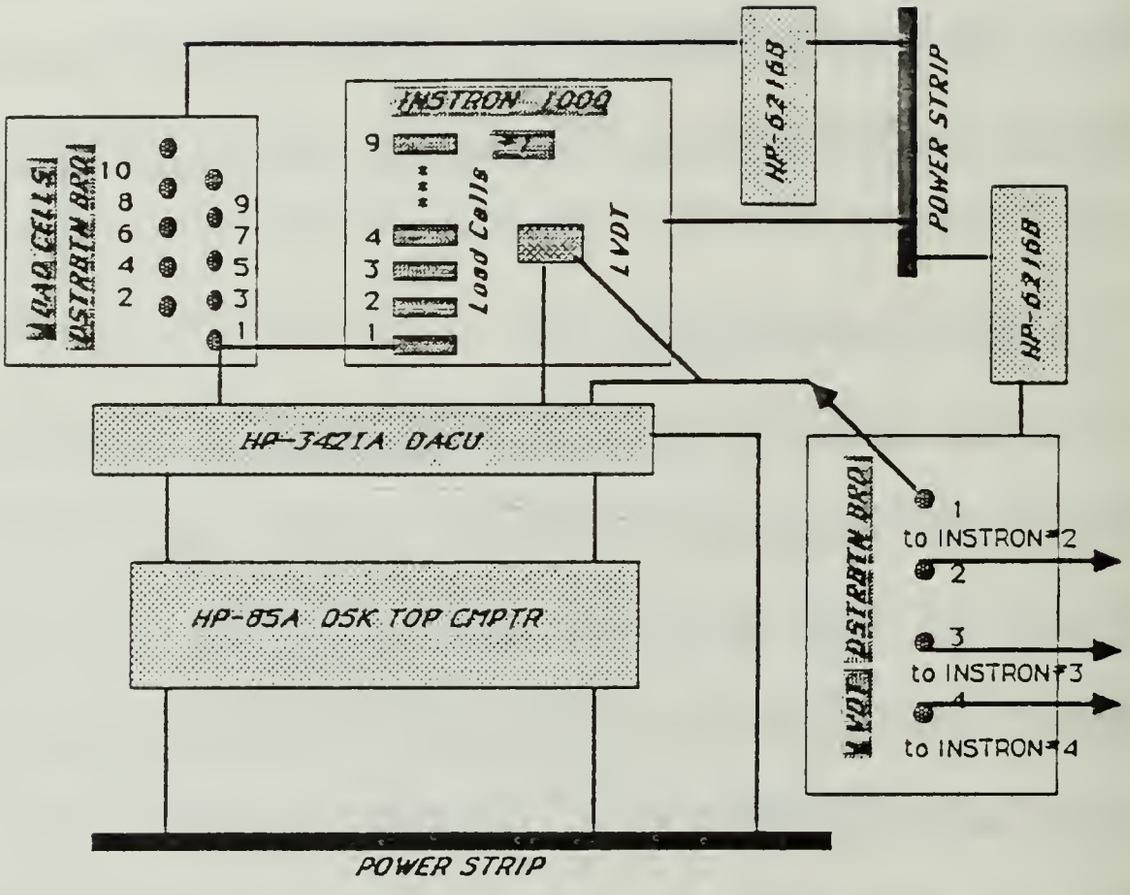

Figure 10a : Block diagram of the overall experimental set-up involving four INSTRON 1000 machines proposed for the Loading Sequence phase.

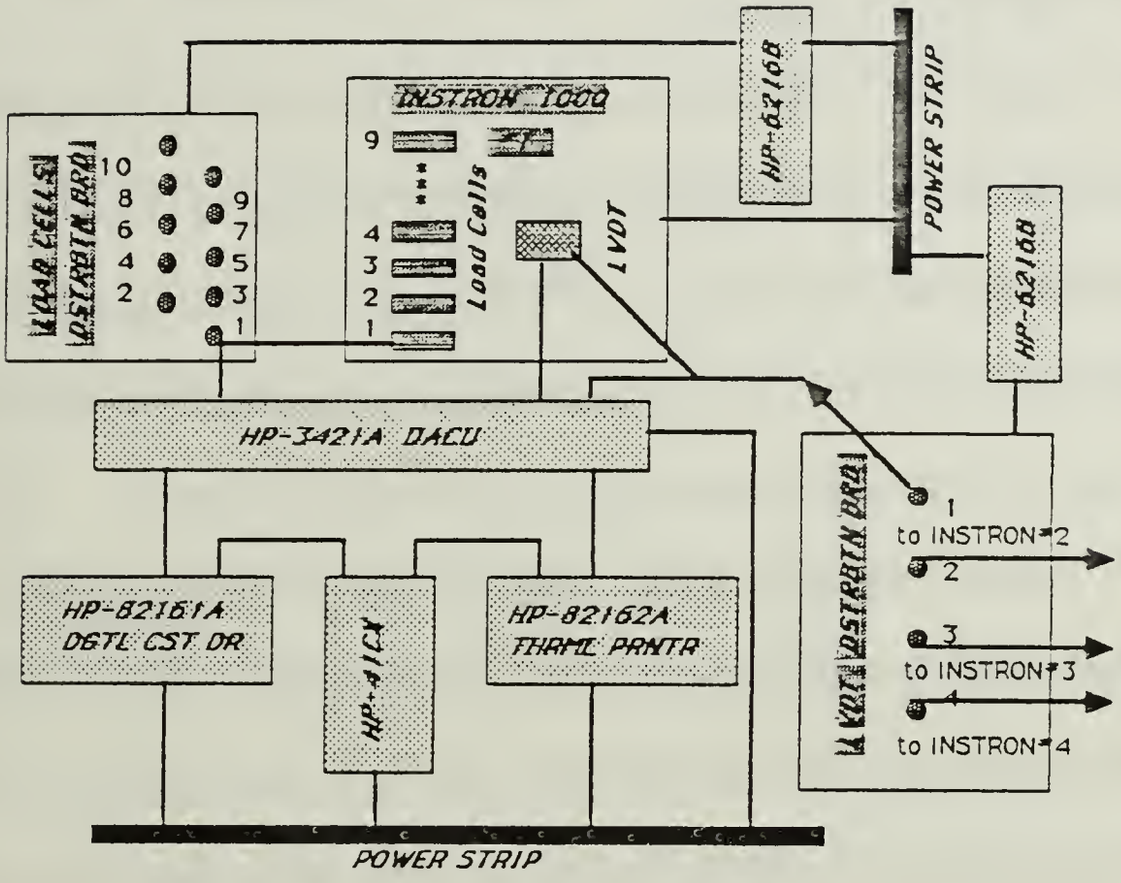

Figure 10b : Block diagram of the overall experimental set-up involving four INSTRON 1000 machines proposed for the Creep-Rupture phase.

IV. DISCUSSION-RESULTS

A. INSTRON LIMITATIONS

According to the INSTRON manual [Ref. 14] the Liquid Crystal Display (**LCD**) indicator for the extension readout of the moving cross-head of the INSTRON between the no-load case and the under load situation, gives an agreement within about 10 % and hence only the latter, which is directly related to the ultimate experiment, was thoroughly examined.

Several attempts were made to obtain displacements for the minimum knob speed setting (i.e 0.5 in/min-MIN) but it turned out that no movement of the cross-head had taken place as it was observed by both the **LCD** and the **DIAL** indicators; the latter was used to monitor the physical displacement as described in the Appendix A. Furthermore it was observed that after a short period of time the **LCD** displacement readout started to decrease with time.

Using the bracketing technique it was found that no matter what the load was (within the capability of the equipment) no stall occured for knob speed settings larger than 0.5 in/min-30 % and the overtravel-limiters

system had finally to interrupt the loading sequence to protect the equipment from overload.

A good number of attempts were also performed at the range of speeds (0.5 in/min-MIN, 0.5 in/min-12 %). This showed completely irrelevant indications (**Table I**) as far as the observed and the expected spceds correlation was concerned and suggest that in actuallity the cross-head had moved so little and in such a random way that no significance could be given to these small Variable Speed Indicator (**VSI**) settings.

Several knob speed settings were tried to evaluate the quality of the response and some representative sample data are given in **Table II** which actually turned out to be in very good agreement with the anticipated results. One can also observe from **Figures 11a, 11b** and **11c** corresponding to the above mentioned table that the functions $d_{DIAL} = f(t)$ $d_{LCD} = f(t)$ and $P = f(t)$ are single valued, monotonically increasing and as the time increases there is a tendency for the displacement and the load intervals to decrease. Having thus verified the anticipated results and observing from the quality of the response, that the helical spring employed

TABLE I

INSTRON 1000 RESPONSE FOR LOW SETTINGS OF THE VARIABLE SPEED INDICATOR

Column 1	Column 2	Column 3	Column 4	Column 5	Column 6	Column 7
3.2	0.025	224	12.0	61	1	12.5
2.8	0.040	254	11.7	61	1	20.0
3.6	0.060	194	11.7	61	1	30.0
2.7	0.075	257	11.7	61	1	37.5
3.0	0.090	591	30.0	63	0	45.0
3.6	0.100	50	3.0	61	2	50.0
1.4	0.110	168	4.0	64	3	55.0
11.3	0.110	167	31.5	63	2	55.0
9.7	0.110	118	19.0	62	2	55.0
12.6	0.110	76	16.0	62	1	55.0
8.9	0.110	945	140.0	85	13	60.0
OBSRVD SPD x(.001in/min)	VRBL SPD IND DIAL SETTING	TOTAL TIME x (sec)	DIAL DSPLCT x (.001 in)	STL LD (P) x (lbs)	LCD DSPL x (.01 in)	EXPCTD SPD x(.001in/min)

TABLE II

TYPICAL DATA BASE SHOWING THE QUALITY OF THE RESPONSE OF THE INSTRON 1000 TESTING EQUIPMENT

Column 1	Column 2	Column 3	Column 4
.13	0	60	0
.25	4	61	0
.50	9	61	1
.75	15	62	1
1.00	22	63	2
1.25	27	63	3
1.50	32	64	3
1.75	37	65	4
2.00	44	66	4
2.25	50	67	5
2.50	56	68	5
2.75	62	69	6
3.00	68	71	7
3.25	79	71	7
3.50	80	73	8
3.75	84	73	9
4.00	86	74	9
4.25	92	75	10
4.50	98	77	10
4.75	104	78	11
5.00	110	79	12
5.25	116	80	12
5.50	122	81	13
5.75	128	83	14
6.00	134	84	14
6.25	139	85	13
6.50	143	87	14
6.75	150	88	14
7.00	155	89	15
7.25	162	91	15
7.50	168	92	16
7.75	174	93	16
8.00	180	94	17
8.25	182	94	18
8.50	187	95	18
8.75	193	97	19
9.00	195	*97	18
TIME x (minutes)	DIAL DSPLMT x(0.001 inch)	TNSL LOAD x (lbs)	LCD DSPLMT x (0.01 inch)
CODES :		*: STAL LOAD	
DATA IDFN :	RUN * 18		
VSI STNG :	.5x.13 in/min		

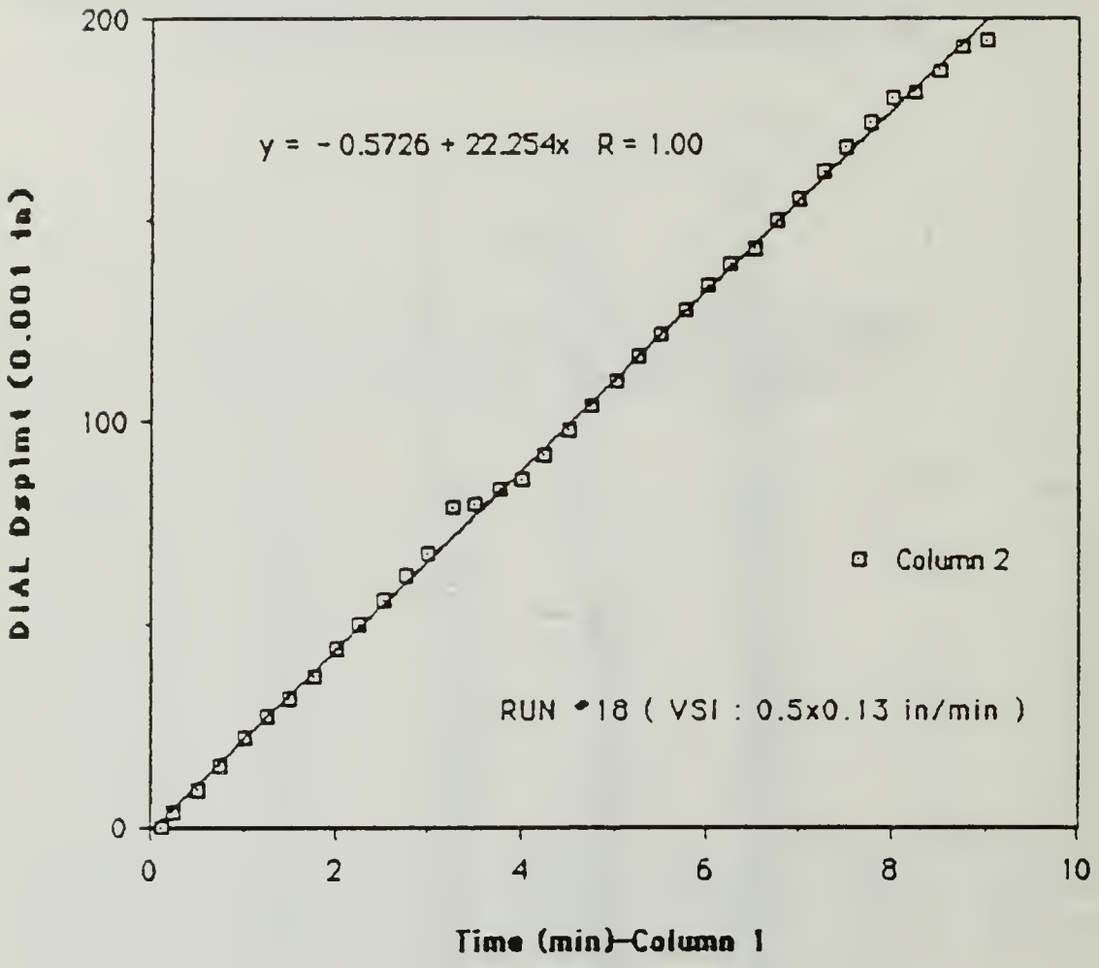

Figure 11a : Typical response for the Loading-Sequence. Variation of physical displacement (DIAL) of the INSTRON 1000 moving cross - head with time.

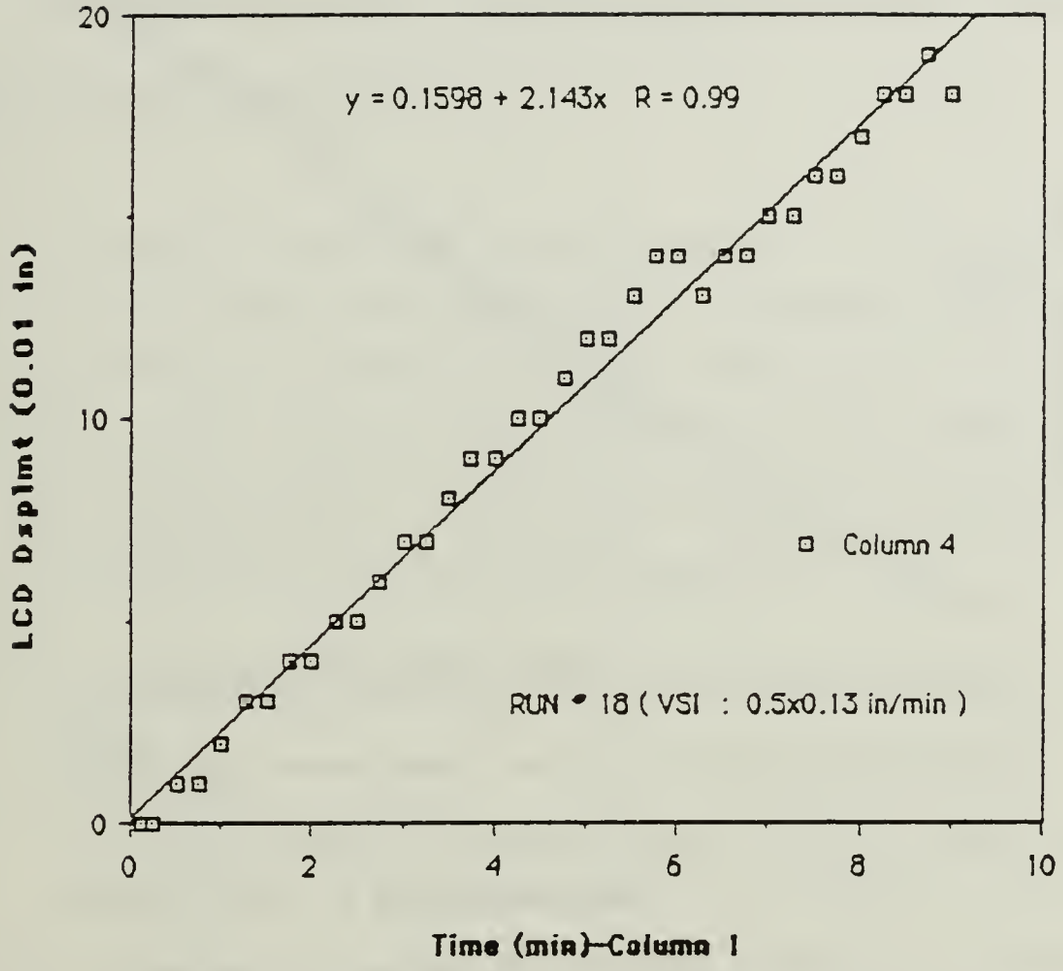

Figure 11b : Typical response for the Loading-Sequence. Variation of displayed displacement (LCD) of the INSTRON 1000 moving cross - head with time.

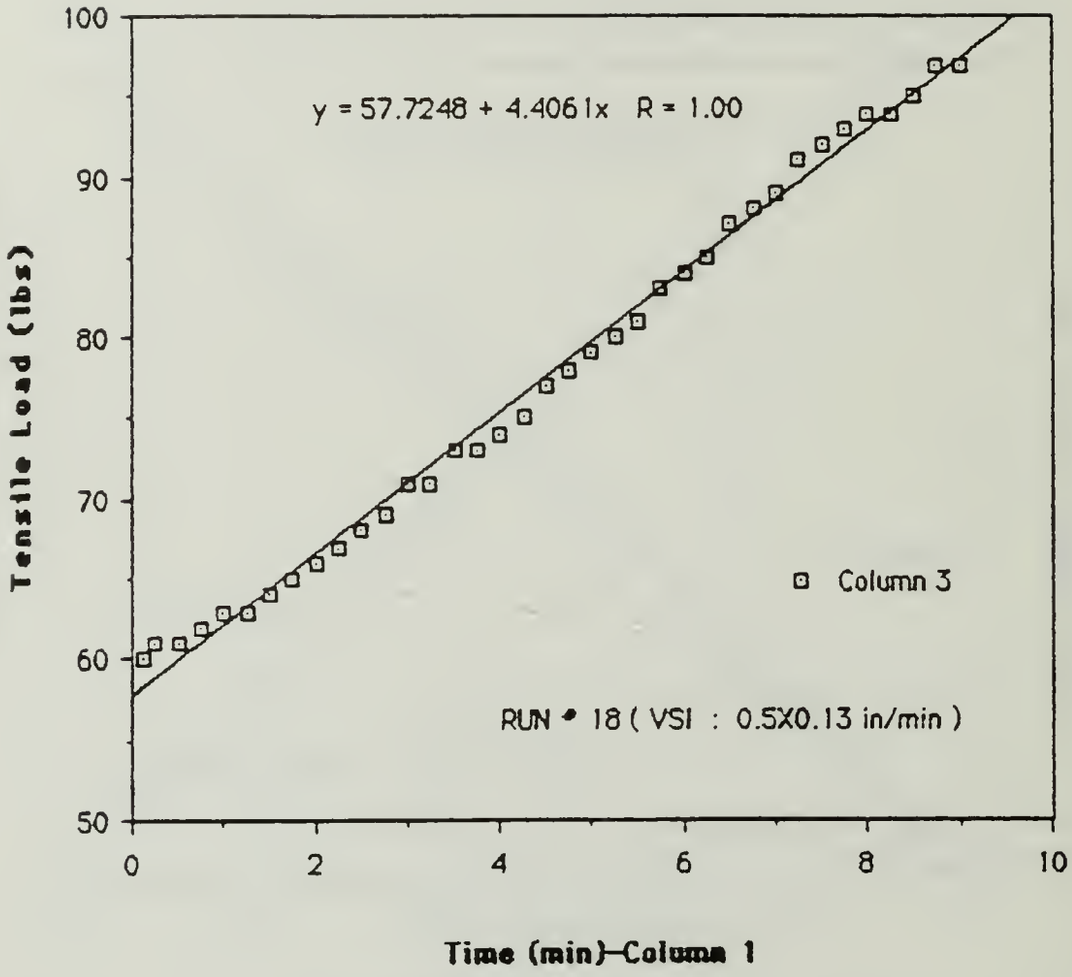

Figure 11c : Typical response for the Loading-Sequence. Variation of tensile load applied to the INSTRON 1000 moving cross - head with time.

managed to represent quite well the linear model assumed, the data base of **Table III** was created by repetition of the loading sequence at various speed settings. A closer look to this data base yielded the following results.

There is always an one to one correspondence between the following pairs of variables of interest:

1. The **LCD** and the **DIAL** displacements. Their relationship appears to be a linear under a slope of one (1) as shown in **Figure 12a**. The greater error (noise) band which is observed to the lower side of the simple curve fit is attributed to the sequence under which the data were manually recorded. Had the data been recorded in the opposite sequence, a greater error band to the upper side of the simple curve fit would have heen observed.

2. The expected speed and the observed speed as shown in **Figure 12b.**

3. The stall load and the Variable Speed Indicator (**VSI**) as shown in **Figure 12c.**

The plot of stall load versus the **VSI** as presented in Figure 12c enables the descission maker to predict the appropriate knob combinations to reach a certain load level without stalling. However this plot is characterized by a lot of scatter in the data and that is why it is also presented in a form to compensate for the mean upper and lower values

TABLE III

DATA BASE OF THE STALL CONDITIONS DURING THE SIMULATION FOR VARIOUS SETTINGS OF THE VARIABLE SPEED INDICATOR

Column 1	Column 2	Column 3	Column 4	Column 5	Column 6	Column 7
0.13	55	2.0	15	13	449	84
0.13	65	14.6	197	22	799	97
0.13	65	19.5	638	65	1961	201
0.13	65	22.0	195	18	532	97
0.13	65	19.4	21	0	65	62
0.13	65	22.3	71	6	187	70
0.13	65	12.9	53	3	246	69
0.13	65	13.0	53	5	254	69
0.13	65	12.9	56	3	260	69
0.13	65	14.1	53	5	224	69
0.13	65	22.4	205	19	550	97
0.14	70	23.5	749	75	1885	226
0.14	70	29.5	411	41	834	148
0.14	70	26.2	194	18	444	95
0.14	70	30.3	163	15	323	93
0.14	70	21.3	50	5	141	68
0.14	70	20.5	57	6	167	69
0.14	70	22.2	90	7	243	76
0.14	70	19.9	147	15	443	88
0.14	70	23.8	57	4	144	69
0.14	70	21.8	110	8	303	80
0.14	70	23.7	60	5	152	69
0.14	70	18.1	165	13	547	92
0.15	75	23.2	975	79	2484	279
0.15	75	34.0	425	43	750	152
0.15	75	33.4	1138	112	1925	321
0.15	75	31.7	866	87	1638	260
0.15	75	30.7	1155	107	2319	323
0.15	75	33.0	1200	125	2185	332
0.15	75	34.5	911	88	1585	229
0.15	75	35.1	1529	143	2615	428
0.15	75	33.2	173	13	295	90
0.15	75	33.9	742	70	1315	225
0.15	75	27.3	182	18	400	94
0.15	75	26.8	112	11	251	81
0.15	75	24.3	168	14	414	92
0.15	75	24.2	394	36	977	142
0.16	80	36.8	1569	153	2560	436
0.16	80	38.9	1587	149	2449	424

VSI STNG x (0.5 in/min)	EXPCTD SPD x(.001in/min)	OBSRVD SPD x(.001in/min)	DIAL DSPLMT x (.001 in)	LCD DSPLMT x (.01 in)	TOTAL TIME x (sec)	STALL LOAD x (lbs)

CONTINUED

TABLE III

DATA BASE OF THE STALL CONDITIONS DURING THE SIMULATION FOR VARIOUS SETTINGS OF THE VARIABLE SPEED INDICATOR

Column 1	Column 2	Column 3	Column 4	Column 5	Column 6	Column 7
0.16	80	39.7	960	90	1451	270
0.16	80	32.7	30	3	53	62
0.16	80	42.0	963	101	1375	274
0.16	80	4.1	165	16	223	90
0.16	80	35.5	467	44	822	166
0.16	80	33.3	531	50	993	183
0.16	80	34.4	770	82	1344	235
0.16	80	33.9	869	81	1537	265
0.16	80	12.2	446	41	2193	272
0.16	80	33.9	716	64	1268	221
0.17	85	49.7	1467	150	1770	433
0.17	85	42.8	1798	159	2516	497
0.17	85	43.7	848	93	1165	248
0.17	85	46.3	414	41	536	145
0.17	85	42.7	1342	120	1885	366
0.17	85	45.2	810	81	810	193
0.17	85	43.5	717	74	990	220
0.17	85	43.8	770	78	1054	223
0.17	85	40.4	995	94	1477	284
0.17	85	40.8	1050	93	1545	299
0.17	85	37.2	1214	92	1956	340
0.18	90	47.5	1681	176	2126	466
0.18	90	49.9	1695	160	2037	467
0.18	90	33.3	1186	113	1287	327
0.18	90	51.9	1441	138	1666	400
0.18	90	40.7	1320	93	1960	370
0.18	90	33.8	989	98	1104	284
0.18	90	49.3	1222	117	1487	340
0.18	90	44.0	1333	97	1818	369
0.18	90	49.8	767	72	925	224
0.18	90	38.6	906	87	927	262
0.18	90	49.5	1346	131	1632	381
0.18	90	52.3	1210	115	1387	340
0.19	95	60.9	515	55	507	172
0.19	95	77.9	2021	304	1557	562
0.19	95	55.6	2105	187	2272	592
0.19	95	48.2	1651	174	2057	462
0.19	95	59.8	824	81	827	242
0.19	95	57.2	913	88	957	262
0.19	95	57.5	645	61	673	200
0.19	95	46.6	1775	267	2157	489

VSI STNG x (0.5 in/min)	EXPCTD SPD x(.001in/min)	OBSRVD SPD x(.001in/min)	DIAL DSPLMT x (.001 in)	LCD DSPLMT x (.01 in)	TOTAL TIME x (sec)	STALL LOAD x (lbs)

CONTINUED

TABLE III

DATA BASE OF THE STALL CONDITIONS DURING THE SIMULATION FOR VARIOUS SETTINGS OF THE VARIABLE SPEED INDICATOR

Column 1	Column 2	Column 3	Column 4	Column 5	Column 6	Column 7
0.19	95	45.1	1677	145	2337	482
0.19	95	45.3	1666	165	2474	513
0.19	95	57.5	390	37	407	141
0.19	95	70.1	1274	107	1091	350
0.19	95	47.6	65	10	92	69
0.20	100	67.9	845	89	747	246
0.20	100	69.6	1250	129	1077	344
0.20	100	65.5	1458	124	1317	371
0.20	100	37.3	2005	241	3224	606
0.20	100	70.1	167	15	143	91
0.20	100	60.2	1152	113	1148	323
0.20	100	47.6	1306	50	1647	359
0.20	100	56.9	1050	114	1107	295
0.20	100	78.5	484	35	370	140
0.20	100	51.1	2145	183	2519	583
0.20	100	47.9	1845	190	2313	524
0.20	100	50.1	1600	130	1917	457
0.20	100	59.5	770	72	777	228
0.20	100	49.5	1556	113	1887	428
0.21	105	72.5	2207	213	1827	612
0.21	105	68.5	1048	115	918	306
0.21	105	59.4	1642	153	1659	451
0.21	105	63.3	1339	118	1270	369
0.21	105	48.9	1710	156	2097	474
0.21	105	58.4	1701	252	1747	474
0.21	105	41.2	1965	126	2865	543
0.22	110	75.0	79	5	57	70
0.22	110	66.1	1627	188	1658	525
0.22	110	80.6	321	32	611	240
0.22	110	101.5	1813	144	1072	400
0.22	110	77.5	1149	111	586	322
0.23	115	74.2	2570	225	1917	585
0.23	115	99.9	1865	181	1120	514
0.23	115	69.7	2116	198	1822	596
0.23	115	86.8	495	50	342	166
0.23	115	83.3	587	60	423	188
0.24	120	91.6	2240	216	1468	783
0.24	120	90.4	883	88	586	253
0.24	120	109.7	426	40	233	126
0.24	120	71.4	1410	140	1185	381

VSI STNG x (0.5 in/min)	EXPCTD SPD x(.001in/min)	OBSRVD SPD x(.001in/min)	DIAL DSPLMT x (.001 in)	LCD DSPLMT x (01 in)	TOTAL TIME x (sec)	STALL LOAD x (lbs)

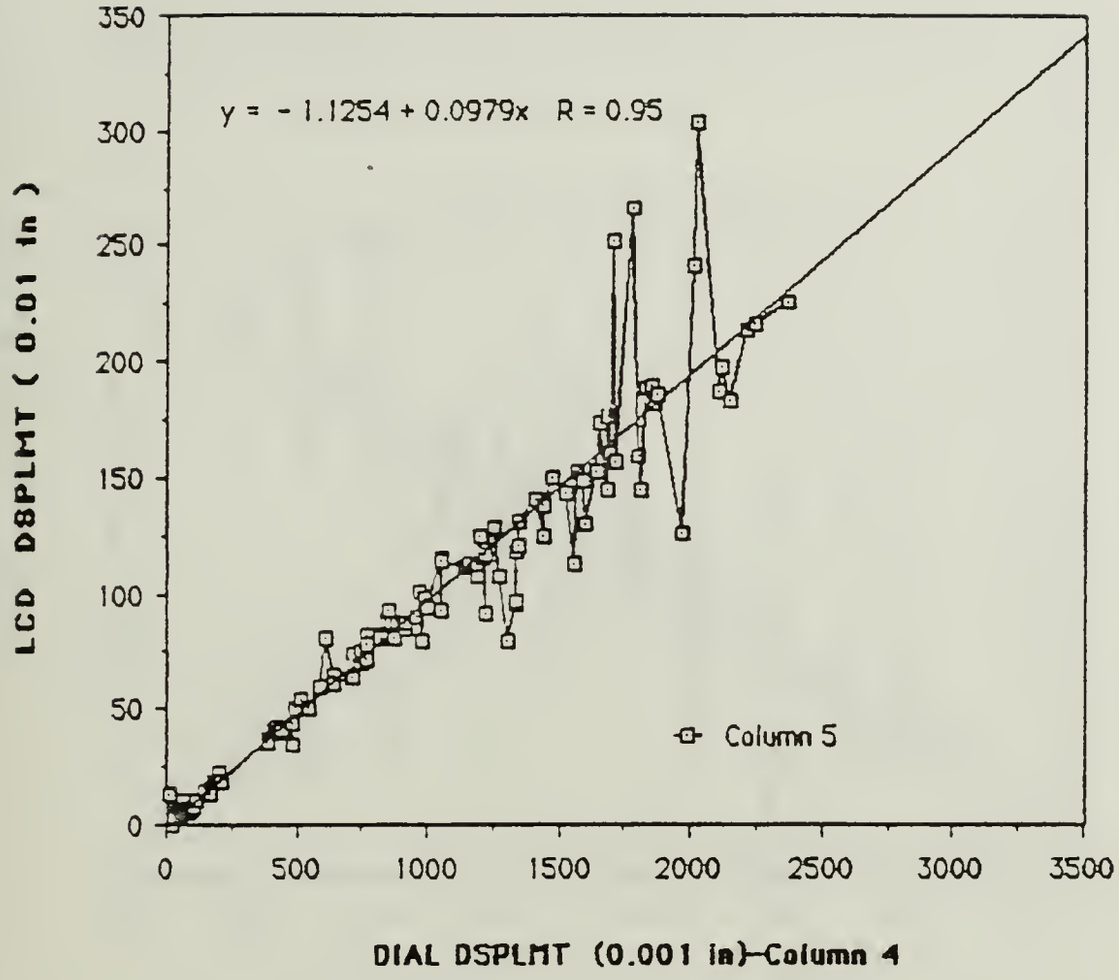

Figure 12a : Quality of the Response of the Simulated Experiment. Relation between physical (DIAL) and displayed (LCD) displacement of INSTRON 1000 moving cross-head at stall conditions.

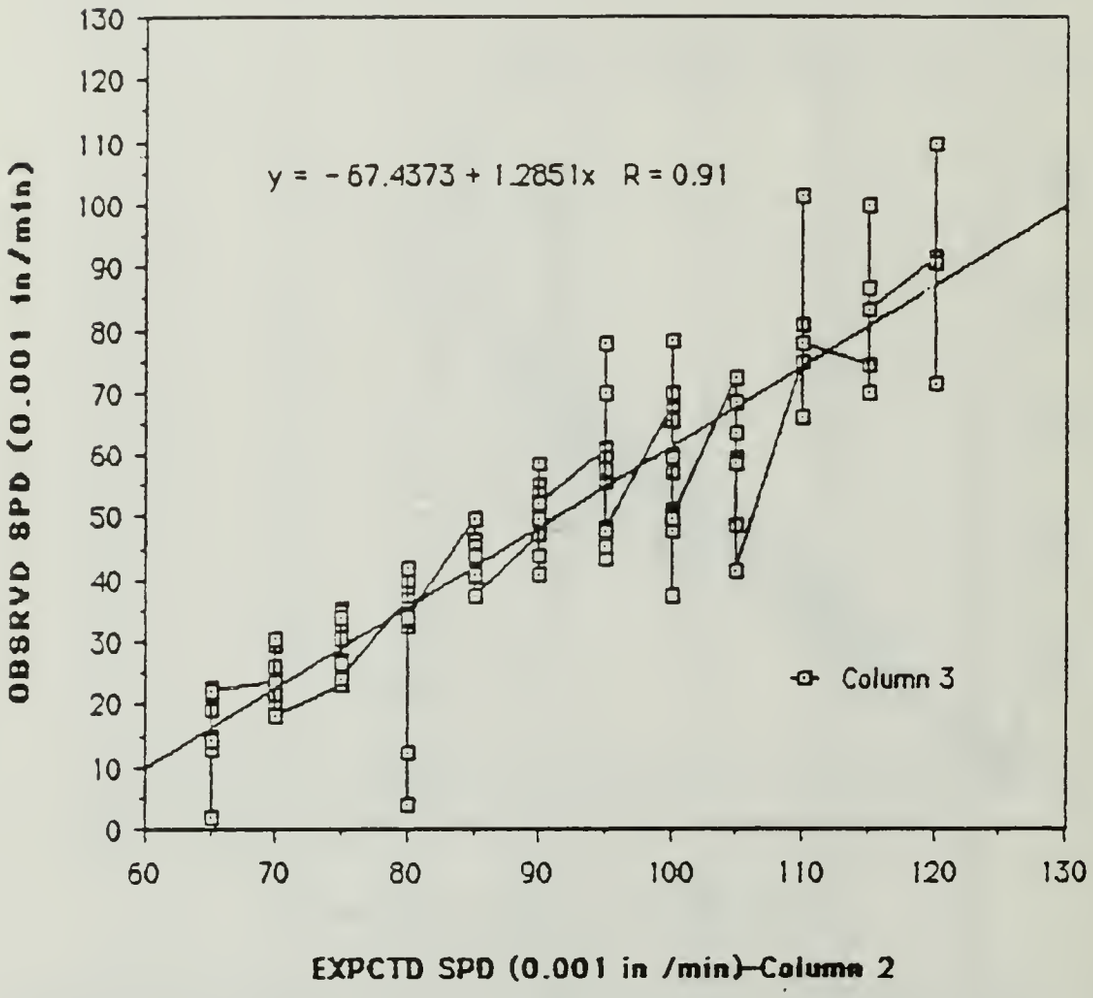

Figure 12b : Quality of the Response of the Simulated Experiment. Relation between observed speed (OBSRVD SPD) and expected speed (EXPCTD SPD) of INSTRON 1000 moving cross-head at stall conditions.

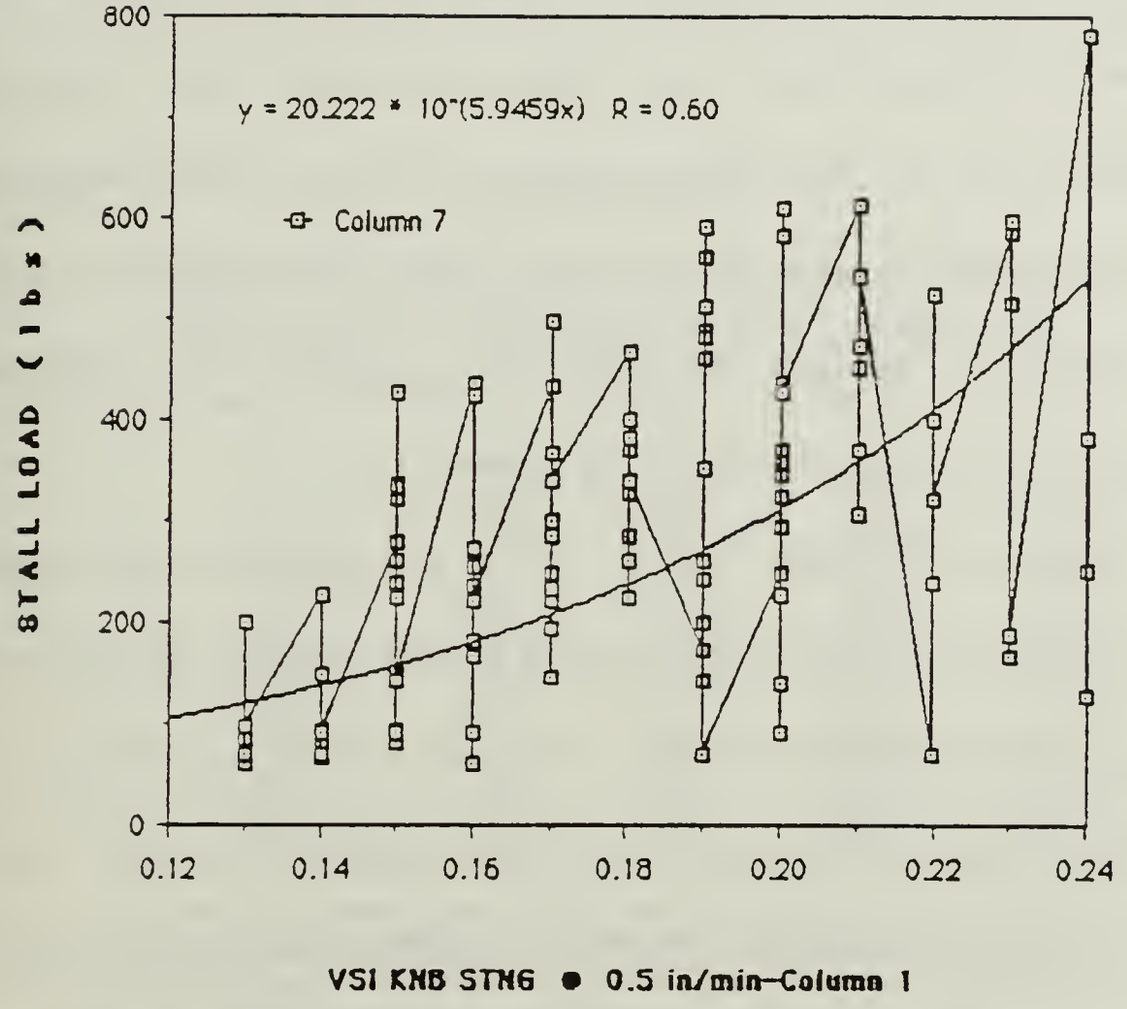

Figure 12c : Quality of the Response of the Simulated Experiment. Relation between achieved stall load and INSTRON 1000 variable speed indicator knob setting (VSI KNB STNG).

values achieved at every **VSI** knob setting as **Figure 12c-1** after the appropriate data manipulation presented in **Table III-A.** It is therefore evident that in order to avoid stall one has to take into account the **VSI** knob setting corresponding to the mean which also gives the higher confidence level in that no stall will occur. For the actual experiment where nine (9) fiber bundles will have to be tested simoultaneously totaling 450 lbs order of magnitude load, Figure 12c-1 suggests that the **VSI** knob setting to be used has to be that of 0.5 in/min-21 %.

The graphs of Figures 12a, b, c, c-1 are characterized by a great amount of scatter which appears to be of increasing magnitude as the **VSI** setting is increased. However this is not true and this indication is only attributed to the limitations of the testing equipment itself. Had the capacity of the INSTRON been larger the scatter would decrease almost to zero. This statement ows its credit to the large amounts of attempts that have been made for **VSI** knob settings larger than 0.24 in which the switch limiter-system had always taken over to interrupt the loading sequence for safety purposes in the neighborhood of 950-975 lbs. Being conservative this means that a stall load of at least 1000 lbs for the **VSI** of 0.25 and 1200 lbs for the **VSI** of 0.26 would have been achieved if capacity were not a

TABLE III-A

MIN, MEAN & MAX VALUES OF PARAMETERS OF INTEREST
FOR VARIOUS VSI SETTINGS AT STALL CONDITIONS

Column 1	Column 2	Column 3	Column 4	Column 5
0.13	65	2.0	16.0	22.8
0.14	70	18.1	19.6	30.3
0.15	75	23.2	30.7	35.4
0.16	80	4.1	31.5	42.0
0.17	85	37.2	43.3	49.7
0.18	90	40.7	50.2	58.6
0.19	95	43.1	60.6	77.9
0.20	100	37.3	58.0	78.5
0.21	105	41.2	58.9	72.5
0.22	110	75.0	80.2	101.5
0.23	115	69.7	82.8	99.9
0.24	120	71.4	90.8	109.7
VSI STNG x(0.5 in./min)	EXPCTD SPD x(.001in/min)	MIN OBS SPD x(.001in/min)	MEAN OBS SD x(.001in/min)	MAX OBS PSD x(.001in/min)

CONTINUED

TABLE III-A

MIN, MEAN & MAX VALUES OF PARAMETERS OF INTEREST
FOR VARIOUS VSI SETTINGS AT STALL CONDITIONS

Column 6	Column 7	Column 8	Column 9	Column 10	Column 11
15.0	141.9	638.0	0.0	14.5	65.0
50.0	187.8	411.0	4.0	17.7	75.0
112.0	714.1	1529.0	11.0	67.4	143.0
30.0	759.4	1587.0	3.0	72.8	153.0
414.0	1022.1	1796.0	41.0	97.7	159.0
767.0	1258.8	1695.0	72.0	116.6	176.0
65.0	1209.3	2105.0	10.0	130.8	304.0
167.0	1258.1	2145.0	15.0	176.6	941.0
1048.0	1658.9	2207.0	115.0	161.9	252.0
79.0	1137.8	1827.0	5.0	106.0	188.0
495.0	1486.6	2370.0	50	142.8	225.0
426.0	1239.8	2240.0	40.0	121.0	216.0
MIN DIAL x (.001 in)	MEAN DIAL x (.001 in)	MAX DIAL x (.001 in)	MIN LCD x (.01 in)	MEAN LCD x (.01 in)	MAX LCD x (.01 in)

CONTINUED

TABLE III-A

MIN, MEAN & MAX VALUES OF PARAMETERS OF INTEREST FOR VARIOUS VSI SETTINGS AT STALL CONDITIONS

Column 12	Column 13	Column 14	Column 15	Column 16	Column 17
65.0	503.4	1961.0	62.0	89.5	201.0
141.0	468.8	1885.0	69.0	105.1	226.0
251.0	1439.5	2615.0	81.0	219.3	428.0
55.0	1356.8	2560.0	62.0	240.7	436.0
536.0	1427.5	2516.0	145.0	296.2	497.0
925.0	1529.7	2126.0	224.0	352.5	467.0
82.0	1338.6	2474.0	69.0	303.4	592.0
143.0	1442.4	3224.0	91.0	341.4	608.0
918.0	1769.0	2865.0	306.0	461.3	612.0
57.0	856.8	1658.0	70.0	311.4	525.0
342.0	1124.8	1917.0	166.0	409.8	596.8
233.0	868.0	1468.0	126.0	385.8	783.0
MIN TIME x (sec)	MEAN TIME x (sec)	MAX TIME x (sec)	MIN STL LD x (lbs)	MEAN STL LD x (lbs)	MAX STL LD x (lbs)

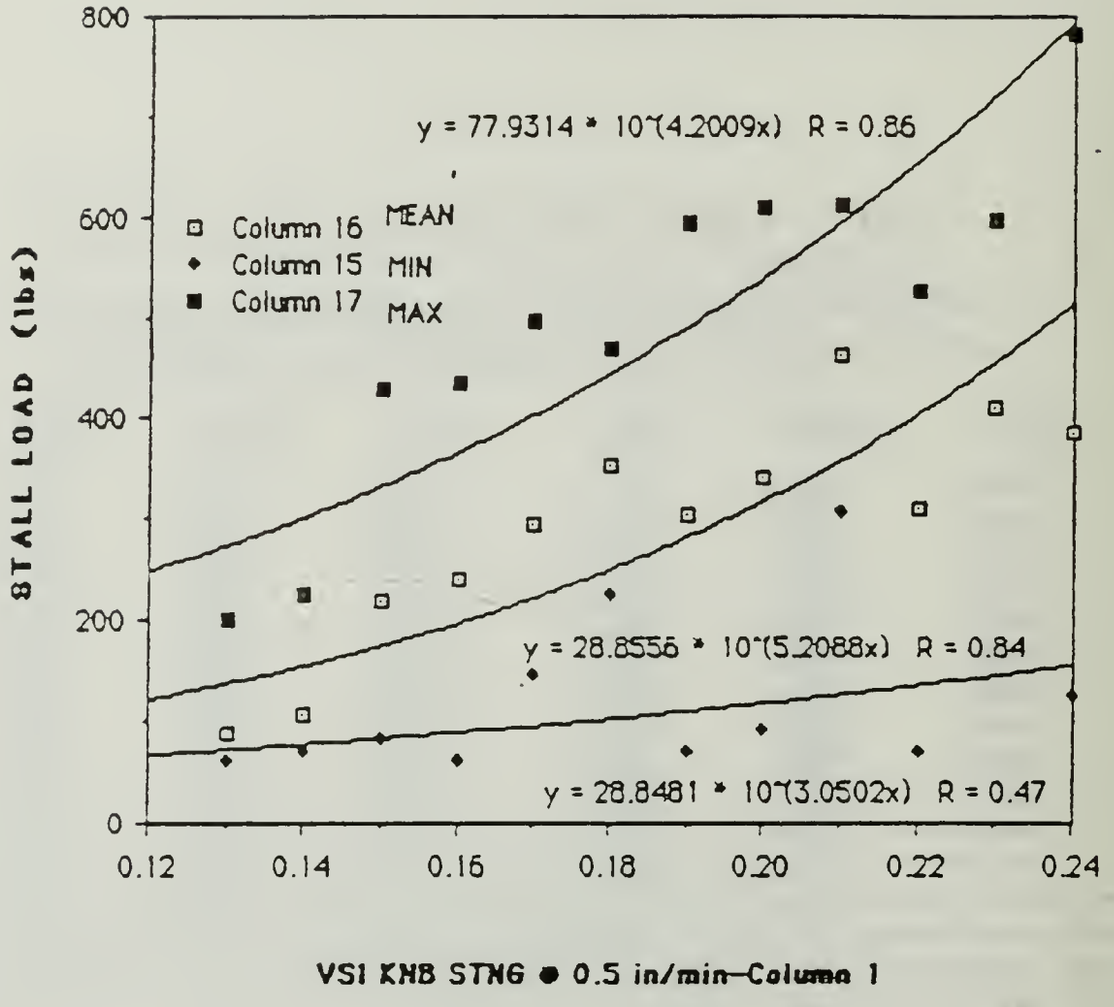

Figure 12c-1 : Response Quality of the Simulated Experiment. Relations between MIN, MEAN and MAX achieved stall load and INSTRON 1000 variable speed indicator knob setting (VSI KNB STNG).

problem. Including these postulated values in Table III-A one can come up with **Figure 12c-2** which clearly shows the decrease of the error band mentioned above.

The accuracy of the **LCD** is limited to 0.01 in and therefore displacements of lower order of magnitude cannot be correctly recorded as for example during the graphite fiber's creep. Roughly the deformation during creep is about 20% of that achieved at the end of the elastic behaviour. Knowing that the elastic deformation is of the order of magnitude of 2 %, for the gauge length of 10 inches to be used, the ultimate creep displacement would be of the order of magnitude of 0.04 in and therefore it is unlikely that the INSTRON **LCD** could record any accurate data during the creep experiment.

Another point worthy of comment is that from the simulation of the actual experiment via the helical spring, it was observed that whenever a stall load level was reached the **LCD** display appeared to decrease in time, the order of magnitude of which was estimated to be about 0.01 in / 20 sec. Hence the **LCD** display cannot be considered a reliable means of recording the fiber's creep data which is of primary importance for life testing. The reason for this decrease in the **LCD** displacement reading lies on the fact

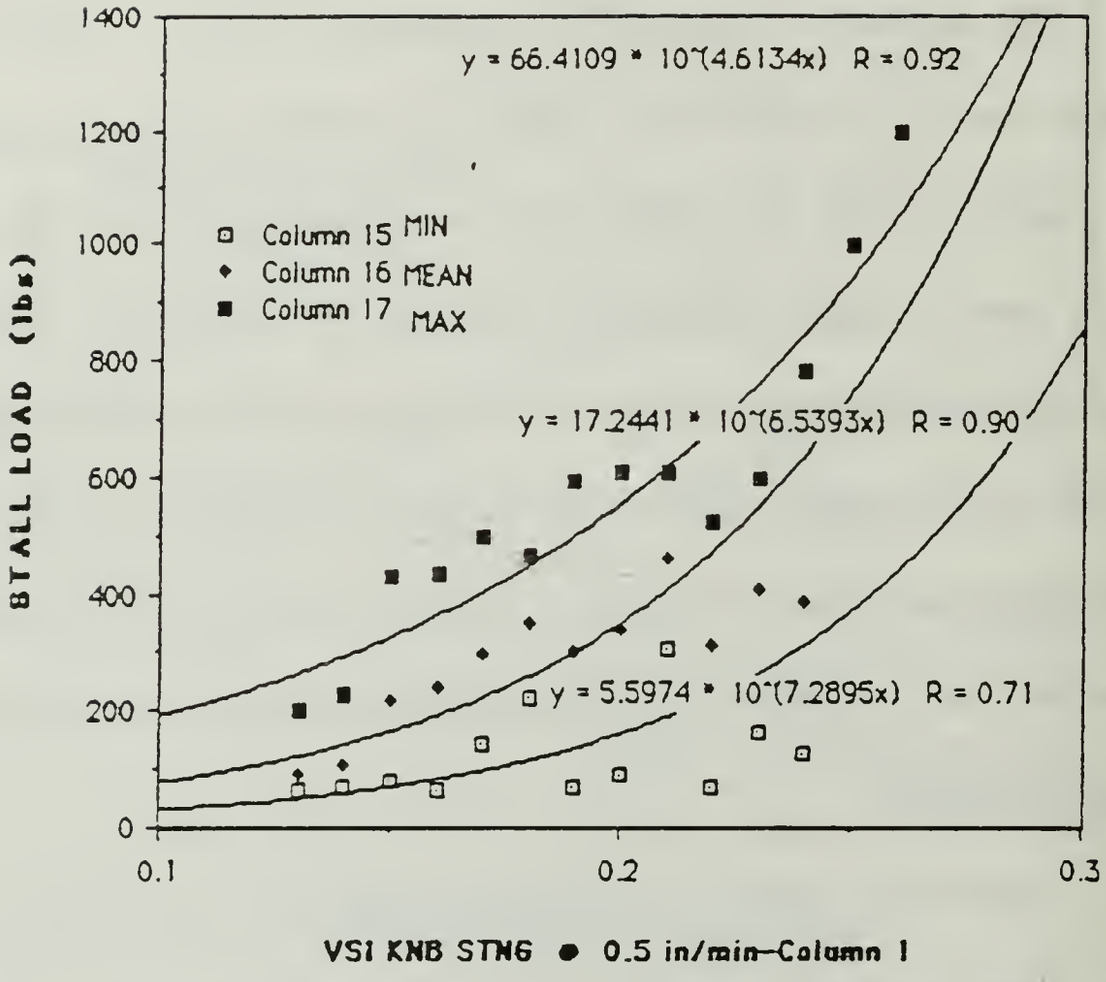

Figure 12c-2 : Response Quality of the Simulated Experiment. Convergence of stall load relations with VSI KNB STNG under theoretically extrapolated conditions.

that this reading is achieved through the Shaft Encoder (**SE**), a device that generates an output in proportion to the revolutions per minute of the Intermediate Drive Shaft (**IDS**) by which it is driven. Consequently in case of a stall, due to the internal friction, the **IDS** is not rotating, no output is generated by the **SE** and hence the decrease in the **LCD** displacement reading.

Finally summarizing the validity of these results one can rely on the INSTRON 1000 only for the loading sequence until the stall load is achieved by merely selecting **VSI** knob settings as dictated by the relatioship of Figure 12c-1, but cannot rely on the **LCD** for the creep-rupture phase and therefore other means of recording and/or displaying the displacement during the creep experiment have to be implemented. Such means is the SCHAEVITZ **LVDT** (for recording) mounted on the loading frame of the INSTRON in conjunction with a high accuracy multimeter as the available FLUKE 8440A to measure and display it's output.

B. LVDT LIMITATIONS

The bracketing technique outlined in Section III of the Appendix A under the title "Procedure" showed that the **LVDT** was totally insensitive

for an input of less than 11.0635 V. This result means that for all practical purposes the output is too low for being able to be recorded and/or displayed for an input less than the 12 V order of magnitude. On this basis the **LVDT** response was then checked at three points namely 24 V, 18 V and 12 V respectively, for the displacements of 0.02 in, 0.04 in and 0.06 inches due to the fact that during creep, the order of magnitude of the creep displacement for the graphite fiber bundles is known to be of the 0.04 order of magnitude (2 % of 20 % of 10 in).

For a positive direction of displacement (i.e 0.02, 0.04, 0.06 in) and after averaging the output of about 10 readings per case, one can come up with **Table IV-A** and observe that , the closer the input voltage (V_{in}) to the calibration value of the 24 V, the better the response and vise versa. In fact the normalized response of the LVDT at the end points of the voltage region (18V-24V) showed almost exactly the same slope, as it was anticipated and a high goodness of fit as shown in **Figures 13a** and **13b.**

For a negative direction of displacement (i.e 0.06, 0.04, 0.02) one can similarly come up with **Table IV-B** which leads to exactly a similar observation as one can see by looking at **Figures 13c** and **13d.**

TABLE IV-A

LVDT OUTPUT FOR VARIOUS INPUTS AND POSITIVE DIRECTION OF DISPLACEMENT

Column 1	Column 2	Column 3	Column 4	Column 5	Column 6	Column 7
0.02	-1.76213	-0.14684	-3.52404	-0.19578	-5.57715	-0.23238
0.04	-1.71797	-0.14316	-3.34925	-0.19218	-5.46213	-0.22759
0.06	-1.31844	-0.10987	-3.29234	-0.18291	-5.22860	-0.21786
DSPLCMNT(in) Pstv Drctn	AVR6 Vout(V) Vin = 12V	Vout / Vin Vin = 12V	AVR6 Vout(V) Vin = 18V	Vout / Vin Vin = 18V	AVR6 Vout(V) Vin = 24V	V out / Vin Vin = 24V

TABLE IV-B

LVDT OUTPUT FOR VARIOUS INPUTS AND NEGATIVE DIRECTION OF DISPLACEMENT

Column 1	Column 2	Column 3	Column 4	Column 5	Column 6	Column 7
0.06	-1.63297	-0.13608	-3.30045	-0.18336	-5.24423	-0.21851
0.04	-1.71655	-0.14305	-3.45410	-0.19189	-5.46877	-0.22787
0.02	-1.76616	-0.14718	-3.53410	-0.19634	-5.59618	-0.23317
DSPLCMNT(in) Ngtv Drctn	AVR6 Vout(V) Vin = 12V	Vout / Vin Vin = 12V	AVR6 Vout(V) Vin = 18V	Vout / Vin Vin = 18V	AVR6 Vout(V) Vin = 24V	V out / Vin Vin = 24V

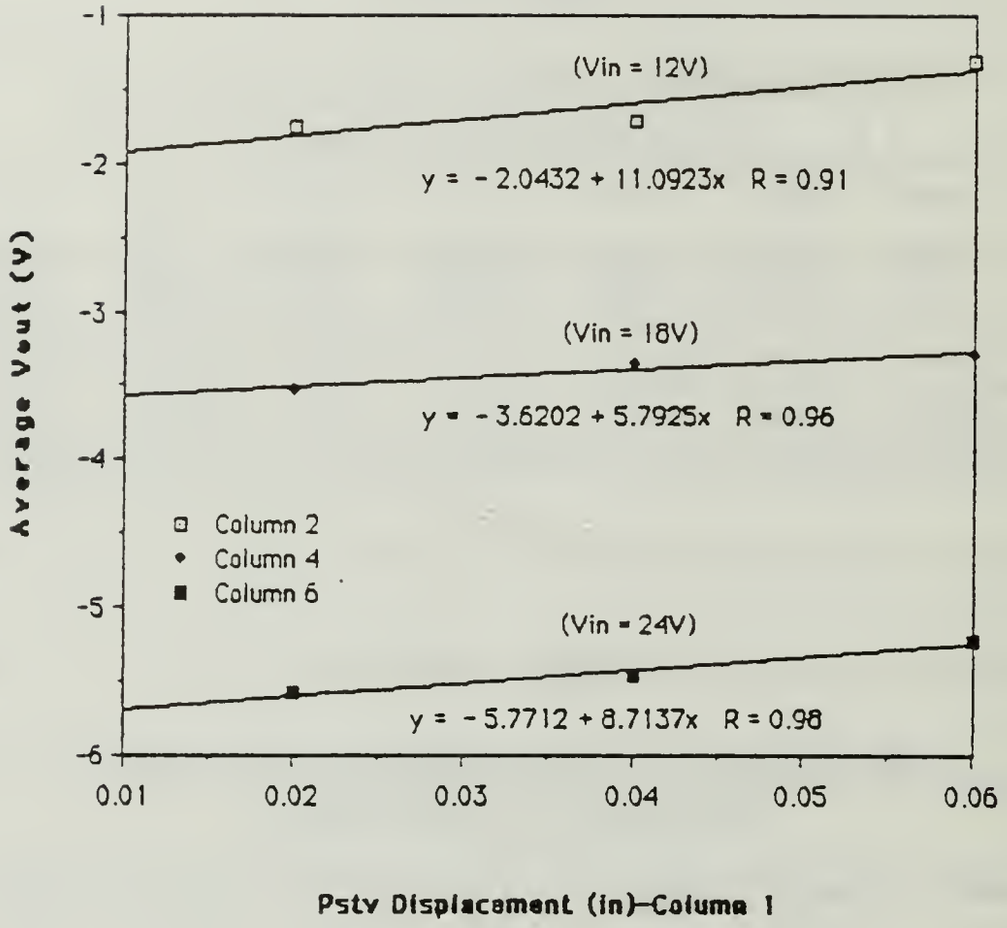

Figure 13a : Response of the LVDT for various inputs and directions of displacement. Variation of Average Vout with Positive displacement.

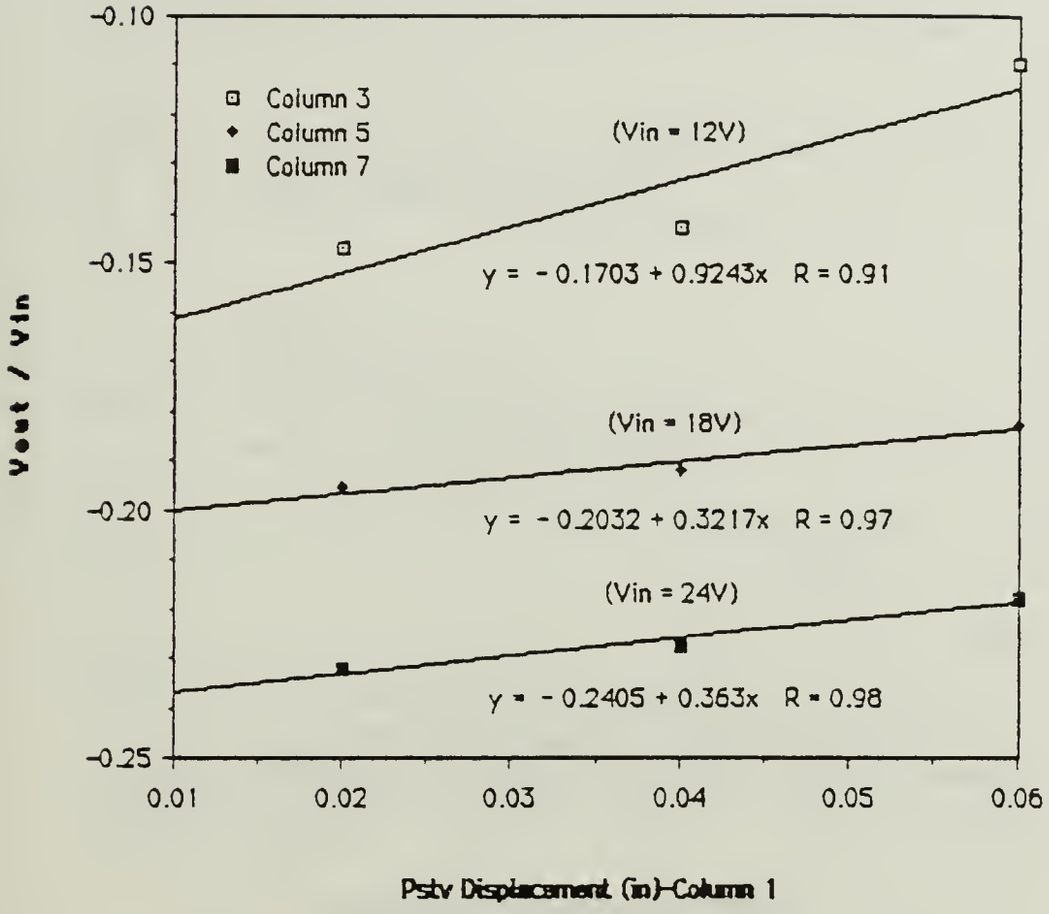

Figure 13b : Response of the LVDT for various inputs and directions of displacement. Variation of (Vout / Vin) with Positive displacement.

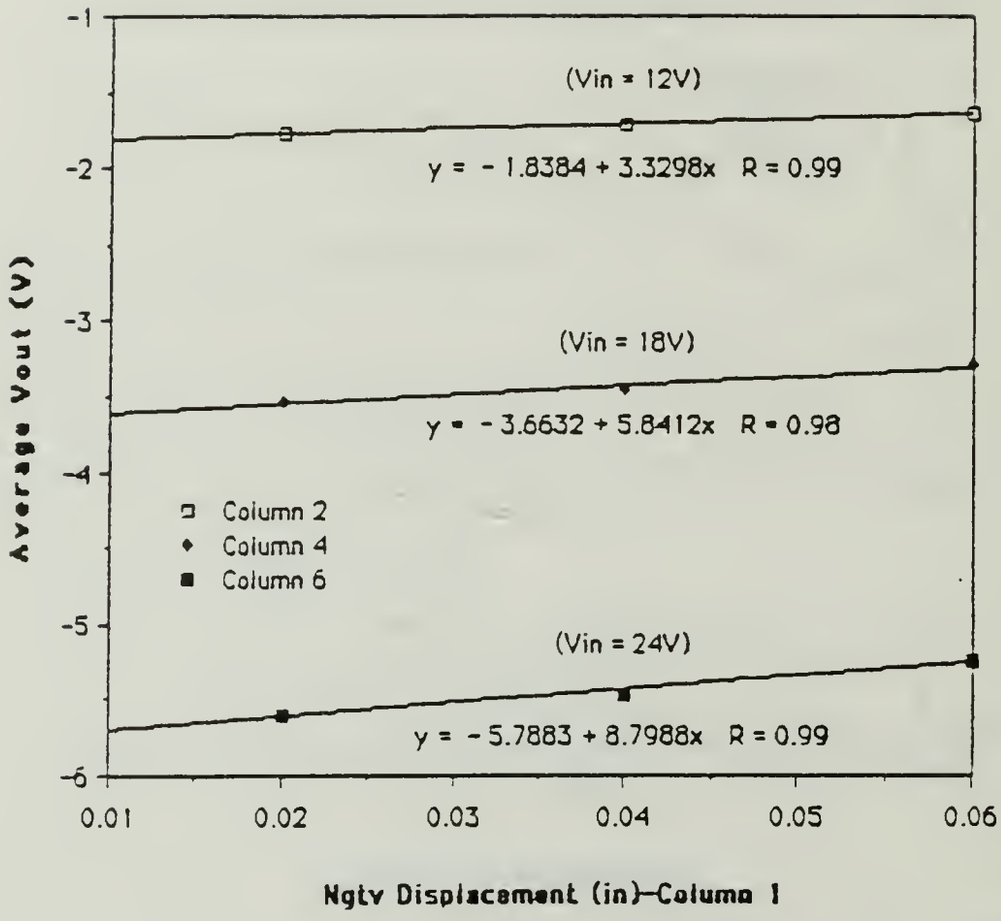

Figure 13c : Response of the LVDT for various inputs and directions of displacement. Variation of Average Vout with Negative displacement.

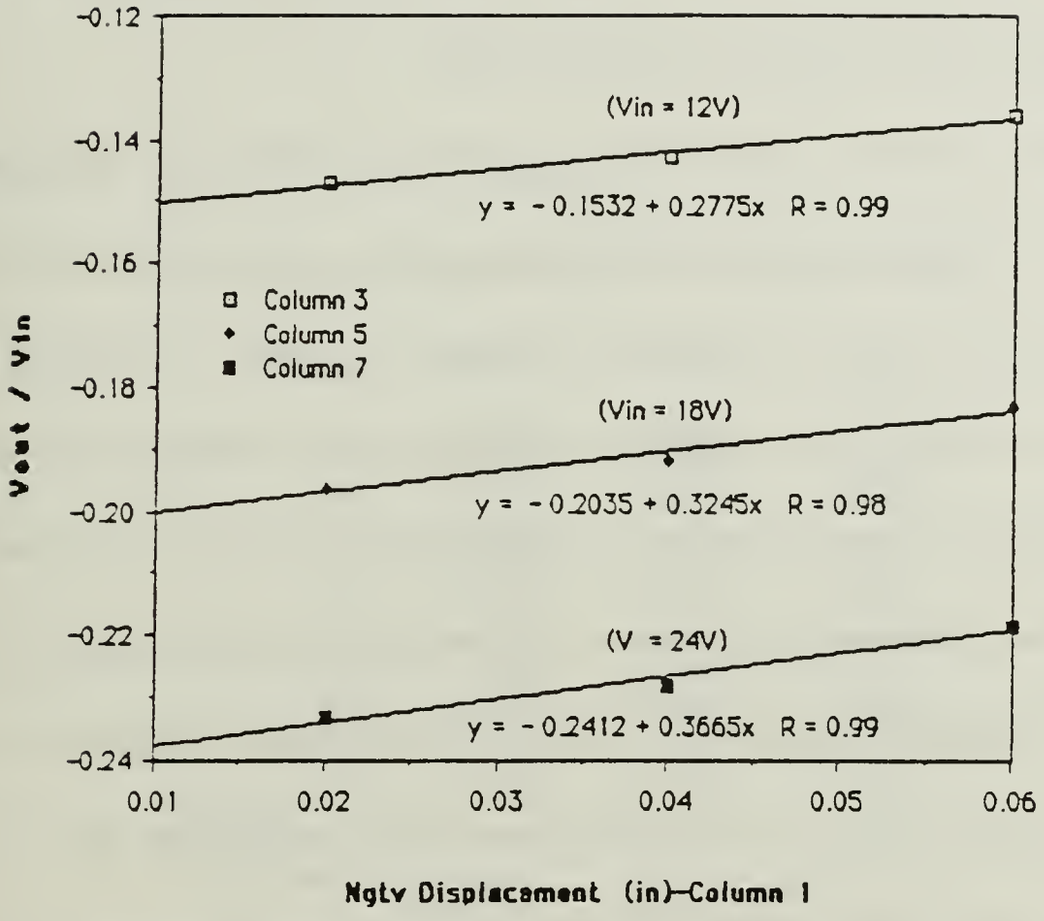

Figure 13d : Response of the LVDT for various inputs and directions of displacement. Variation of (Vout / Vin) with Negative displacement.

Furthermore by comparing Figures 13b and 13d one can see that for the voltage region (18V-24V) the difference in slope of the corresponding curves is only at the third decimal point (less than 0.5 %).

Consequently for this region the **LVDT** response is almost independent of the direction of displacement.

The stability of the LVDT in time was checked by recording its' output at a step inteval of 5 seconds for about 1 hour at the input voltage check points of 12v, 18V and 24V as shown in **Table V**. Plotting of the results in **Figures 14a, 14b** and **14c** shows that although the output is pretty stable with time prior to its' stabilization overshoots for a period of 10 to 20 seconds depending on the input voltage used (the lower the input voltage the longer the overshoot) and finally stabilizes rather quickly under a damped oscillation. It is believed that this is the reason that the data recorded during the initial run of the experiment showed that the cross-head moved up and down. Furthermore the reason that a polarity check did not reveal any faults, is that the amplitude of the oscillation is very small (0.0001V) compared to the output of the LVDT which is of the order of several volts.

The check of the time dependence was made possible by monitoring the output of the **LVDT** in the neighborhood of 1 hour, 10 hours and 15 hours

TABLE V

TYPICAL LVDT TIME RESPONSE FOR VARIOUS INPUTS

Column 1	Column 2	Column 3	Column 4
0	-1.72075	-3.47150	-5.46130
5	-1.71997	-3.44820	-5.46330
10	-1.71879	-3.45970	-5.46180
15	-1.72059	-3.45760	-5.46180
20	-1.71967	-3.45760	-5.46180
25	-1.71824	-3.45760	-5.46180
30	-1.72016	-3.45760	-5.46180
35	-1.71930	-3.45760	-5.46180
40	-1.71788	-3.45760	-5.46180
45	-1.71135	-3.45760	-5.46180
50	-1.71099	-3.45760	-5.46180
TIME (sec)	Vout (V) @ Vin = 12V	Vout (V) @ Vin = 18V	Vout (V) @ Vin = 24V

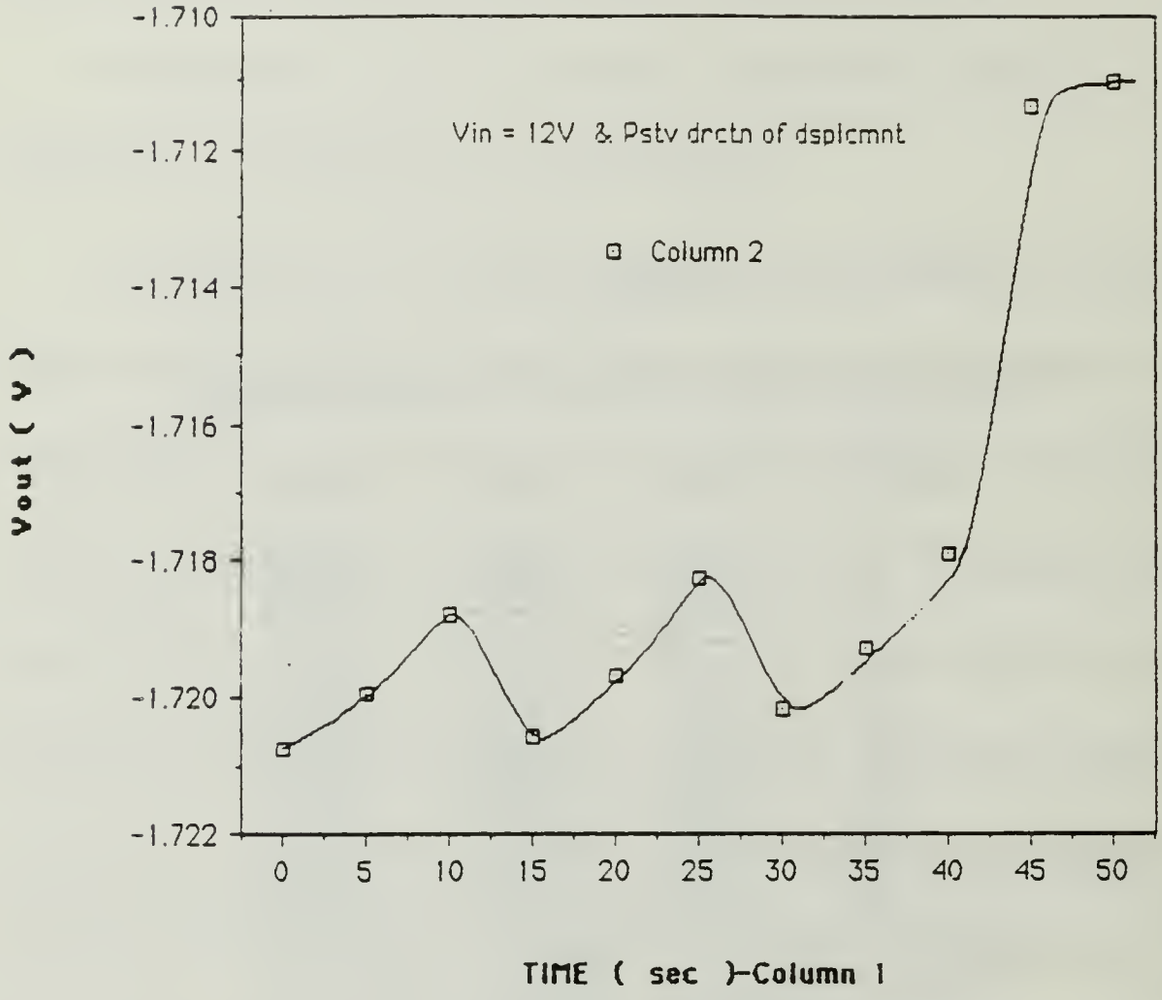

Figure 14a : Time response of the LVDT for Vin = 12V.

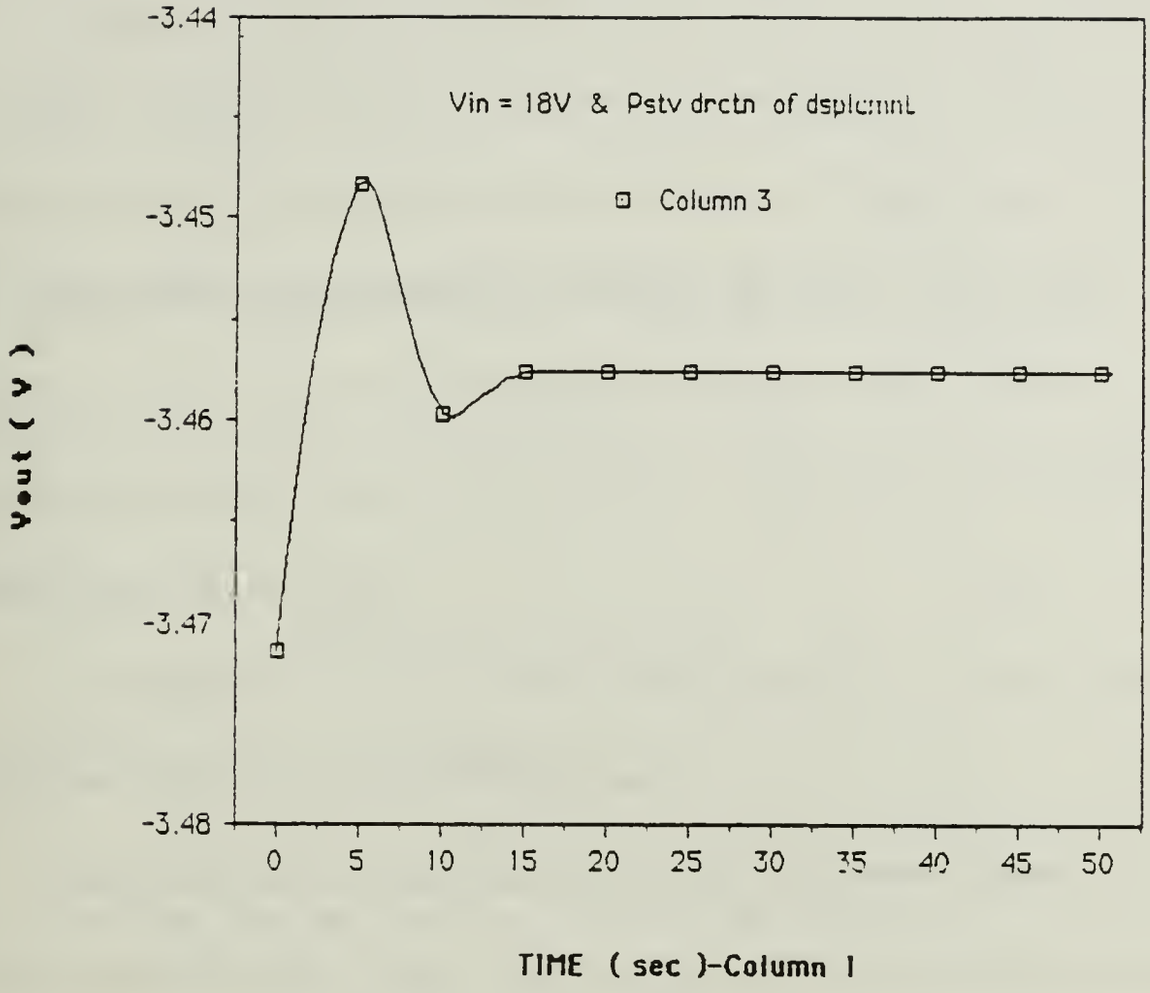

Figure 14b : Time response of the LVDT for Vin = 18V.

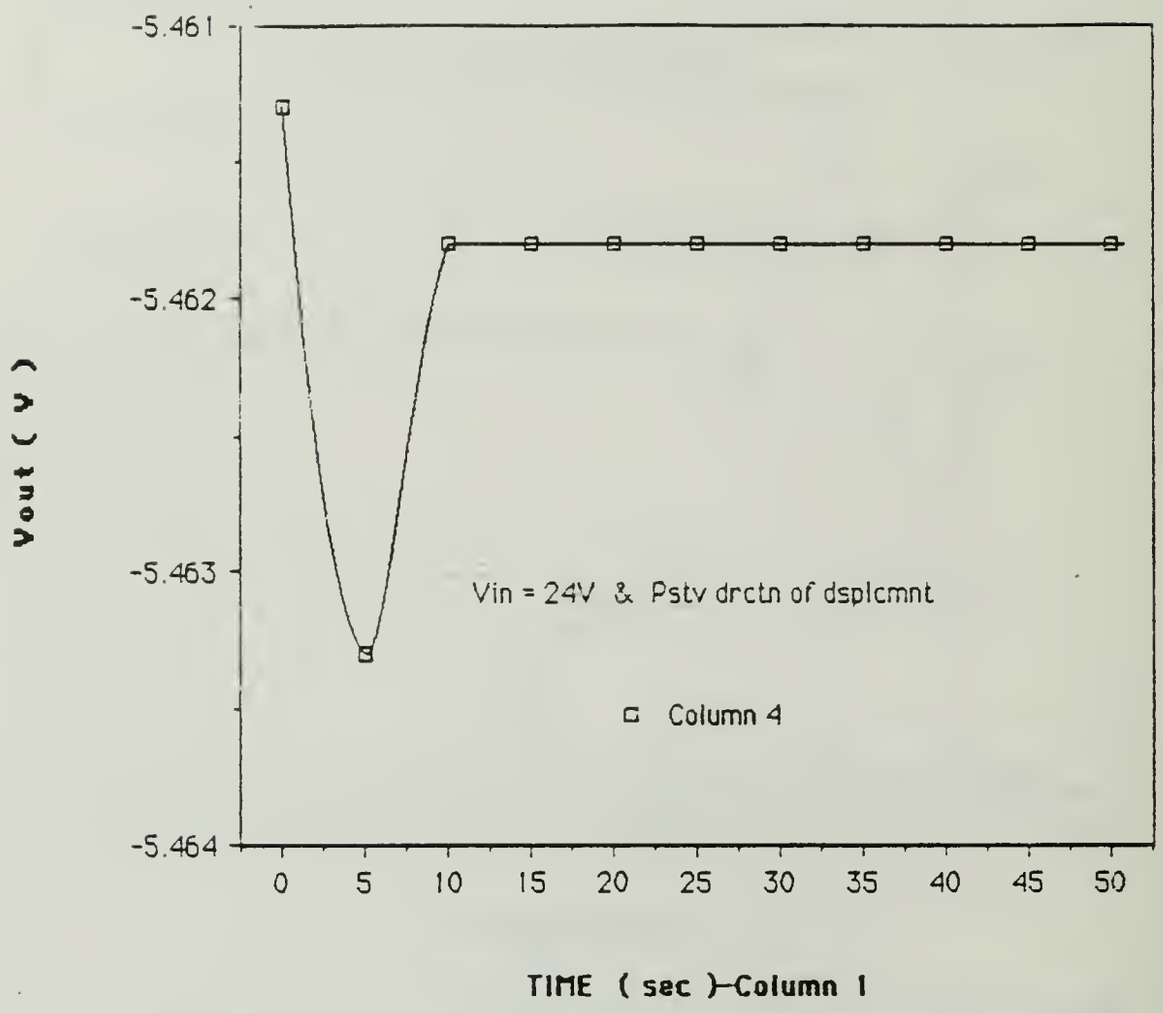

Figure 14c : Time response of the LVDT for Vin = 24V.

for the same displacements of 0.02, 0.04 and 0.06 inch in both directions and for the same input voltage check points (12V, 18V and 24 V). The results are presented in **Tables V-A** and **V-B** and when plotted as in **Figures 15a** and **15b** showed that the minimum time dependance (less than 10^{-4} relative errror) is achieved for both directions of displacement at 24V and at about 0.04 in displacement. Although negligible (less than $2x10^{-3}$ relative error) the time dependance at 18V was almost constant with a shallow minimum at about 0.03-0.055 in, whereas no minimum point was identified in the 12V case.

Consequently for the entire voltage region (12V -24V) the **LVDT** response shows negligible time dependence.

Since the area of interest as far as the creep is concerned is the region between 0.020 in and 0.025 inches, drifting in time does not seem to be a serious problem for any input voltage within the above specified region; however a slight dependence can be observed in the lower half of this voltage region and hence it is prudent to use the 24V input voltage for the **LVDT**s that are going to be used.

TABLE V-A

LVDT RELATIVE ERROR FOR VARIOUS INPUTS AND POSITIVE DIRECTION OF DISPLACEMENT

Column 1	Column 2	Column 3	Column 4
0.02	0.00003●	0.00128●	0.00154●
0.04	0.00081●	0.00129●	0.00002•
0.06	0.00132●	0.00141●	0.00159•
DSPLCMNT(in) Pstv Drctn	DVout / Vin Vin = 12V	DVout / Vin Vin = 18V	DVout / Vin Vin = 24V
CODES :	● : 1hr		• :10hrs

TABLE V-B

LVDT RELATIVE ERROR FOR VARIOUS INPUTS AND NEGATIVE DIRECTION OF DISPLACEMENT

Column 1	Column 2	Column 3	Column 4
0.06	0.00029*	0.00105●	0.00164●
0.04	0.00051●	0.00111•	0.00007●
0.02	0.00003●	0.00146●	0.00157●
DSPLCMNT(in) Ngtv Drctn	DVout / Vin Vin = 12V	DVout / Vin Vin = 18V	DVout / Vin Vin = 24V
CODES :	* :15 hrs	• :10hrs	● : 1hr

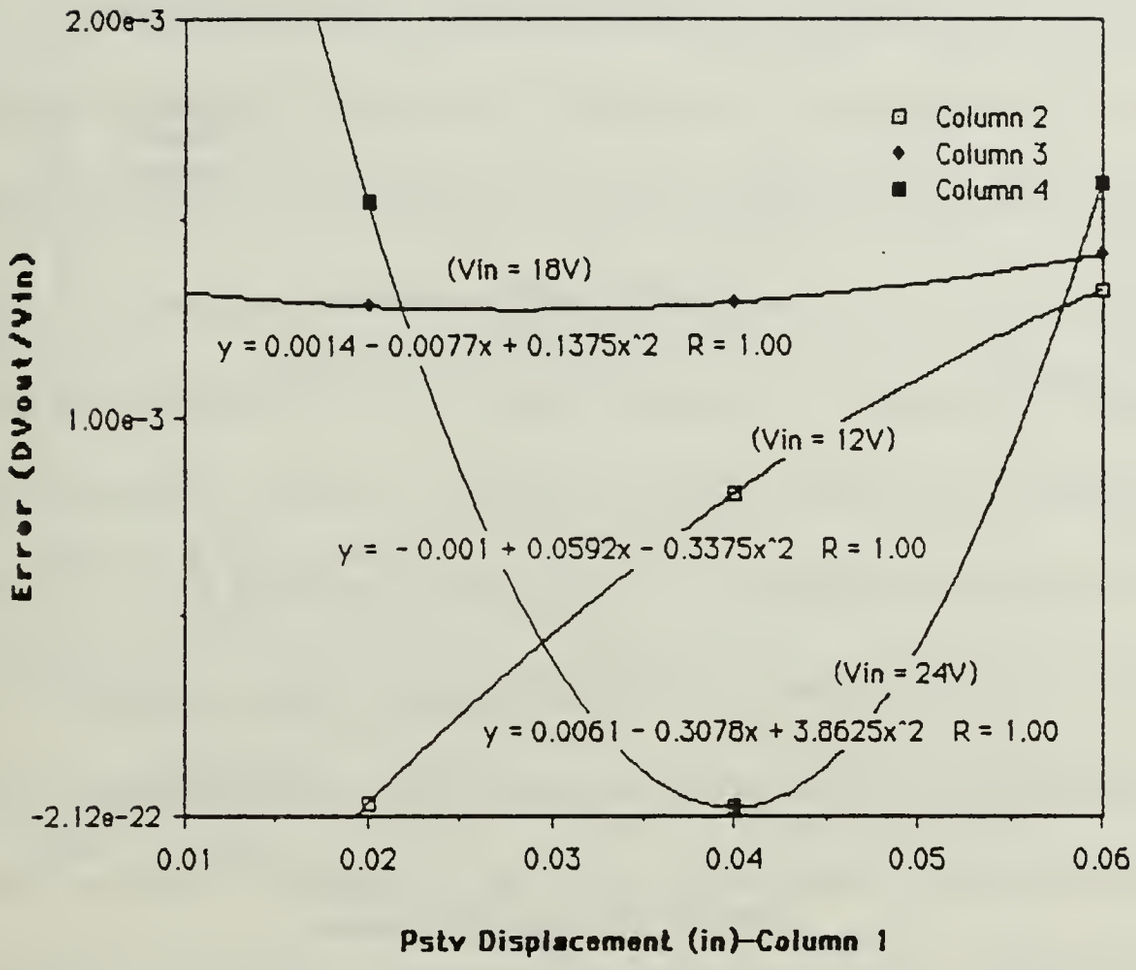

Figure 15a : LVDT relative error for various inputs and Positive direction of displacement.

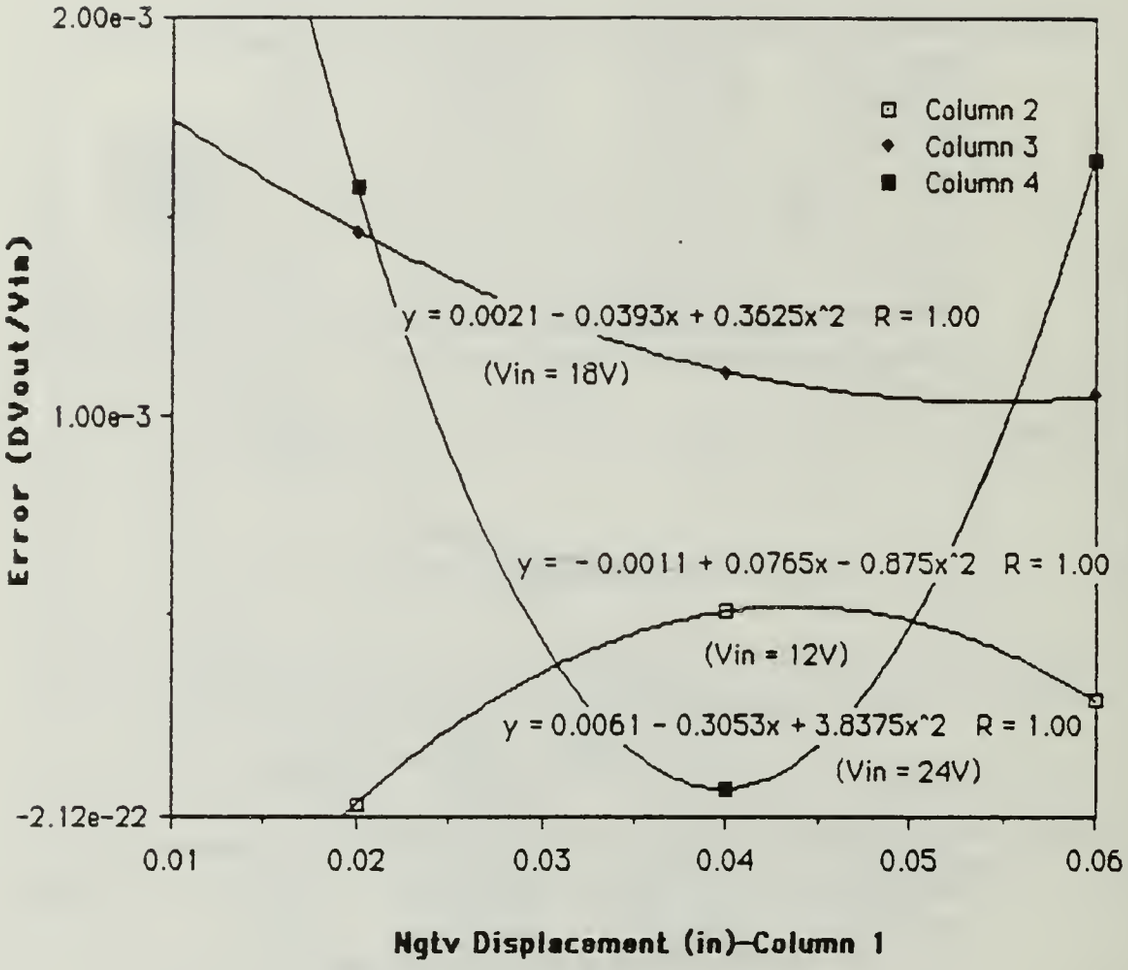

Figure 15b : LVDT relative error for various inputs and Negative direction of displacement.

V. CONCLUSIONS- RECOMMENDATIONS

In identifying the characterization methodology for efficient strength to life data generation by testing fiber bundles (each may consist of ten thousand (10^4) filaments) it was made clear that in order for one to arrive to meaningfull statistical data, ***long*** periods of time and a very ***efficient*** data acquisition system is required. The high efficiency of the data acquisition system is primarily needed during the loading phase because the life prediction is based on the ***conditional probability*** that no failures have occurred during the loading sequence and this probability can be calculated only if the number of failures that occured during the loading sequence is known; in the stress rupture phase, the more accurately the number of failures is recorded the better the results. Furthermore the data accuracy during the loading sequence is what gives rise to an accurate ***lower tail*** of the Weibull life distribution which is cruisial in safe life prediction calculations.

The data accuracy during the loading sequence are influenced by the limitations of the testing equipment and the data acquisition system.

The limitations of the testing equipment were examined by a mechanical spring simulation and it was found that in order to avoid irregular indications during the loading sequence caused by the stall of the equipment due to internal friction, the data base of Table III-A and/or Figure 12c-1 have to be used whereas for the 450 lbs load level of interest (simoultaneous testing of nine (9) graphite bundles Hercules AS4 including the control bundle) the cross-head speed setting has to be higher than 0.5 in /min level with the variable speed indicator at 21%.

The limitations of the testing equipment during the creep-rupture phase were also examined by simulation and it was found that indeed the LVDT output is very small. More specifically, for the recommended excitation voltage of the 24V where the time dependence errors are almost inexistent a creep displacement of 0. 0001 inch corresponds to a difference in output slightly less than 0.001V which dictates that the five digits resolution mode has to be used by the data acquisition system. The reason that the data recorded during the initial run of the experiment was considered unreliable (in that it showed that the cross-head moved up and down, whereas only upward displacement is theoretically expected from monotonic creep) lies on the fact that even though the LVDT output is

stable with time, prior to the composite sample stabilization, it overshoots and stabilizes rather quickly (within a few minutes) under a damped oscillation. This oscillation is relatively small (of the 0.0001V order of magnitude) compared to the LVDT output which is of the order of several volts.

The data acquisition system used is not capable of recording data at a rate faster than 0.04 readings/sec. According to the available literature this result appears to be within the design constraints of the instruments since an interface loop involving only the HP-41CX calculator and the HP-3421A DACU can barely give 1 reading/sec. It is therefore obvious why the recording rate decreases substantially when the cassette drive and the thermal printer are also included in the loop, given that they are considered slow units in the first place. On the other hand the data logger routine used had been modified to record data at hundredths of seconds that is 50 times faster than the theoretical capability of the data acquisition unit itself. Finally due to the limitations of the HP-41CX calculator the advanced commands could not be used (AUTOZERO OFF, AUTORANGING, etc.) which can also substantially increase the recording rate. Under the above circumstances it is recommended to substitute the existing data acquisition

system with a simpler one composed of the the HP-3421A DACU and the HP-85 desk top computer at least during the loading sequence. The obvious advantages of such a system which can give a reading rate per second as fast as 3, 9 or 11 (for 5, 4 or 3 digits of resolution repectively) are:

1. No other peripherals that might limit the recording rates will have to be connected since the HP-85 has its own printer and cassette drive.

2. More programming flexibility will be available through the use of the advanced commands.

3. Substantial difference in memory capacity (319 vs16K).

4. During the loading sequence there is no need to record the LVDT output due to the relative rapid changes, a fact which saves one channel and at the same time provides the opportunity to use the three digits of resolution mode (N3) which can more than triple the recording rate.

APPENDIX A

I. INSTRON 1000 DESCRIPTION-OPERATING PRINCIPLES

A. GENERAL

The INSTRON model 1000 Universal Testing Instrument shown in **Figure A-1** is set to accept a main power input of 120 ±10 VAC, single phase, 50-60 Hz and by means of it's own power transformer, the necessary AC voltages are provided to the various systems of the equipment.

All the major units of the instrument as well as their sub-units are described with respect to Figure A-1 by an item number given in parenthesis next to the unit under description.

B. MAJOR UNITS

These can be thought of being the loading frame (1), the drive train assembly and the control console (19).

1. Loading Frame

This is the part of the equipment where the test specimens are mounted and the loading (tension or compression) is applied.

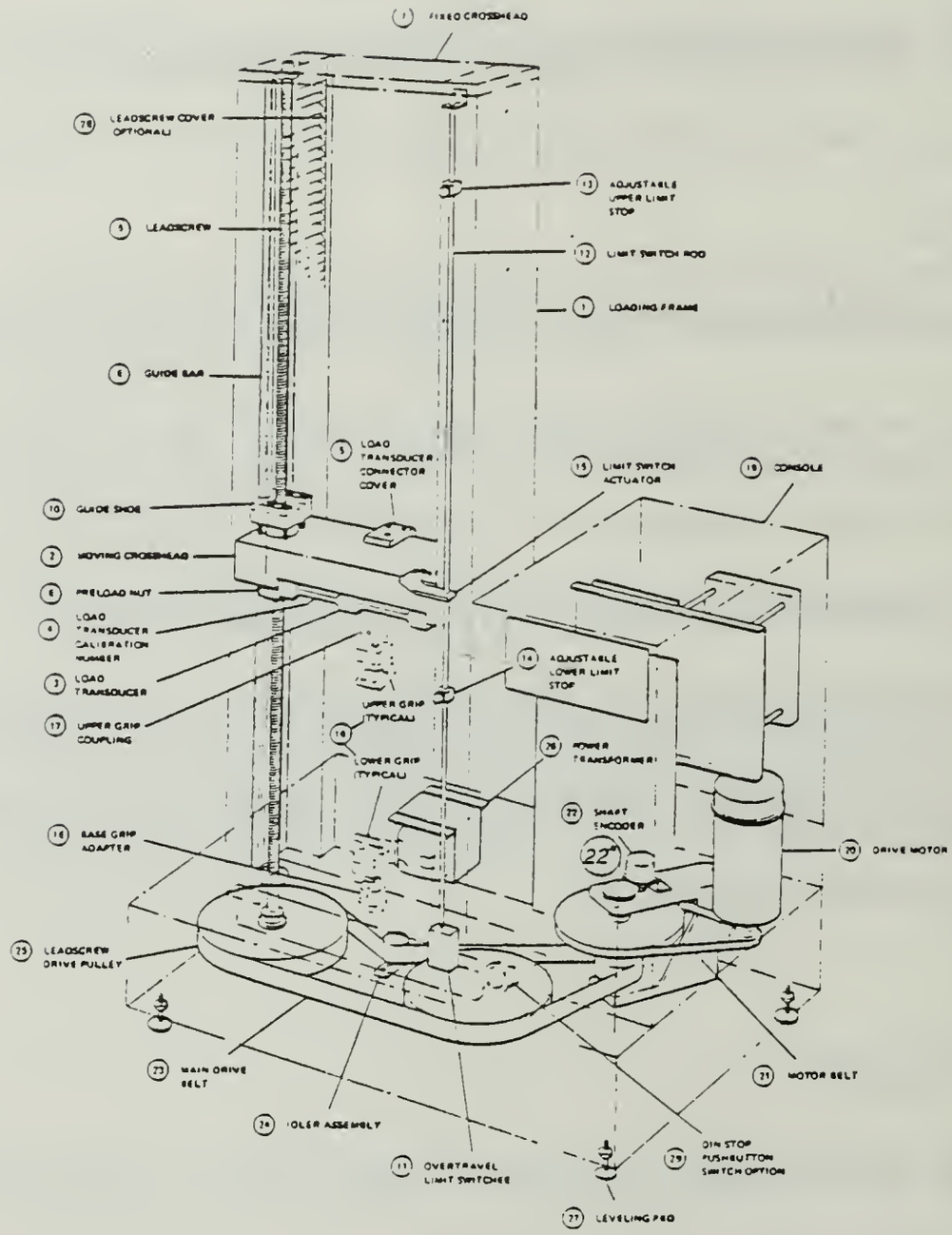

Figure A-1 : Major Units and sub units of the testing Equipment.

2. Drive Train

This is a series of several units the prime function of each one can be described as follows:

a. Drive Motor (20)
It's rotary motion is transfered to an intermediate drive shaft by means of a motor belt (21).

b. Intermediate Shaft (22*)
Its rotary motion is in turn transfered to the leadscrew drive pulleys (25) by means of the main drive belt (23).

c. Leadscrew Drive Pulleys (25)
These are rotated by the main drive belt (23) and are nechanically connected to the leadscrews (6).

d. Leadscrews (6)
These are threaded rods which are at the top supported by the fixed cross-head structure (7) and can turn the moving cross-head (2) at commanded speeds.

e. Moving Cross-Head (2)
This is the element within the loading frame (1), that applies the loads to the test specimen at commanded speeds.

3. Control Console

This part of the equipment serves as a housing for the controls and the indicator systems (19). A detailed view of it's front and rear panel is presented in **Figure A-2**.

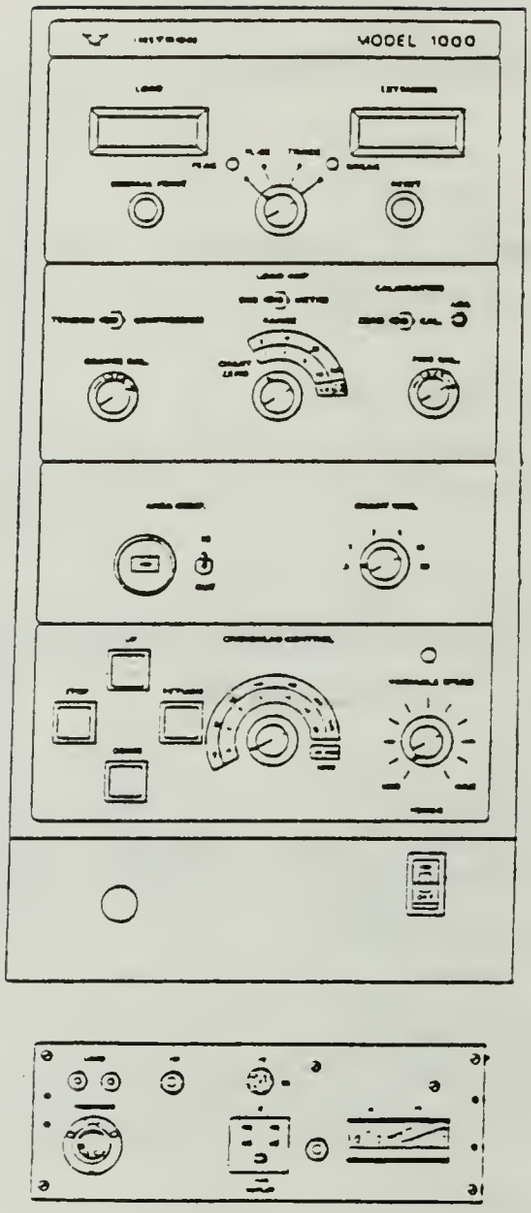

Figure A-2 : Front and rear Control Panels of the testing Equipment.

C. OTHER IMPORTANT FEATURES

Among the important features of the INSTRON 1000 which are described in full detail in the manual of the equipment [Ref. 14], the following two need to be generally described:

1. Overtravel-Limiters System

The purpose of this system is to protect the Load Transducer (**LT**, 3) from overload by stopping the moving cross-head (2). This is achieved in the following sequence:

a. Setting the adjustable upper and lower limit stops (13,14) in appropriate positions on the limit switch rod (12).

b. Activating the overtravel limit switches (11) after the limit switch actuator (15) which is mounted on the moving cross-head, gets in touch with either one of the adjustable stops.

2. IMC Digital Processor/Controller model 700 (**IMC DP/C**)

The purpose of this feature shown in **Figure A-3** is associated with the upgrading of the INSTRON 1000 so that testing of viscoelastic materials could also be possible. More specifically this unit is capable to create a constant stress level in time, using the applied load as the control variable which is of prime importance during the creep. This is achieved by the following sequence:

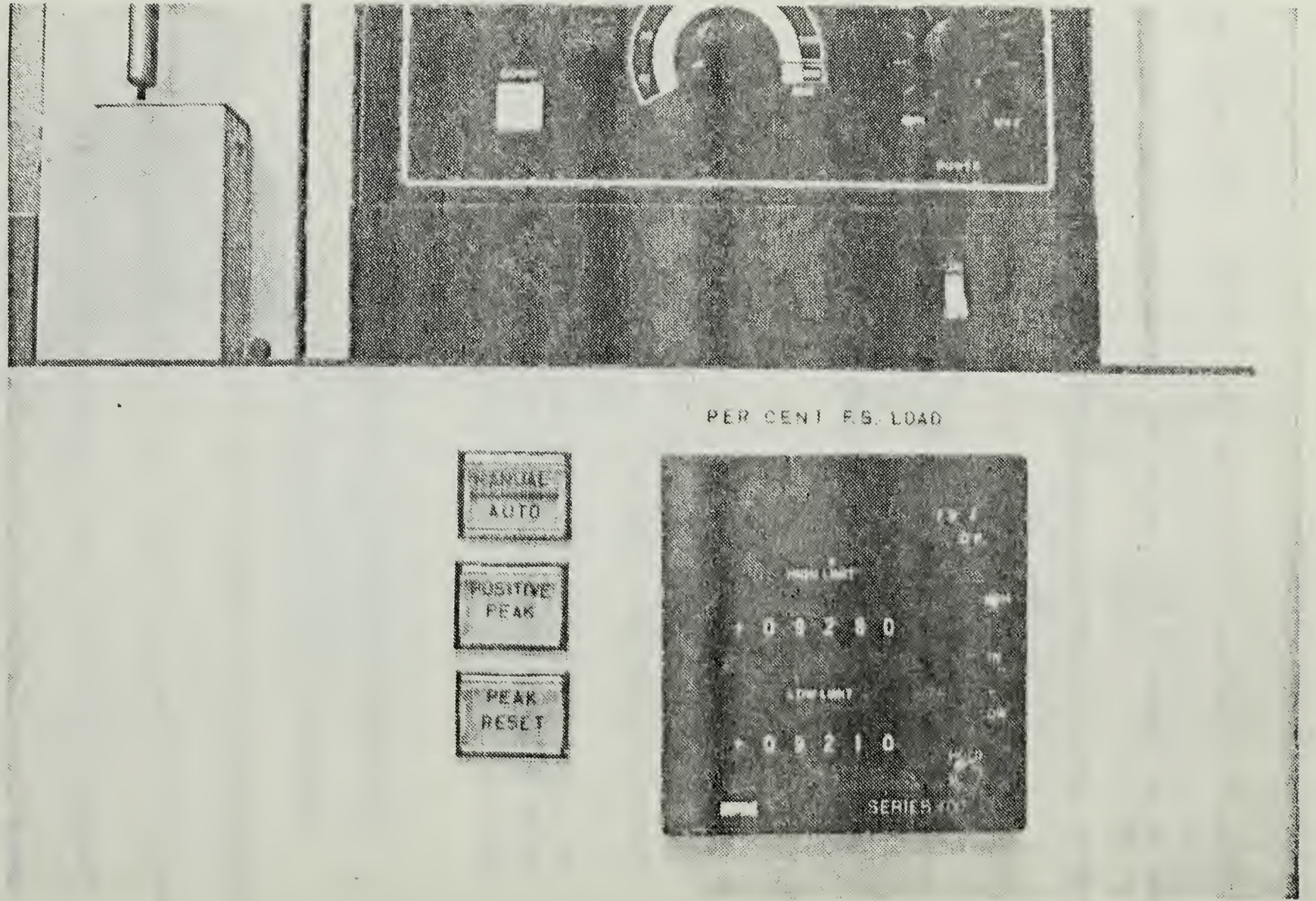

Figure A-3 : IMC Digital Processor/Controller feature.

a. Setting the desired maximum and minimum load levels on the face of the **IMC DP/C** defining thus the permissible band of the load variation.

b. Activating the automatic mode by selecting the appropriate button on the face of the **IMC DP/C** which allows the moving cross-head to move under its control to the desired maximum setting and then continually adjust to correct for the effects of the creep, within the range setting of the previous step.

D. FUNCTIONS

1. Load Measurement

The load measurement is achieved by means of a calibrated Load Transducer (LT, 3) that has to be installed into the moving cross-head. There are three options in calibrated **LT**s (10, 100 and 1000 lbs) dependent on the anticipated load level. The input of the transducer is transformed to an electrical signal by means of a LINEAR VARIABLE DIFFERENTIAL TRANSFORMER (**LVDT**). This is a sensitive device that can measure minute deflections of the load transducer in the load weighting system and is composed of two major elements shown in **Figure A-4**:

a. The **LVDT** coil assembly (2*) and

b. The **LVDT** core assembly (4*).

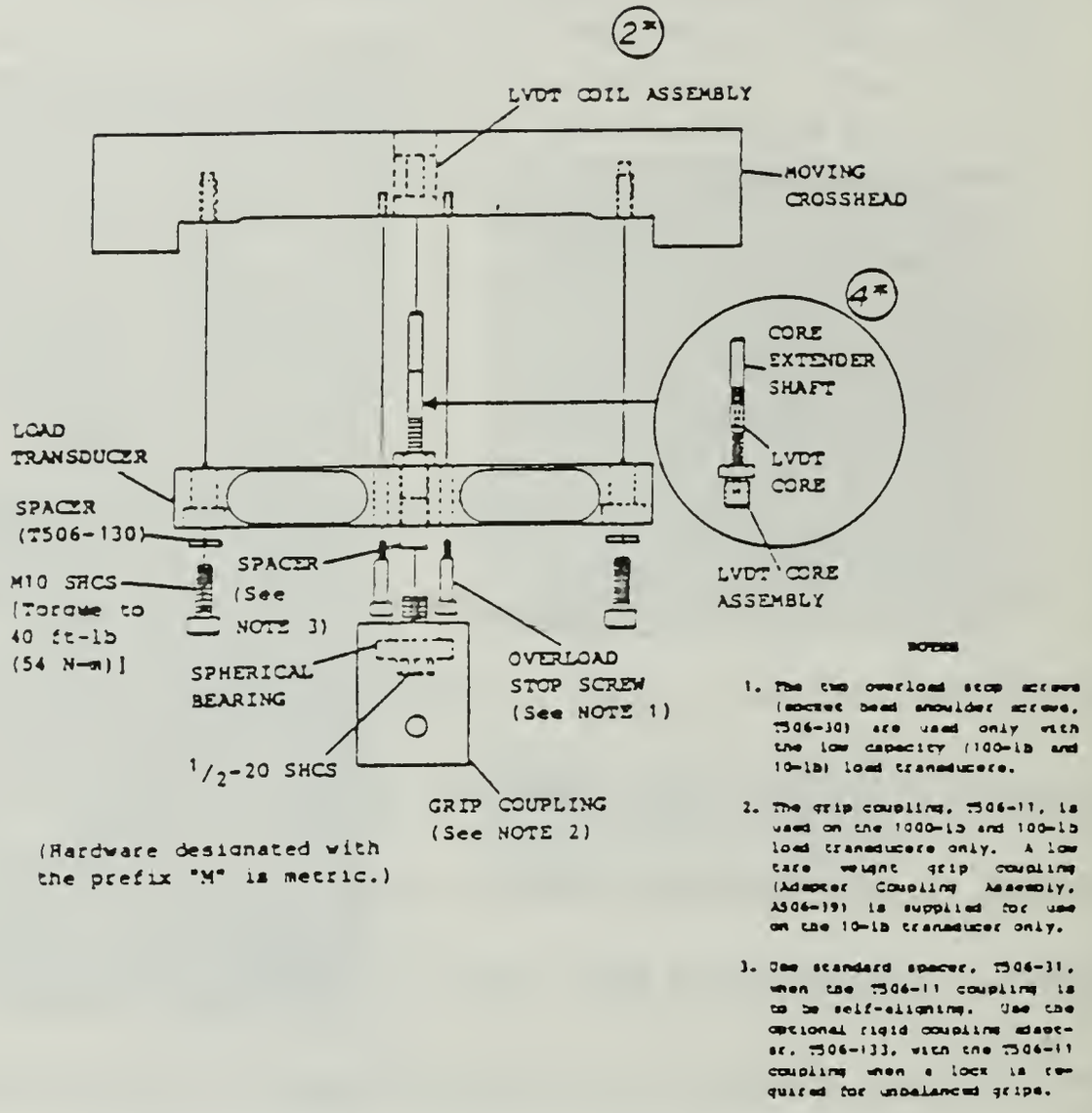

Figure A-4 : LVDT coil and core assemblies.

It's transformed electrical signal is finally digitally displayed to a Liquid Crystal Display (**LCD**) panel located at the upper right corner of the front side of the console, at a frequency dependent on the commanded cross head speed.

2. Extension Measurement

The extension measurement of the moving cross-head is achieved by utilizing a SHAFT ENCODER (**SE**, 22), a device which generates an output in proportion to the revolutions per minute of the intermediate shaft (**IS**, 22*) by which it is driven. This output is an incremental measure of the displacement of the moving cross-head and it is also used as a feedback to maintain the commanded speed. The defficiency of the extension measurement system lies on the fact that no output can be generated by the **SE** in any case case the equipment could not overcome its own internal friction as in a case of a partial or total stall.

3. Creep Monitoring

This function is achieved via the enhancement feature of the **IMC DP/C** which is capable of creating a constant stress level in time using the applied load as the control variable. Thus, by setting the desired band of load variation the moving cross head moves under the **IMC DP/C** control by continually adjusting to the effects of the creep.

II. INSTRON 1000 LIMITATIONS

A. OBJECTIVES

The objectives with respect to the INSTRON 1000 limitations were:

1. To evaluate the minimum speed that the INSTRON can be operated without stalling.

2. To convert this speed to a combination of the INSTRON labeled controls.

3. To check whether this speed is load dependent or in otherwords given a physically verified speed check whether one is able to predict the corresponding stall load.

4. To find out any other limitations that will become apparent during the simulation experiment.

B. THEORETICAL MODEL

A practical way to present a relationship between a load level (**p**) and the equipment cross-head speed (**v**), is to follow the simple relations presented below where **t** represents time and **l** a physically measured displacement:

(A-1) $$(p/t)*(1/p) = 1/t$$

(A-2) $$1/t = v$$

(A-3) $$p = v*[1/(1/p)]*t$$

Given that the ratio (**1/p**) can be thought of representing the elastic constant of a linear model one could anticipate the following results:

1. The functions of **l = f(t)** and **p = f(t)** to be single valued and monotonically increasing.

2. As load increases the displacement and time intervals have to show a tendency to decrease.

C. MECHANICAL SET-UP

A helical spring as the one shown in **Figure A-5** was decided to be used for the simulation experiment provided that both the cross-head speed (**v**) and the time (**t**) could be easily recorded, because it was cosidered the best solution from the safety standpoint.

Under the requirements of comforming with the necessary safety precautions for the operator and the equipment limitations, the mechanical set-up shown in **Figures A-6** and **A 7** was designed which provided the capability of easily achieving the target load level of the 450 lbs order of

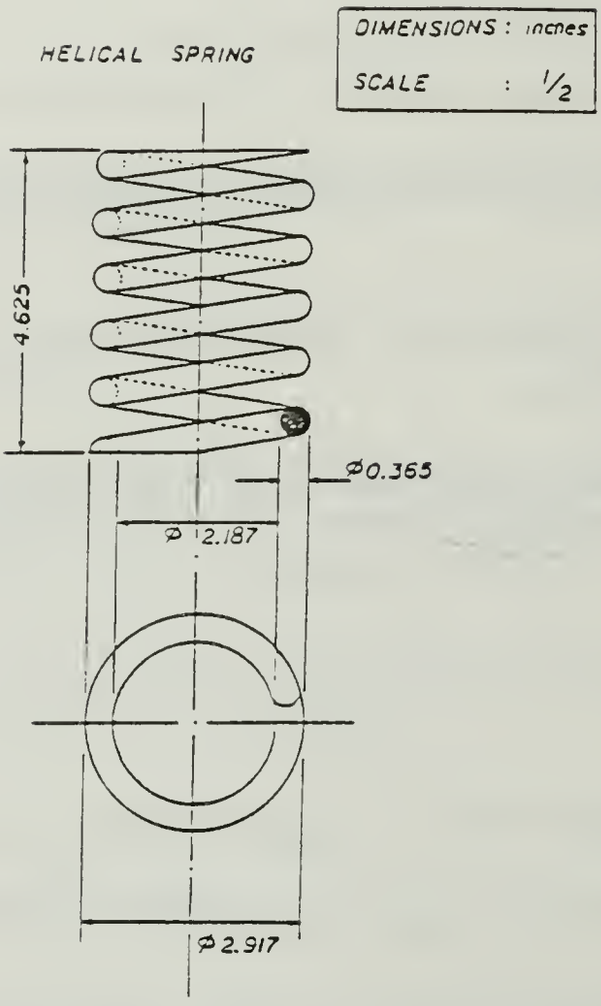

Figure A-5 : Helical Spring employed for the Simulation.

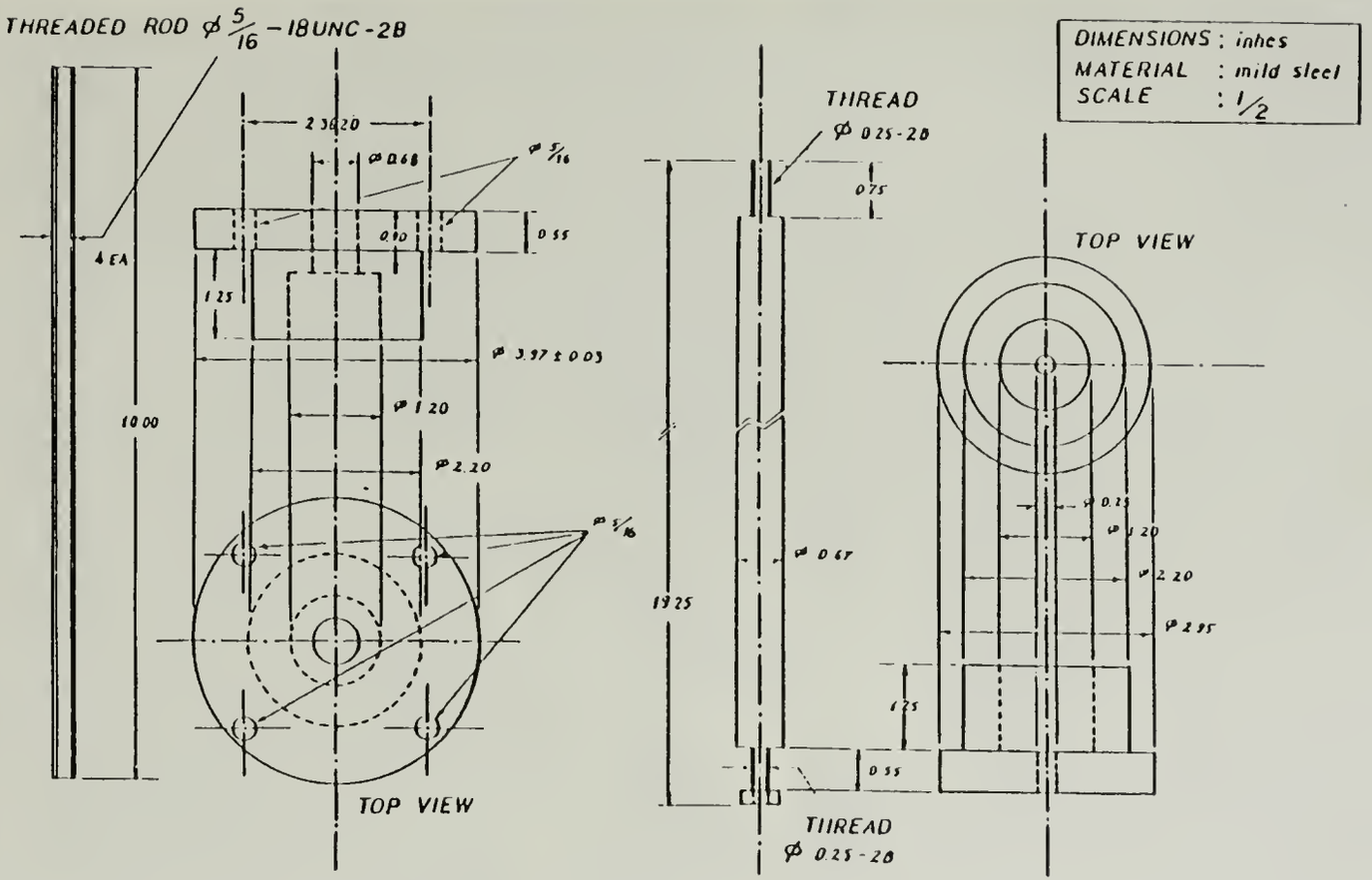

MECHANICAL SET UP PARTS FOR SIMULATION

Figure A-6 : Mechanical Set-Up components designed for the Simulation.

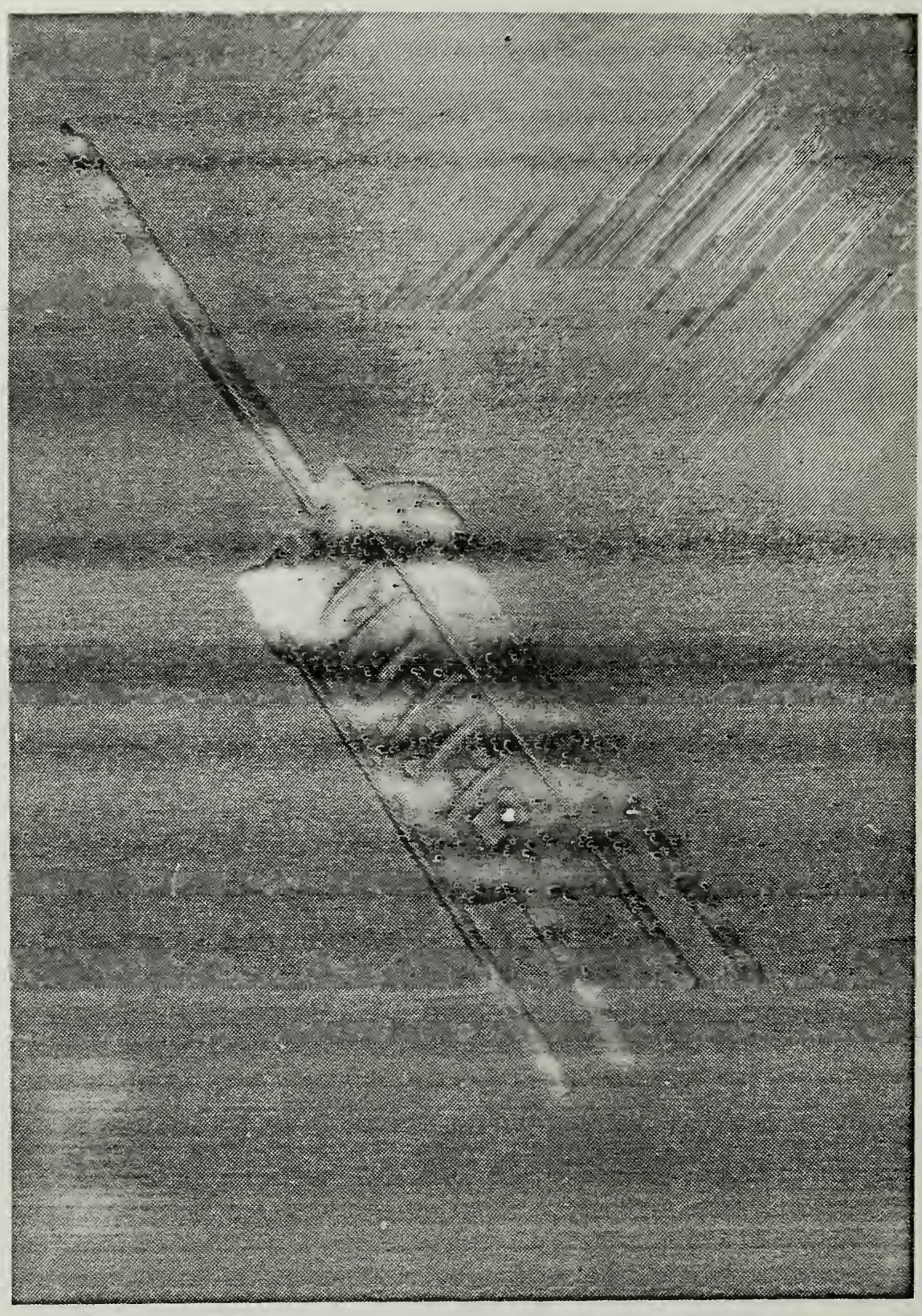

Figure A-7 : Assembled components for the Simulation.

magnitude. On the other hand since one could not rely on the INSTRON cross-head control knob markings for the evaluation of (**v**) due to inherent limitations of the equipment [Ref. 14] and therefore a dial indicator (**DIAL**) capable to measure displacement in 0.001 of an inch (ten times better resolution than that of the **LCD** meter) was also used during the simulation procedure as shown in **Figure A-8**.

The overall mechanical set-up for the simulation of the loading sequence is shown in **Figure A-9**.

D. METHODOLOGY

The methodology followed consisted basically of:

1. Evaluating the quality of the response as outlined in steps B.1 and B.2 above.

2. Determining the lower threshold speed that the INSTRON could be operated without producing irrelevant indications and the stall load corresponding to each one of the selected speeds, using the method of bracketing between selected upper and lower bounds.

3. Observing the quality of agreement between the **DIAL** indicator utilized and the **LCD** meter.

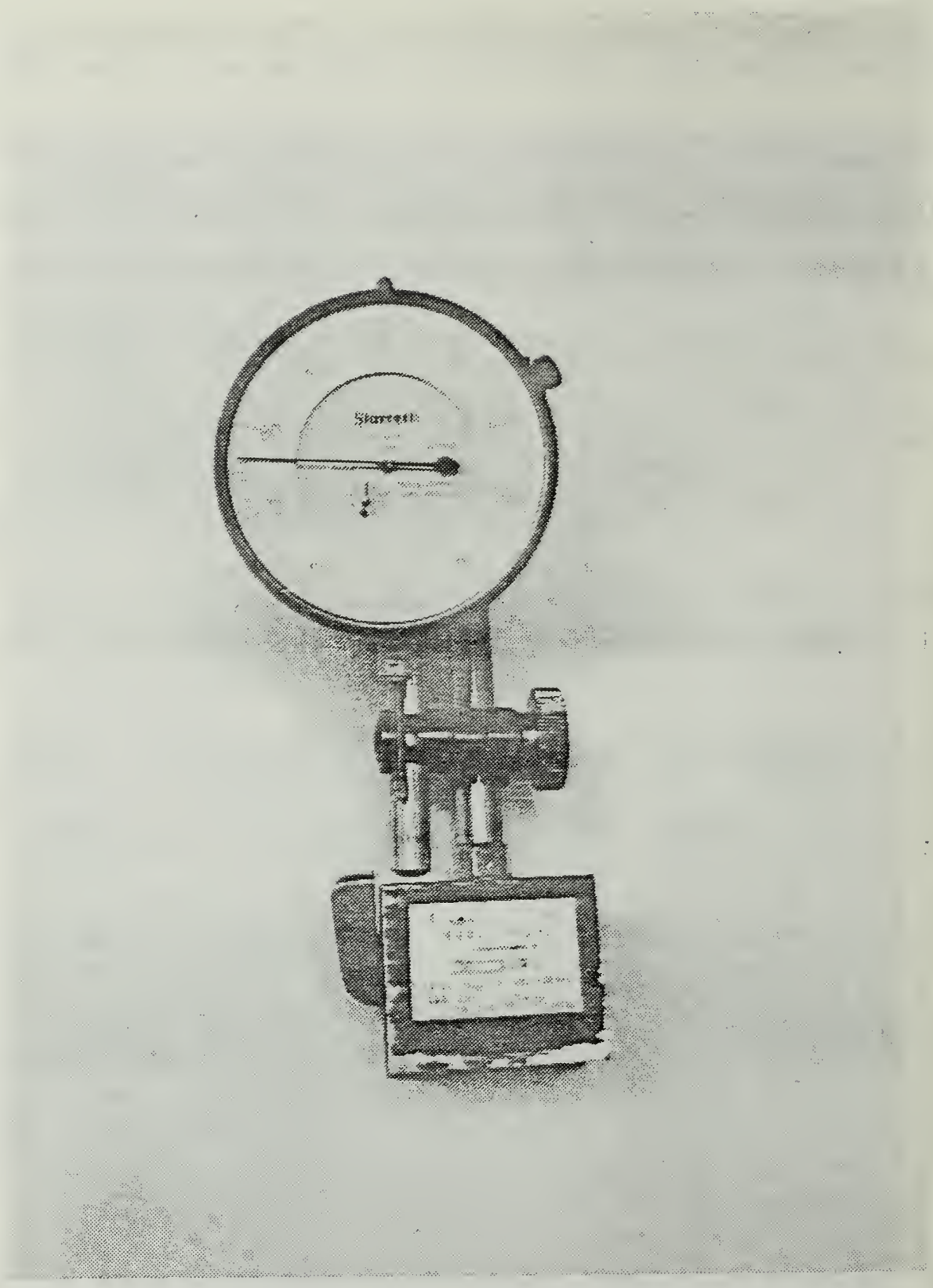

Figure A-8 : Dial indicator employed to measure the physical displacement of the INSTRON 1000 moving cross-head.

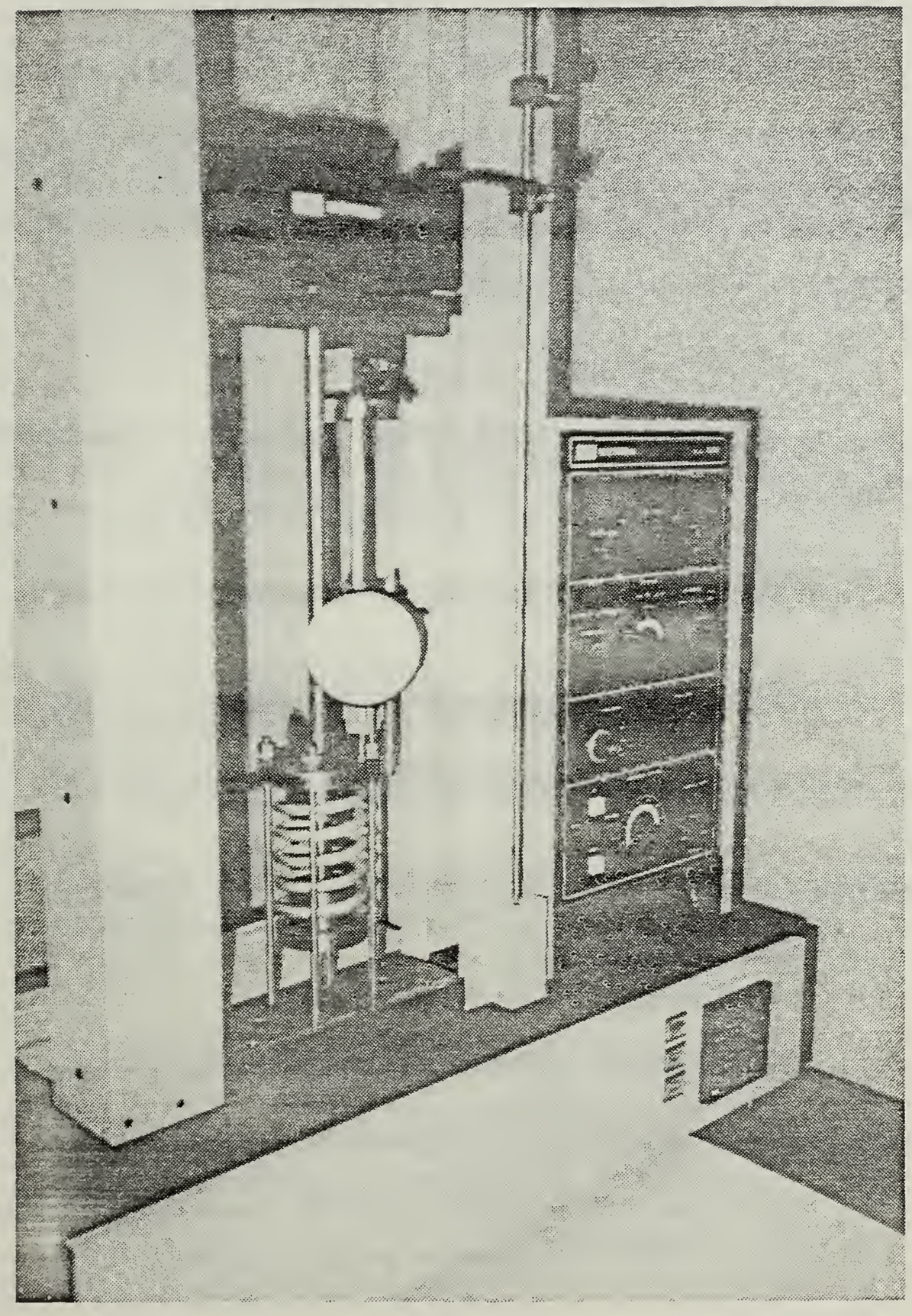

Figure A-9 : Overall Mechanical Set-Up during the Simulation.

E. DETAILED PROCEDURES

The detailed procedures used to achieve the data base available are presented below in a check list form to provide for ease in reproducing parts or the totallity of the results, under the desired incremental values depending on the application of interest.

1. Familiarization

Make sure that you are thoroughly familiar with the controls of the INSTRON as well as that you have already read and comprehended the following istructions.

CAUTION

DO NOT ATTEMPT TO OPERATE THE INSTRON UNLESS YOU ARE FEELING COMFORTABLY WITH ITS CONTROLS AND THE FOLLOWING INSTRUCTIONS

2. No-load case

a. Identify the Load Transducer on the cross-head.

b. Calibrate the INSTRON accordingly [Ref.14 : ch. 5]

(1) Go through steps 1 and 2 of the calibration procedure (page 5-2).

(2) If using the 100 lb or the 10 lb capacity Load Transducers go through steps 3 ,4 and 5 (pages 5-2 & 5-3).

(a) For the 100 lb capacity Load Transducer go through step 6a (page 5-4) anyway, and NOTE (page 5-4) as well as steps 7b, 7c (page 5-5) only if necessary.

(b) For the 10 lb capacity Load Transducer go through step 6b (page 5-4).

(3) If using the 1000 lb capacity load transducer go through NOTE and step 6a (page 5-3) anyway , and step 7a (page 5-4) only if necessary.

c. Set cross-head control knob to 10/.5.

d. Set variable speed knob to 0.1 (first position next to MIN) and observe illumination of the corresponding red light.

e. Set physical displacement scale (**DIAL**) to starting reference.

f. Based on the settings of thc previous two steps make a rough calculation of what the maximum displacement will be according to the formula:

(DISPLACEMENT) = (SPEED) X (TIME)

and set the upper limit stop. TIME has to be assumed that of the step 2j for the No-Load case and 3c for the load conditions. The lower limit stop has to be set so that it matches with the physical displacement starting reference.

g. Set stop watch to starting reference .

h. Make sure that the appropriate record equipment (lists, pencil, eraser) is handy in front of you and that you have understood how the data recording will be performed.

i. Simultaneously start the watch timer and push the white UP button (tension) and observe it's illumination as well as, that red STOP button's light is turned off.

j. Record physical and LCD displacements at one (1) minute intervals for the first ten (10) minutes, at ten (10) minute intervals for the first hour; if the INSTRON will stop earlier do not forget to record stall time and load level.

k. Push red STOP button and observe it's illumination as well as that the white UP buttons' light is turned off.

l. Push yellow RETURN button and observe it's illumination as well as that the red STOP buttons' light is turned off.

CAUTION

THE RETURN SPEED IS ALWAYS 20 in/min (500 mm/min)
AND THEREFORE BE ALLERT TO PUSH THE STOP BUTTON
IN CASE ANY FAILURE OCCURS TO THE LOWER LIMIT STOP

m. Set variable speed knob to 0.2 (second position next to MIN) and observe illumination of the corresponding red light.

n. Repeat steps 2e up to 2l above.

o. Set the variable speed knob to 0.3 (third position next to MIN) observe the illumination of the corresponding red light and repeat step 2n above. If the INSTRON will not stall do not exceed 2/3 of the Load Transducer capacity.

p. Obtain plots of the physical displacement versus time with parameter the four different speed settings outlined in steps 2c, d m and o.

3. Under load case

a. Repeat steps a to i of paragraph 2. (No-Load case).

b. Repeat step f of paragraph 2.

c. Record **DIAL** and **LCD** displacements as well as force at one half (1/2) minute intervals for the first ten (10) minutes; hopefully the INSTRON will stall; do not forget to record stall time and load.

d. Repeat steps 2k and 2l.

e. Repeat in the order given the following steps: 2m, 2e, 2f, 2g, 2h, 2i, 3c, 2k and 2l.

f. Repeat in the order given the following steps: 2o, 2e, 2f, 2g, 2h, 2i, 3c, 2k and 2l.

g. Obtain plots of the physical displacement and the applied load versus time with parameter the four differnt speed settings outlined in steps 2c, d, m and o.

III. CREEP-DISPLACEMENT/STABILITY OF THE LVDT

A. BACKGROUND

It is known that for the graphite fiber bundles the order of magnitude of the displacement during a normal loading sequence at a constant stres rate **R** is about 2% (0.02). It is also known that the graphite fiber bundles are viscoelastic and therefore they creep and the total creep displacement is known to be of the 0.004 order of magnitude or in otherwords 20% of the maximum displacement achieved at the end of the loading sequence. Due to the small numbers that one has to deal with, during the creep experiment for a gauge length of **l = 10 in** it is necesary to use a very accurate device that will be capable of recording and/or displaying the minute differences in displacement during the creep. This is the point where the (**LVDT**) comes into play because the minute creep displacements of the cross-head of the INSTRON can be converted to voltages of the 0.1 mV order of magnitude which fortunately can be recorded and/or displayed using high accuracy multimeters. And since it is this creep-rupture behavior that can lead to strength-life data, the need to be familiar with the problems that may arise

like the one according to which no output has been recorded although the INSTRON cross-head had moved, is therefore obvious. Some possible explanations of the problem just described could be either the very small magnitude of the voltage output or drifting in time.

B. OBJECTIVES

Therefore the objective is to test the stability of the **LVDT** with respect to the following variables:

1. The Input Voltage (**Vin**).
2. The Direction of Displacement (**d+**) or (**d-**).
3. The Time (**t**).
4. The Temperature (**T**).

Based on the fact that the actual experiment will be conducted essentially in constant room temperature ie. within temperature differences of less than five (5) degrees, the stability of the **LVDT** with respect to the temperature does not appear to be significant.

C. PROCEDURE

To implement the above mentioned objective the set-up presented in **Figure A-10** was used which is composed of the following components:

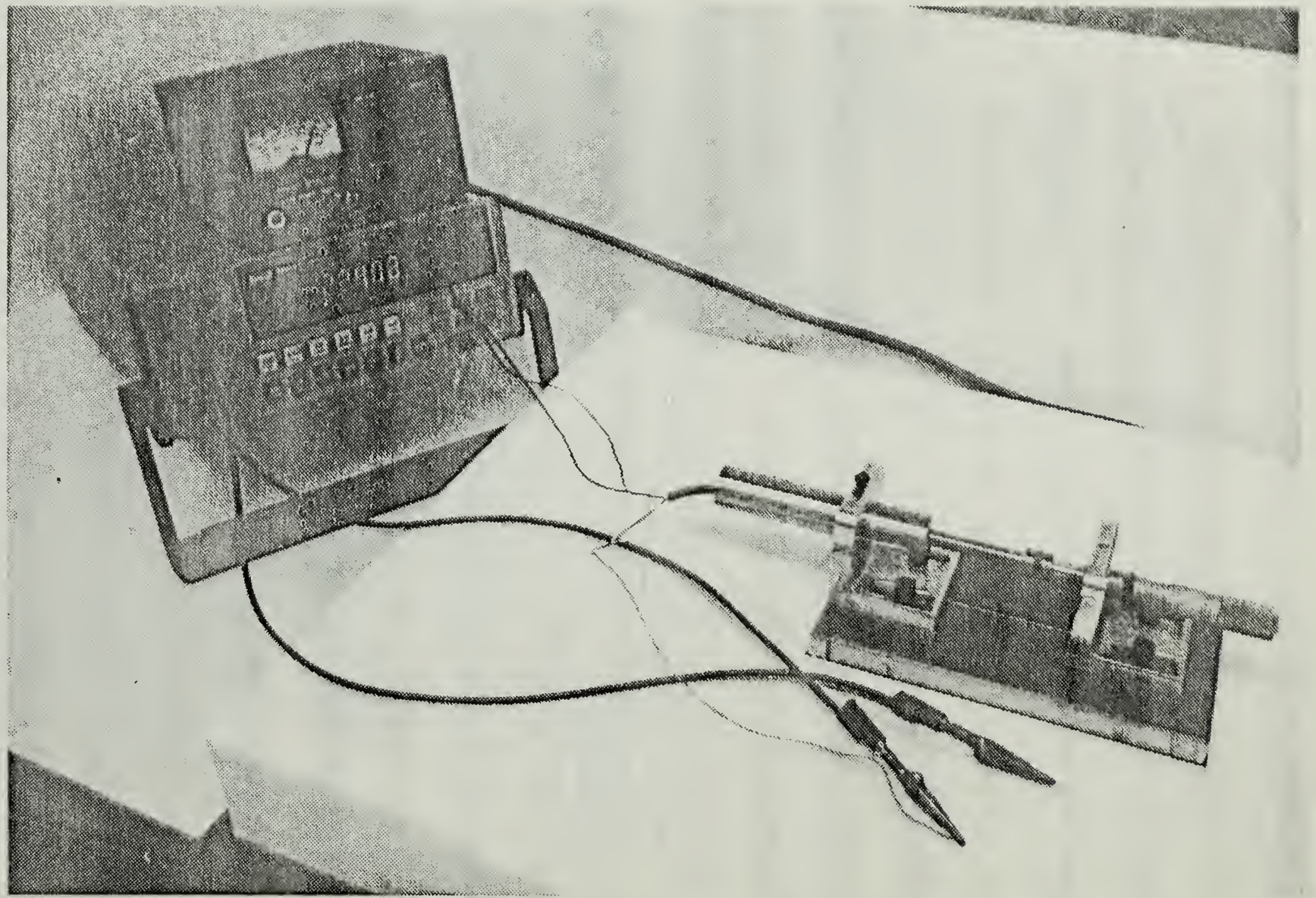

Figure A-10: Experimental Set-Up used for the evaluation of the response of the LVDT.

1. A regulated position test stand for the mounting of both parts of the **LVDT**. The core was mounted on a micrometer's vernier by which a fully controlable insertion of the core at increments of 0.001 in was possible.

2. A power supply (HP-1616B) by which the control of the input voltage V_{in} was possible.

3. A high accuracy multimeter (FLUKE 8840A) for the exact measurement of the output.

The maximum input of the SCHAEVITZ **LVDT** is 24V and therefore for time saving purposes the " bracketing technique " was used between the limits of 24V,12V and 1V respectively. If this technique would show that some voltage region was immaterial, bracketing would have been then applied for the remaining voltage region of interest.

For positive direction of displacement the output voltage of at least three (3) points was obtained, for various selected values of the input voltage (at least 3), and repetition of the same procedure for the negative direction of displacement was accomplished.

The anticipated results according to the specifications were:

1. The output of the **LVDT** to be independent of V_{in} .
   Check : The ratios of V_{out}/V_{in} versus **d**, plot under the same slope.

2. The output of the **LVDT** to be independent of **d+** or **d−** .
   Check : The curves of V_{out}/V_{in} versus **d+** and V_{out}/V_{in} versus **d−** coincide.

3. The linearity of the **LVDT**.
   Check : Curves are straight lines.

APPENDIX B

1. POINTS OF CONTACT

The Hewlett-Packard engineers/technicians who served as points of contact in the recording rate optimization problem of the HP-3421A DACU and their telephone numbers are listed below for further contacts if necessary:

1. Tom Turney : (408) 988-7304
2. Russ Mc Ugh : (415) 857 8241
3. Ashley Werrpass : (415) 857-5673

2. OFFICIAL CORRESPONDENCE WITH HEWLETT-PACKARD

According to HP-IL Module OWNER'S MANUAL [Ref. 17 : p. 63] the following official letter was forwarded to the Customer Support Division of the Hewlett-Packard Co. The purpose of this letter was to explain the existing situation with respect to the slow data acquisition rate of the HP-3421A DACU, have the Company confirm the information released by phone about the recording rate capabilities of the equipment depending on the peripherals used within the HP-IL and finally have it propose viable solutions utilizing the already available equipment.

DEPARTMENT OF THE NAVY
NAVAL POSTGRADUATE SCHOOL
MONTEREY, CA 93943-5100

IN REPLY REFER TO

Curriculum of Aeronautical Engineering
Major (HAF) D.M. Petridis, Code 31
Monterey, CA 93943-5000
November the 21st 1986

Dear Sirs,

I am an officer of the Greek Air Force, currently stationed at the U.S Naval Postgraduate School, for a Master of Science Degree in Aeronautical Engineering. My thesis research is related to the graphite fibers tensile testing, in an effort to obtain a strength-life data base that will serve in predicting the service life of a component made of graphite fiber composites, given that the strength of the fibers is known.

The experimental set-up is composed of a tensile testing equipment (INSTRON 1000) where the graphite fiber bundles are mounted. Failures of individual fibers within the bundles are transfered to an HP-3421A Data Acquisition Control Unit by means of a set of high precision load cells (INTERFACE SSM-100). Installed in this unit are two 10 channel multiplexer boards (44462A-OPTION 020). During the experiment, data are recorded using the HP-IL communications circuit as shown in the attached block diagram. The HP-44468A Data Acquisition Control Pac provided the basic data logger software program. This program was modified to permit the recording of time in hundredths of seconds and edited to reduce the number of data registers used. A copy of this program and its output are also attached to this letter. Contrary to what is advertised in page 32 of the Operating, Programming and Configuration Manual of the 3421A the reading rates obtained are of the 0.04 order of magnitude (see attached plot).

A preliminary telephone contact with your offices in Palo Alto on September the 29th [(415) 857-8175] provided us with the information according to which the reading rates reduce to N5(1)/N4(2)/N3(2) if the HP-41CX is interfaced to the 3421A as shown in the attached block diagram and can be substantially improved to N5(3)/N4(9)/N3(11) respectively, in

case the calculator, the thermal printer (HP-82162A) and the digital cassete drive (HP-82161A) are substituted by the HP-85A desk top computer.

Similar information was provided by your offices in Santa Clara [(408) 988-7304] on October the 27th, and Palo Alto [(415) 857-8241/5673] on October the 31st and suggestions to use programming utilizing the so called advanced commands (AUTOZERO OFF and the less digits of resolution possible) were also made .

Based on the information provided so far, you are kindly requested for the following:

1. To confirm by letter the above information and if possible provide us with any insight associated with the substantial reduction of the reading rates in case the 3421A is interfaced with either the hand-held calculator or the desk-top computer.

2. To make any helpful comments on the modified HP-44468A Data Logger Routine and also inform us whether any faster reading rates could be obtained by reducing and/or by-passing a number of the HP devices in the loop; if this is the case what are your suggestions for the optimum scheme?

3. To inform us about the reasons that will improve the recording rate in case the HP-85A is interfaced to the 3421A via the HP-IL.

4. What increase of recording rate can be achieved through the advanced commands with either one, the HP-41CX calculator or the HP-85A computer.

Your early reply will be greatly appreciated. In the mean time we remain,

Sincerely yours

Major (HAF) D.M .Petridis

PS : In case you have any questions please call the Naval Postgraduate School Aeronautical Engineering Curriculum Office at (408) 646-2491/2 and leave your message.

If later than December the 15th 1986, please forward your answer to my thesis advisor in the following address :

U.S Naval Postgraduate School
Department of Aeronautical Engineering
Dr. Edward M. Wu, Code 67Wt
Monterey, CA 93943-5000

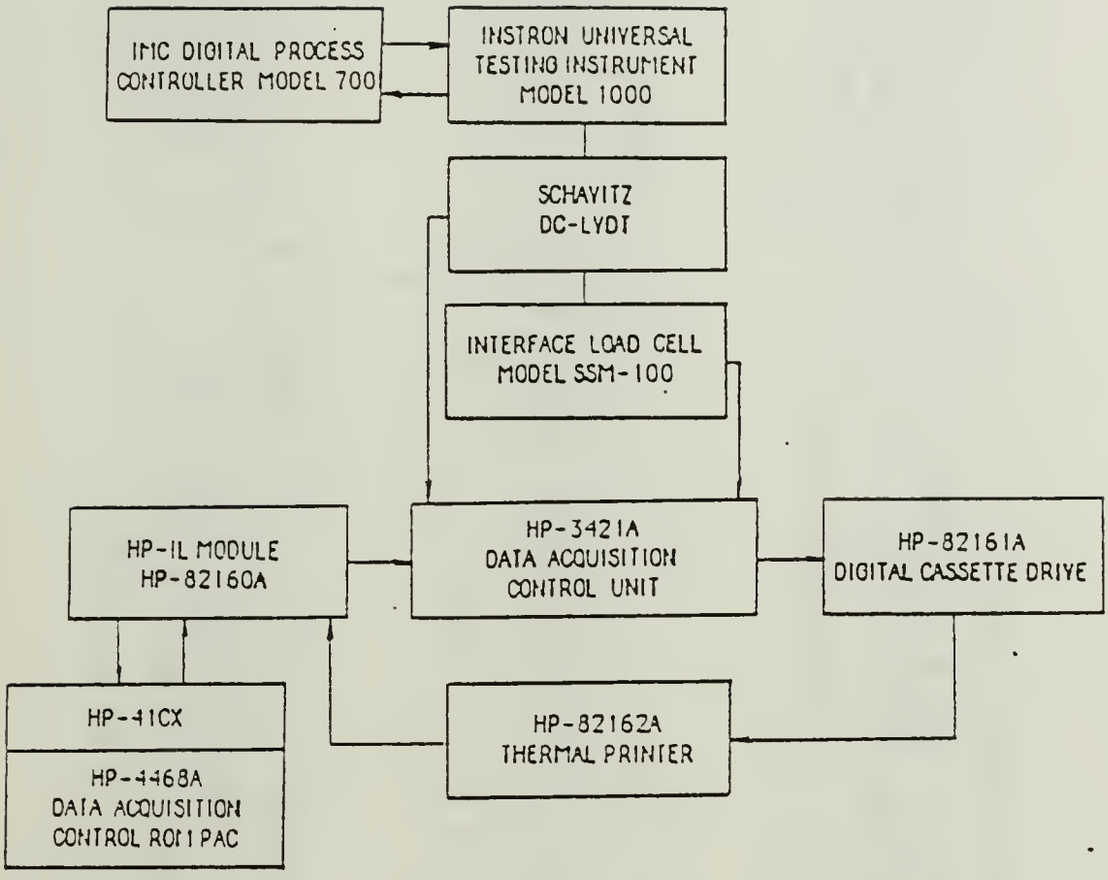
IMC DIGITAL PROCESS CONTROLLER MODEL 700
INSTRON UNIVERSAL TESTING INSTRUMENT MODEL 1000
SCHAVITZ DC-LVDT
INTERFACE LOAD CELL MODEL SSM-100
HP-IL MODULE HP-82160A
HP-3421A DATA ACQUISITION CONTROL UNIT
HP-82161A DIGITAL CASSETTE DRIVE
HP-41CX
HP-4468A DATA ACQUISITION CONTROL ROM PAC
HP-82162A THERMAL PRINTER

APPENDIX A

PROGRAM LISTING

```
DATA LOGGER
 01 LBL "LOGM"
 02 SF 10
 03 GTO 35
 04 LBL "DLM"
 05 CF 10
 06 LBL 35
 07 SF 12
 08 SF 27
 09 " HP 3421A"
 10 AVIEW
 11 CLKY
 12 "DATA LOGGER"
 13 AVIEW
 14 CF 12
 15 "DLM"
 16 32
 17 AK
 18 "CLKY"
 19 -32
 20 AK
 21 "LOG"
 22 35
 23 AK
 24 CF 13
 25 RCL 35
 26 ENTER
 27 INT
 28 X=Y?
 29 GTO 31
 30 X<>Y
 31 FRC
 32 1 E3
 33 *
 34 STO 35
 35 LBL 31
 36 "NEW ? Y/N"
 37 AON
 38 FC? 10
 39 PROMPT
 40 AOFF
 41 ASTO Y
 42 "Y"
 43 ASTO X
 44 X=Y
 45 GTO 01
 46 "EDIT ? Y/N"
 47 AON
 48 FC? 10
 49 PROMPT
 50 CF 10
 51 AOFF
 52 ASTO X
 53 "Y"
 54 ASTO Y
 55 X=Y?
 56 GTO 04
 57 SF 12
 58 "-+-EDITOR-+-"
 59 AVIEW
 60 CF 12
 61 GTO 18
 62 LBL F
 63 "DCV"
 64 AVIEW
 65 1
 66 GTO 02
 67 LBL 02
 68 1 E2
 69 +
 70 1 E-7
 71 *
 72 RCL 05
 73 +
 74 ISG 35
 75 ABS
 76 SF 25
 77 RCL IND 35
 78 FS?C 25
 79 GTO 10
 80 DSE 35
 81 ABS
 82 "OUT OF ROOM"
 83 AVIEW
 84 PSE
 85 FS? 10
 86 GTO 16
 87 GTO 04
 88 LBL 10
 89 RDN
 90 FS? 10
 91 GTO 21
 92 STO IND 35
 93 GTO 03
 94 LBL 21
 95 STO 04
 96 RCL 06
 97 39
 98 +
 99 STO 08
100 1 E-3
101 *
102 RCL 35
103 1
104 -
105 STO 07
106 LASTX
107 +
108 +
109 STO 06
110 LBL 22
111 RCL IND 07
112 STO IND 06
113 DSE 07
114 ABS
115 DSE 06
116 GTO 22
117 RCL 04
118 STO IND 08
119 RCL 08
120 INT
121 38
122 -
123 STO 06
124 GTO 03
125 LBL 01
126 CLX
127 STO 30
128 37
129 STO 35
```

Figure A.1. Modified HP44468A Data Logger Routine

```
130 LBL 03
131 FIX 0
132 CF 29
133 "FIRST CH?"
134 CF 22
135 AOFF
136 PROMPT
137 FC? 22
138 GTO 04
139 ENTER
140 "LAST CH?"
141 PROMPT
142 CLA
143 ARCL Y
144 "|— "
145 ARCL X
146 AVIEW
147 1000
148 /
149 +
150 STO 05
151 CF 23
152 "FUNCTION?"
153 PROMPT
154 FS? 23
155 GTO 19
156 "PRESS FN KEY"
157 PROMPT
158 LBL 19
159 CF 22
160 "USER0-83 ?"
161 PROMPT
162 FS? 22
163 GTO 20
164 "LAST SETUP"
165 AVIEW
166 PSE
167 "NOT STORED"
168 AVIEW
169 PSE
170 GTO 03
171 LBL 20
172 INT
173 ABS
174 84
175 X<=Y?
176 GTO 19
177 RDN
178 "USER"
179 ARCL X
180 AVIEW
181 16
182 +
183 GTO 02
184 LBL 04
185 FS? 10
186 GTO 16
187 37
188 RCL 35
189 X<=Y?
190 STOP
191 1 E-3
192 *
193 38
194 +
195 STO 35
196 CF 09
197 "RECORD Y/N"
198 CF 23
199 AON
200 PROMPT
201 CF 20
202 FC?23
203 SF 20
204 ASTO Y
205 "Y"
206 ASTO X
207 X=Y?
208 SF 09
209 "RECORD"
210 FC? 09
211 "|-OFF"
212 AVIEW
213 FC? 55
214 GTO 06
215 "PRINT? Y/N"
216 CF 23
217 AON
218 PROMPT
219 CF 21
220 FC? 23
221 SF 21
222 ASTO Y
223 "Y"
224 LAST X
225 CF 08
226 X=Y?
227 SF 08
228 SF 21
229 FC? 08
230 CF 21
231 "PRINT"
232 FC? 08
233 "|-OFF"
234 AVIEW
235 LBL 06
236 AOFF
237 SF 29
238 SF 28
239 XROM  "ALM"
240 X<0?
241 GTO 05
242 PWRDN
243 OFF
244 LBL 05
245 XEQ "DLMLM"
246 ISG 32
247 GTO 29
248 1
249 "|"
250 SF 25
251 CLAL
252 CF 25
253 PWRDN
254 OFF
255 LBL 29
256 RCL 34
257 X=0?
258 GTO 05
259 PWRDN
260 OFF
261 GTO 05
262 OFF
263 LBL 18
264 SF 10
265 CF 29
266 FIX 0
267 36
268 RCL 35
269 X<=Y?
270 37
271 STO 35.
272 LBL 16
273 "COMMAND ?"
```

Figure A.1. Modified HP44468A Data Logger Routine (cont'd)

```
274 AON
275 PROMPT
276 AVIEW
277 ASTO 'X
278 "LIST"
279 ASTO Y
280 X=Y?
281 GTO 07
282 "INSERT"
283 ASO Y
284 X=Y?
285 GTO 09
286 "DELETE"
287 ASTO Y
288 X=Y?
289 GTO 12
290 "END"
291 ASTO Y
292 X=Y?
293 GTO 17
294 "HELP"
295 ASTO Y
296 X=Y?
297 GTO 14
298 "INVALID CMD"
299 AVIEW
300 PSE
301 GTO 16
302 LBL 17
303 "*END EDITOR*"
304 AVIEW
305 PSE
306 CF 10
307 GTO 04
308 LBL 12
309 CF 22
310 "NUMBER ?"
311 AOFF
312 PROMPT
313 FC? 22
314 GTO 16
315 INT
316 ABS
317 "DELETE"
318 ARCL X
319 AVIEW
320 38
321 +
322 RCL 35
323 X<>Y
324 X>Y?
325 GTO 13
326 X=Y?
327 GTO 36
328 X<>Y
329 1
330 -
331 1 E-3
332 *
333 +
334 STO 06
335 LBL 15
336 RCL 06
337 1
338 +
339 RCL IND X
340 STO IND 06
341 ISG 06
342 GTO 15
343 LBL 36
344 DSE 35
345 ABS
346 GTO 16
347 LBL 14
348 "LIST"
349 AVIEW
350 PSE
351 "INSERT"
352 AVIEW
353 PSE
354 "DELETE"
355 AVIEW
356 PSE
357 "END"
358 AVIEW
359 PSE
360 GTO 16
361 LBL 13
362 "NONEXISTENT"
363 AVIEW
364 PSE
365 GTO 16
366 LBL 07
367 37
368 RCL 35
369 X<=Y?
370 GTO 16
371 STO 02
372 FIX 0
373 1 E-3
374 *
375 38
376 +
377 STO 35
378 LBL 08
379 RCL IND 35
380 STO 01
381 XROM "DECODE"
382 ASTO 00
383 CLA
384 RCL 35
385 INT
386 38
387 -
388 ARCL X
389 ":-: "
390 RCL IND 35
391 ENTER
392 INT
393 ARCL X
394 RDN
395 FRC
396 1 E3
397 *
398 INT
399 ":--"
400 ARCL X
401 ":-, "
402 ARCL 00
403 AVIEW
404 ISG 35
405 GTO 08
406 RCL 02
407 STO 35
408 GTO 16
409 LBL 09
410 CF 22
411 AOFF
412 "AFTER NUMR ?"
413 PROMPT
414 FC? 22
415 GTO 16
416 X<0?
417 -1
```

Figure A.1. Modified HP44468A Data Logger Routine (cont'd)

```
418 RCL 35
419 38
420 -
421 X<>Y
422 X>Y?
423 GTO 13
424 STO 06
425 "AFTER "
426 ARCL X
427 AVIEW
428 GTO 03
429 END
```

Figure A.1. Modified HP44468A Data Logger Routine (con'd)

```
DATA LOGGER OUTPUT FORMAT
 01 LBL "DLMLM"
 02 "C"
 03 CF 29
 04 FC? 08
 05 CF 21
 06 RCL 35
 07 STO 01
 08 2
 09 LBL 10
 10 3
 11 +
 12 RCL IND 01
 13 ENTER
 14 FRC
 15 1 E3
 16 *
 17 INT
 18 X<>Y
 19 INT
 20 -
 21 +
 22 ISG 01
 23 GTO 10
 24 FIX 0
 25 CLA
 26 ARCL 32
 27 FC? 09
 28 GTO 03
 29 SF 25
 30 CREATE
 31 FS?C 25
 32 GTO 03
 33 PURGE
 34 CREATE
 35 LBL 03
 36 "PASS "
 37 ARCL 32
 38 AVIEW
 39 CLA
 40 ARCL 32
 41 0
 42 FS? 09
 43 SEEKR
 44 CLA
 45 DATE
 46 STO 00
 47 FIX 4
 48 ADATE
 49 TIME
 50 STO 01
 51 FIX 6
 52 ATIME
 53 FC? 08
 54 AVIEW
 55 PRA
 56 ADV
 57 .001
 58 FS? 09
 59 WRTRX
 60 2
 61 STO 33
 62 CF 10
 63 LBL 02
 64 RCL IND 35
 65 STO 01
 66 XROM "DECODE"
 67 ASTO 00
 68 ASHF
 69 ASTO 36
 70 2
 71 STO 37
 72 LBL 04
 73 FIX 0
 74 CLA
 75 RCL 01
 76 XEQ IND 36
 77 FS?C 10
 78 ASTO 00
 79 STO IND 37
 80 CLA
 81 RCL 01
 82 INT
 83 ARCL X
 84 RCL IND 37
 85 ISG 37
 86 SIGN
 87 ":-: "
 88 ENG 5
 89 ARCL X
 90 ":- "
 91 ARCL 00
 92 FC? 08
 93 AVIEW
 94 PRA
 95 CF 10
 96 ISG 01
 97 GTO 04
 98 CLA
 99 FIX 0
100 ARCL 32
101 RCL 33
102 FS? 09
103 SEEKR
104 RCL IND 35
105 STO 01
106 RCL 37
107 ST+ 33
108 1
109 -
110 1 E3
111 /
112 FS? 09
113 WRTRX
114 ADV
115 ISG 35
116 GTO 02
117 RCL 35
118 FRC
119 38
120 +
121 STO 35
122 RTN
123 END
```

Figure A.2. Modified HP44468A Output Format Routine

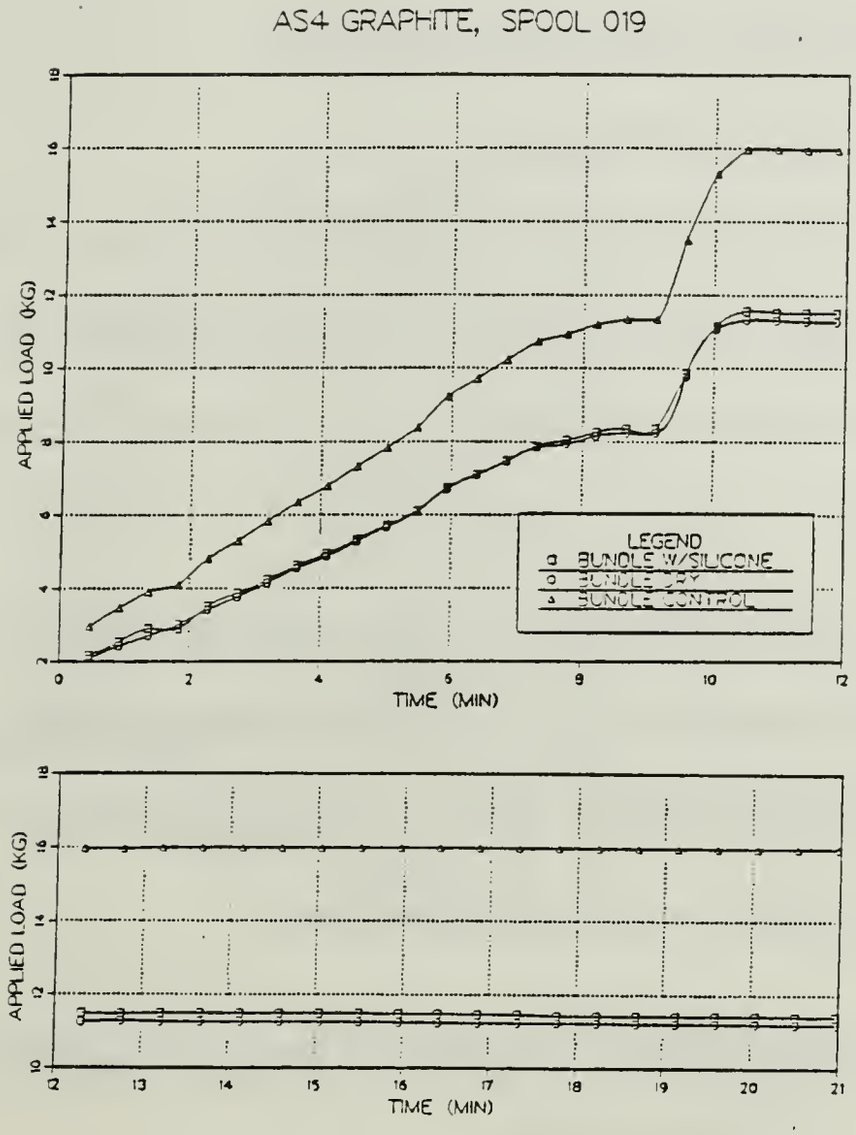

Figure 8.2a. Test 2: Load-Time curves. Maximum constant load on the control sample was 16.003 kilograms.

APPENDIX C

1. ESTIMATION OF POWER SUPPLIES NEEDED

a. Load Cells (LC) Case

The Specifications of the HP-6216B give a voltage range of 0-25V DC and a current range of 0-400mA, whereas the recommended excitation voltage of the INTERFACE LCs is 10V DC and their resistance 350 ± 3.5Ω.

A parallel solution evidently does not work as it can be easily observed by **Figure C-1** where the current through the loop exceeds what is dictated by the power supply specifications for the recommended excitation voltage of the LCs as shown below:

$$I_S = V_S^{REC}/R_{12} = V_S^{REC}/\Sigma^2_{i=1}(1/R) = 10V/2*(1/38.888\Omega)$$
$$I_S = 0.514\ A > 0.400\ A$$

A series solution involving two (2) INSTRONs in which nine (9) LCs are connected in parallel as shown in **Figure C-2** suggests that no

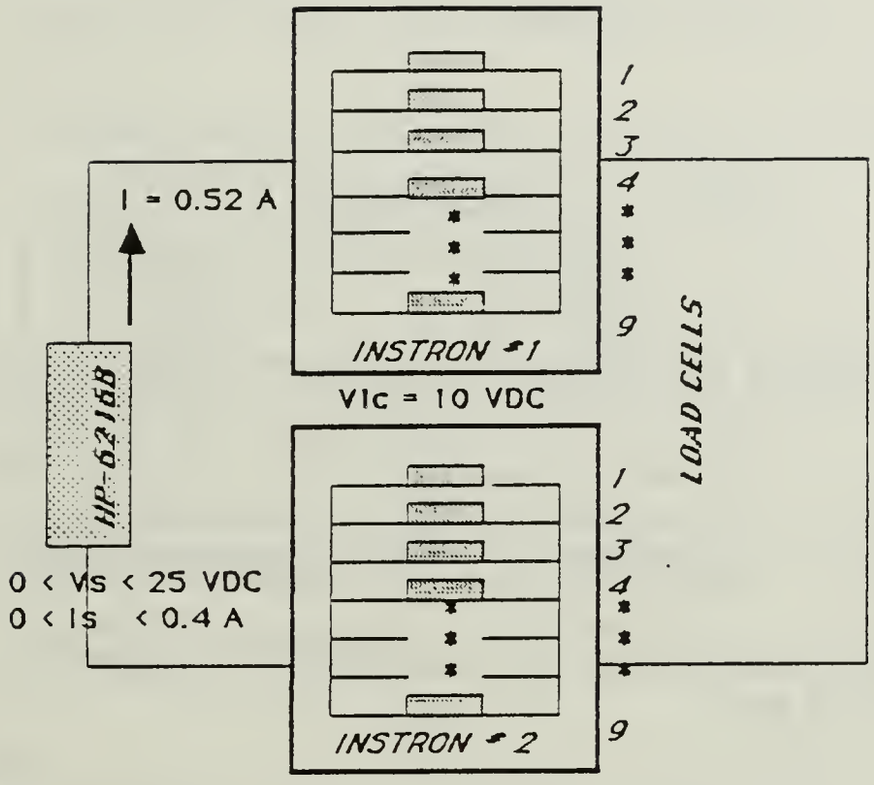

Figure C-1 : Load Cell Sets connected in parallel.

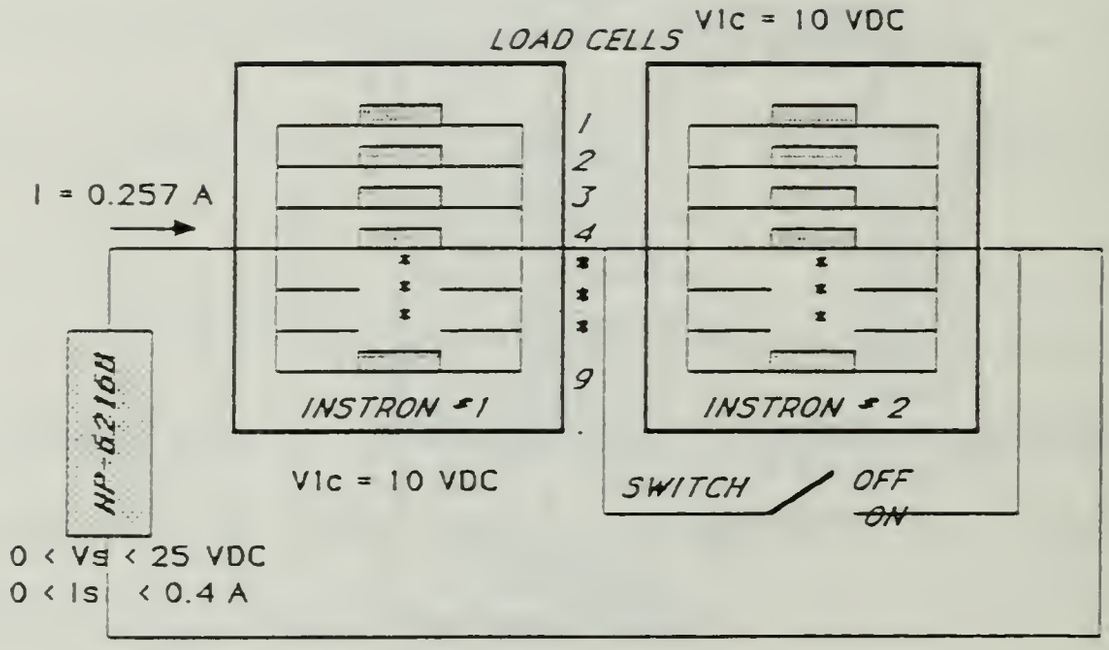

Figure C-2 : Load Cell Sets connected in series.

more than two (2) **LC** sets can be powered by one (1) HP-6216B power supply as shown below:

Switch **ON** : $\Sigma^{9}_{i=1}$ (1/R) = $1/R_{tot}$ = 9 * (1/350) = 0.257 (1/Ω)

R_{tot} = 38.888 Ω

$I_{lc} = V_{lc}^{REC}/R_{tot}$ = 10V/38.888 Ω = 0.257 A

Switch **OFF**: $V_S > V1_{lc} + V2_{lc} = 2 * (V1_{lc}) = 2 * (R_{tot} * I_{lc})$

$V1_{lc} + V2_{lc}$ = 2*38.888*0.257 V = 19.989 V

Hence MAX V_S = 25 V > 19.989 V

However this conclusion does not take into account the possible failure of one **LC** (short-circuit). If this is the case the rest of the LCs will be possibly ruined and consequently it is not worthy of taking the risk.

Therefore it is decided to use four (4) power supplies, one for every **LC** set.

b. **LVDT** case

According to the specifications of the **LVDT** the recommended excitation voltage is 24V and the highest output resistance $10^6\Omega$.

Obviously in this case the series solution does not work since the maximum capacity of the power supply is only 25V and therefore only parallel connection schemes need to be examined. Under the specification

conditions the loop is limited by the 400mA current and hence by a total more than two (2) **LC** sets can be powered by one (1) HP-6216B power resistance of 60 Ω as shown below:

$$MAX\ I_S = V_S^{REC}/R_{tot} \text{ or } R_{tot} = V_S^{REC}/MAX\ I_S = 24V/0.4A = 60\Omega$$

Hence one possible yet economic situation is the one shown in **Figure C-3** where the four (4) **LVDT**s are connected in parallel to the power supply yieling a total resistance of 60Ω. According to this situation each LVDT amounts for a resistance of 240 Ω << 10^6 Ω and a current of 100mA. This fact means a voltage differential of 24V which is well within the capabilities of the HP-6216B power supply.

Therefore given that the **LVDT**s' reliability is very high and that their wiring connections will be spatially that far appart, that the short circuit probability is very remote, one (1) power supply is adequate for all the **LVDT**s that will be externally mounted to the fixed cross-heads of the INSTRON machines.

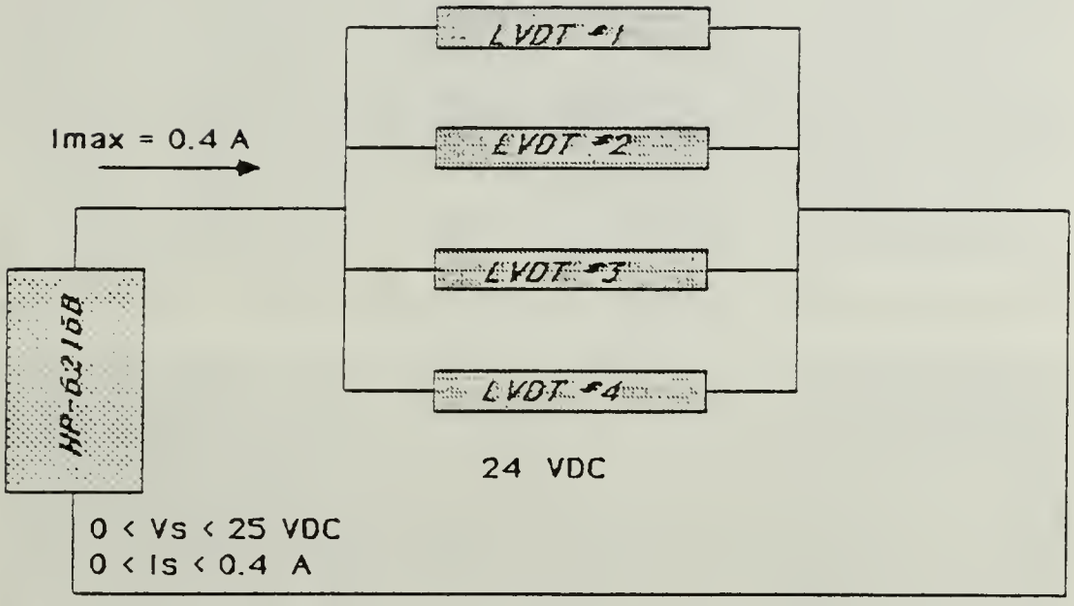

Figure C-3 : LVDTs connected in parallel.

2. IMPLEMENTATION OF THE OVERALL EXPERIMENTAL SET-UP

The necessary procedures for the implementation of this task follow in a check list format. However in case clarifications are needed the manuals have to be consulted accordingly [Refs. 14, 15, 16 & 17].

a. Identification of the appropriate **LT**s to be installed in the moving cross-head of the INSTRONs. In this case the 1000 lbs **LT**s had to be used since the order of magnitude of the load at the end of the loading sequence for the test of nine (9) fiber bundles simoultaneously has been dctermined to be of the 450 lbs order of magnitude.

b. Removal of the existing 100 lbs **LT**s from the INSTRONs' cross-heads, removal of the **LVDT**s from the 100 **LT**s and installation to the 1000 **LT**s. Installation of the 1000 **LT**s into the moving cross-heads and calibration of the equipment in accordance with INSTRON 1000 manual [Ref. 15], (**Figure A-4**).

c. Installation of the **L**oad **C**ells (**LC**)/**U**pper **D**ifferential **M**echanism **S**ystem (**UDMS**) into the moving cross-heads and of the **L**ower **D**ifferential **M**echanism **S**ystem (**LDMS**) into the lower end of the fixed cross-heads as shown in **Figures C-4 & C-5**.

d. Connection of the **LC** wirings to the specifically fabricated **D**istribution **B**oards (**DB**) by soldering (**Figure C-6a**).

e. Connection of the **DB**s to the HP-3421A DACUs and to the HP-6216Bs (excitation voltage of the **LC**s) by appropriately marked wiring, according to the correspodence given in **Table VI**.

f. Mounting of the **LVDT**s to the INSTRONs fixed cross-heads by utilizing the specificaly designed attachement pads in

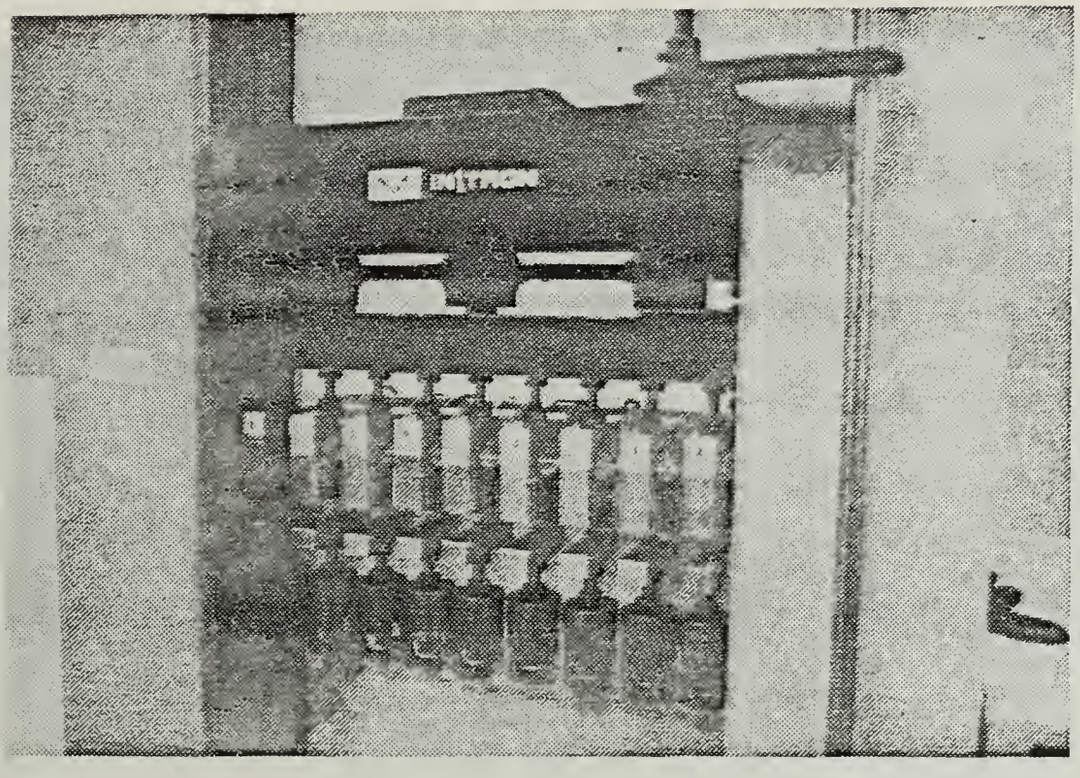

Figure C-4 : Load Cells/Upper Differential Mechanism system.

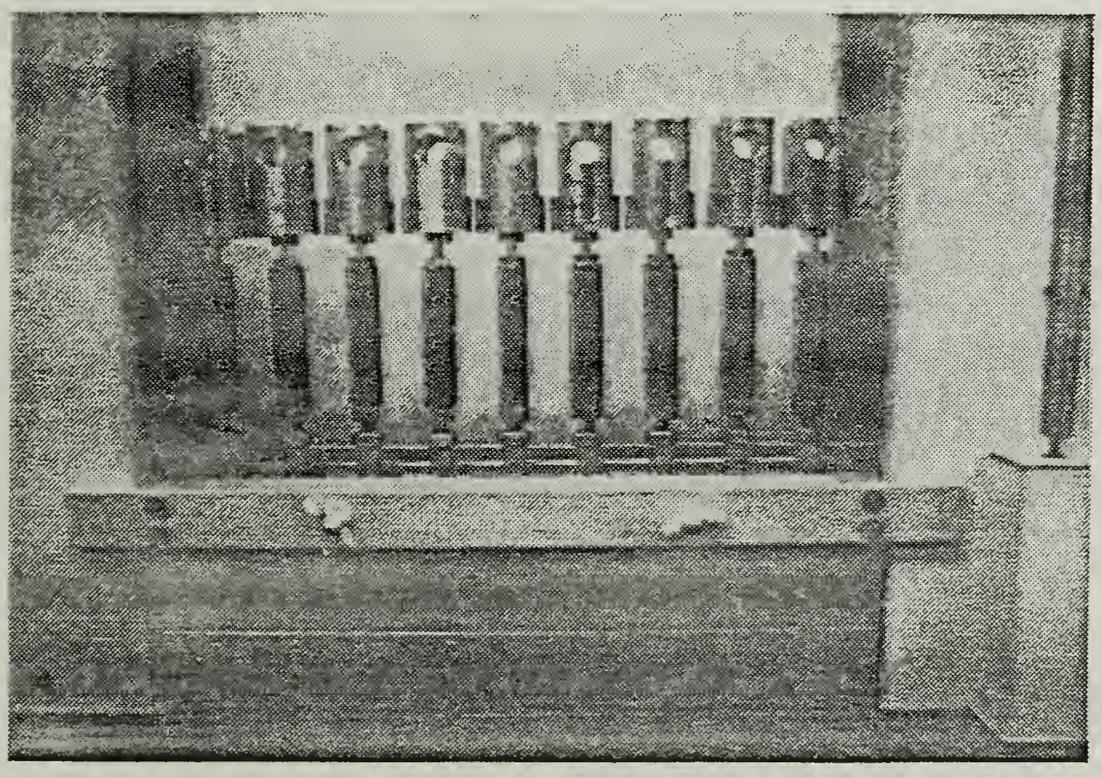

Figure C-5 : Lower Differential Mechanism system.

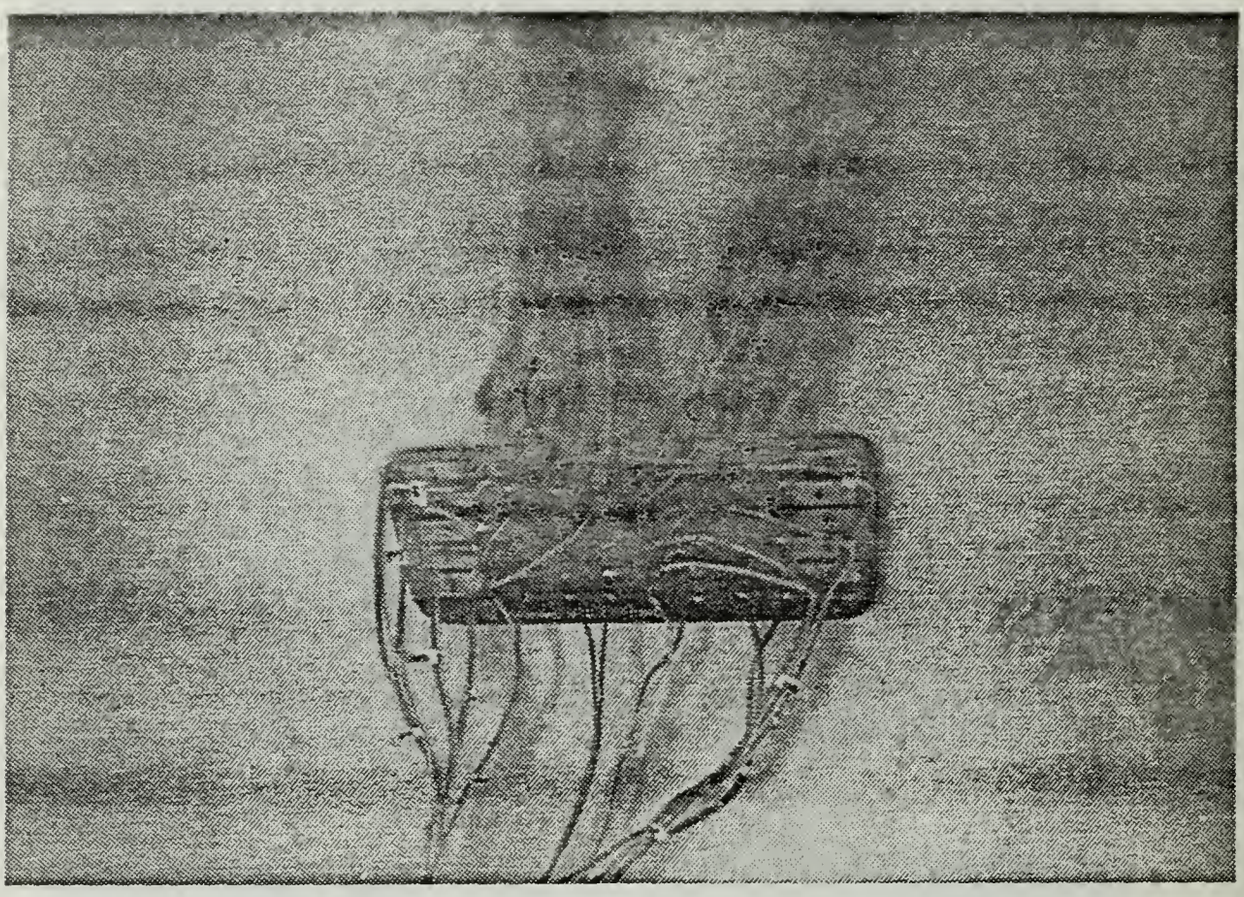

Figure C-6a : Load Cells' Distribution Board.

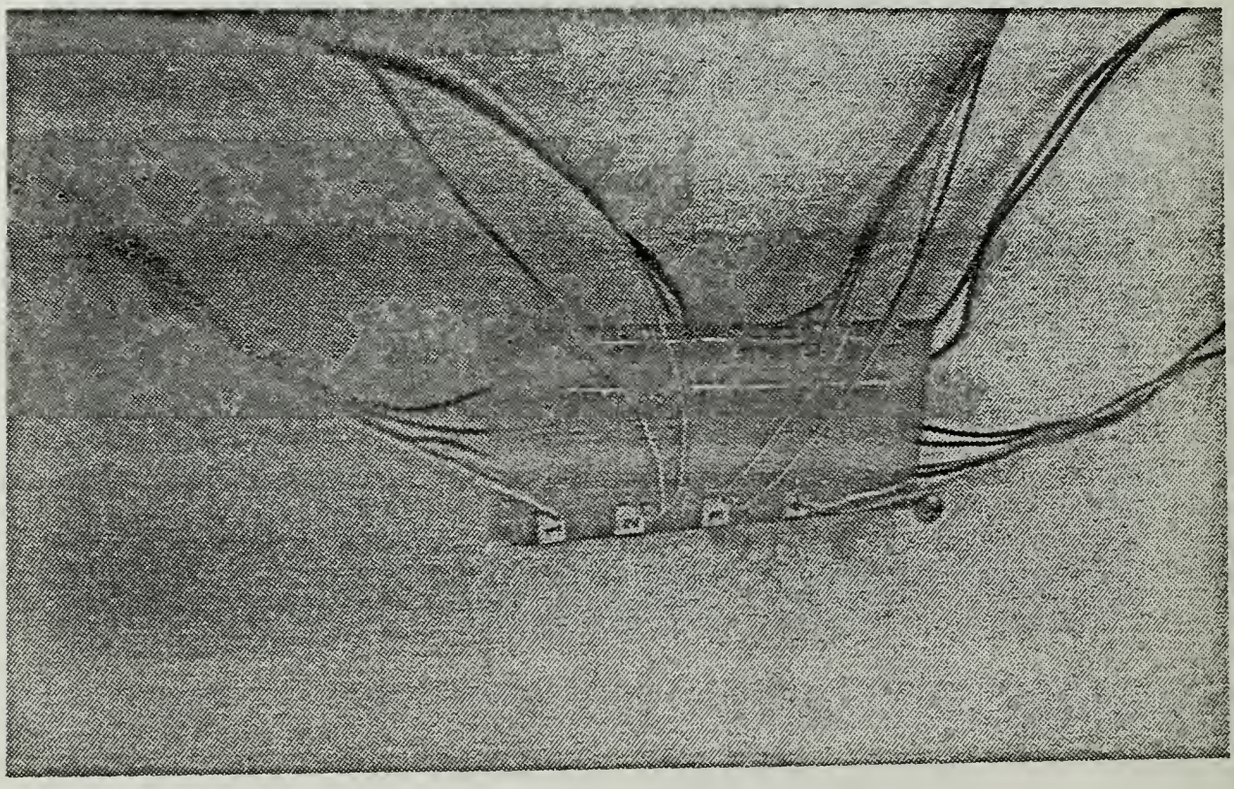

Figure C-6b : LVDTs' Distribution Board.

TABLE VI

LOAD CELLS & LVDT TO HP-3421A DACU
WIRING CONNECTIONS

HP - 3421A DACU

SLOT 0 (LOWER BUS)		SLOT 1 (UPPER BUS)	
CHANNEL #	CONNECTED ITEM	CHANNEL #	CONNECTED ITEM
0	Actuator	0	Load Cell#8
1	Actuator	1	Load Cell#9
2	L.C Exctn Vltge	2	LVDT
3	Load Cell#1	3	LVDT Exctn Vltge
4	Load Cell#2		
5	Load Cell#3		
6	Load Cell#4		
7	Load Cell#5		
8	Load Cell#6		
9	Load Cell#7		

predetermined locations so that no negative voltage outputs could be obtained that could delay the data acquisition rate (**Figure C-7**).

g. Connection of the **LVDT**s wiring to another specifically fabricated **d**istribution **b**oard (**db**) by soldering (**Figure C-6b**).

h. Connection of the **db** to the HP-6216B (excitation voltage of the **LVDT**s) and to the HP-3421A DACUs by appropriately marked wiring according to the correspondence given in Table VI.

i. Connection of the HP-85 desk top computer to the HP-3421A DACUs through the **HP-IL** for the monitoring of the loading sequence.

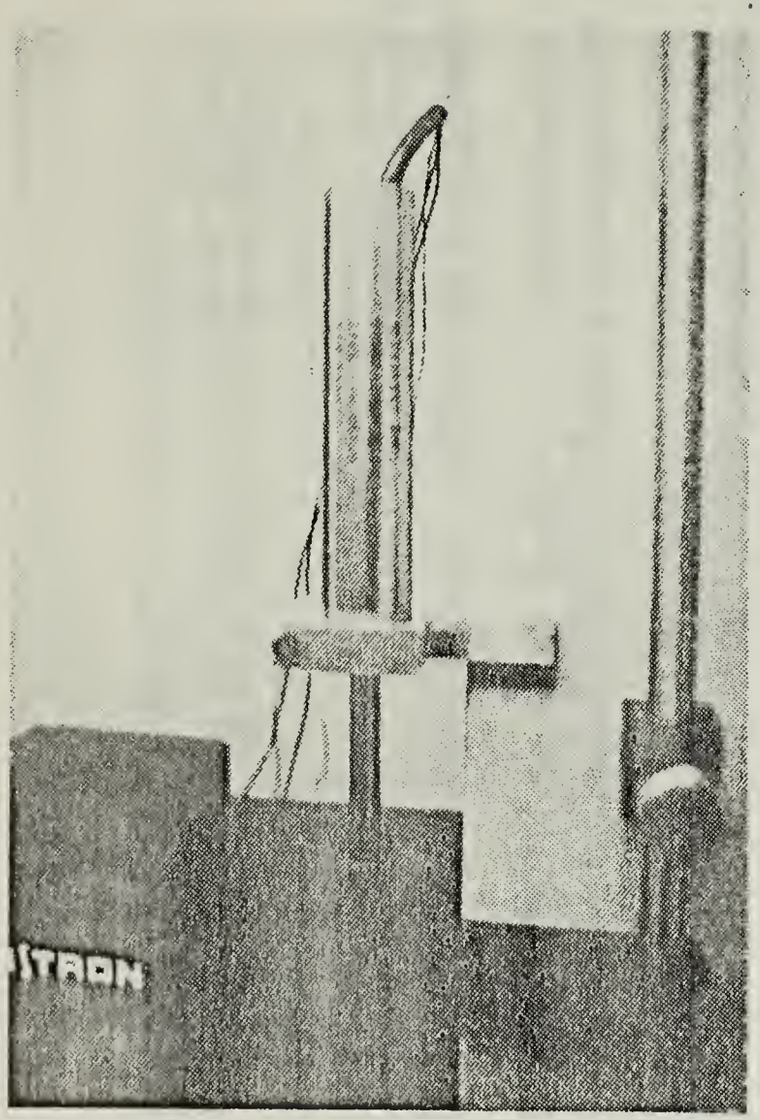

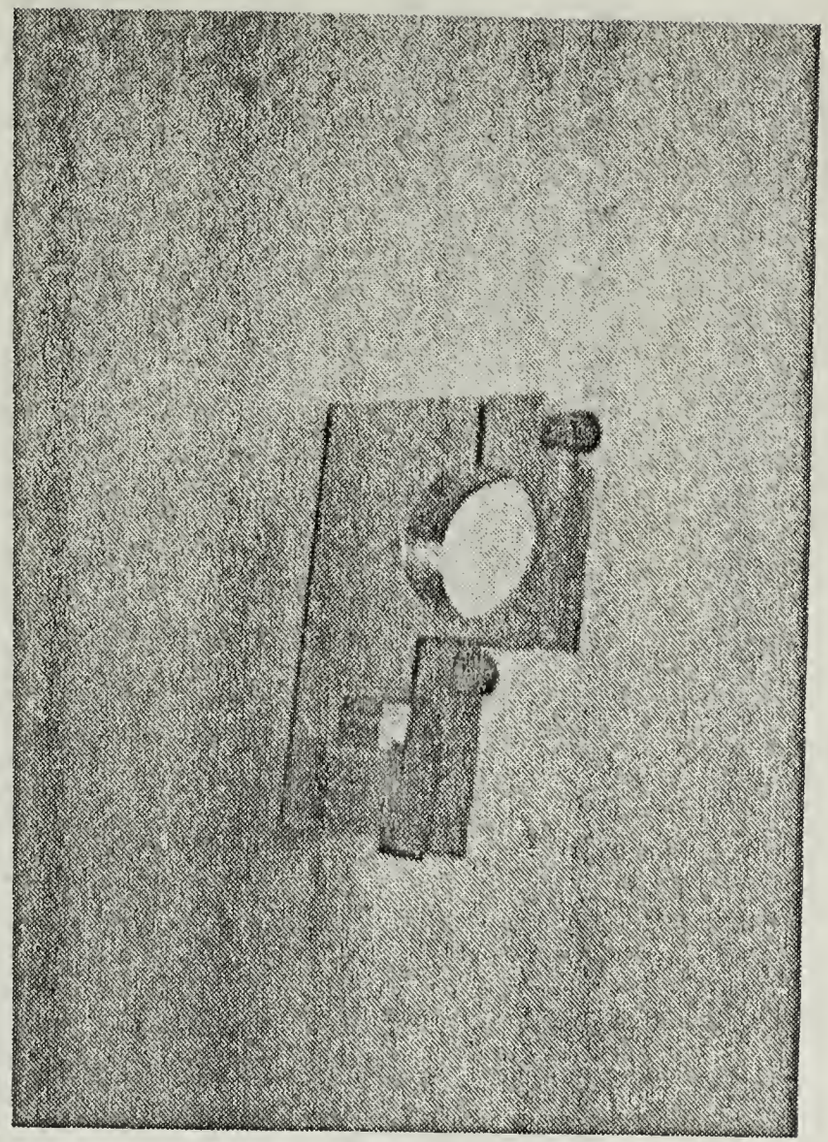

Figure C-7 : LVDT to INSTRON 1000 attachment pads.

LIST OF REFERENCES

1. Tsai, Stephen W., Composites Design 1986, USAF Materials Laboratory, Dayton, Ohio, 1986.

2. Carozzo, Fred D., Jr., Experimental Procedure for Lifetime Testing of Graphite Bundles under Constant Load, M.S. Thesis, Naval Postgraduate School, Monterey, California, March 1986.

3. Rosen, Walter B., Mechanics of Composite Strengthening, Fiber Composite Materials, American Society for Metals, Park, Ohio, 1965.

4. Phoenix, S. L. and Wu, E. M., Statistics for the Time Dependent Failure of Kevlar 49/Epoxy Composites: Micromechanical Modeling and Data Interpetation, UCRL-53365, Lawrence Livermore National Laboratory, Livermore, California, March 1983.

5. Phoenix, S. L., Statistics for the Strength of Bundles of Fibers in a Matrix, Encyclopedia of Materials Science and Engineering, Pergamon Press, 1982.

6. Rosen, Walter B., " Tensile Failures of Fibrous Composites," AIAA Journal, Vol. 2, No. 11, November 1964.

7. Phoenix, S. L., " Statistical Modeling of the Time and Temperature Dependent Failure of Fibrous Composites," in Proceedings of the 9th U.S National Congress of Applied Mechanics, Cornell University, Ithaca, New York, 1982.

8. Coleman, B. D., " Statistics and Time Dependence of Mechanical Breakdown in Fibers," Journal of Applied Physics, Chapter 29, pp. 393-399, 1958.

9. Harlow, D. G. and Phoenix, S. L., " The Chain of Bundles Probability Model for the Strength of Fibrous Materials I : Analysis and Conjectures,"Journal of Composite Materials, pp.12,195, 1978.

10. Harlow, D. G. and Phoenix S. L., " The Chain of Bundles Probability Model for the Strength of Fibrous Materials II : A Numerical Study of Convergence," Journal of Composite Materials, pp. 12 ,314, 1978.

11. Harlow, D. G. and Phoenix S. L., " Probability Distributions for the Strength of Composite Materials I : Two Level Bounds," International Journal of Fracture, p. 16, 1981.

12. Harlow, D. G. and Phoenix S. L., " Probability Distributions for the Strength of Composite Materials II : A Convergent Sequence of Tight Bounds," International Journal of Fracture , p. 17, 1981.

13. Smith, R. L., " A Probability Model for Fibrous Composites with Local Load Sharing," Proceedings of Royal Society of London, Series A, pp. 372,359, 1980.

14. INSTRON, Universal Testing Instrument, Model 1000, Manual No. M-10-1000-4/-5/-6, January 1983.

15. Hewlett-Packard, HP-82160A, HP-IL Module, OWNER'S MANUAL, February 1981.

16. Hewlett-Packard, 44468A DATA ACQUISITION / CONTROL ROM PAC, December 1982.

17. Hewlett-Packard, Operating Programming and Configuration Manual, Model 3421A Data Acquisition/Control Unit, March 1983.

BIBLIOGRAPHY

Broutman, L. J., Fracture & Fatigue, Composite Materials, Volume 5, Academic Press, 1974.

Jones, R. M., Mechanics of Composite Materials, Mc Graw-Hill, 1975.

Niemann. G., Maschinenelemente, Springer Verlag, Band I., 1975.

Phoenix, S. L., Fiber Composite Statistics, Lecture Notes at Sibley School of Mechanical and Aerospace Engineering, Cornell University, Ithaca New York, 1982.

Piggott, M. R., Load Bearing Fiber Composites, Pergamon Press, 1980.

Smith, C. O., Introduction to Reliability in Design, Robert E. Krieger Co., 1983.

Spiegel, M. R., Probability and Statistics, Schaum's Outline Series, Mc Graw-Hill, 1975.

Wu, E. M., Advanced Aircraft Construction, Lecture Notes for Naval Postgraduate School course AE-4103, Monterey, California, 1986.

Wu, E. M., Reliability in Structures and Materials, Lecture notes for Naval Postgrfaduate School course AE-4102, Monterey, California, 1986.

INITIAL DISTRIBUTION LIST

		No. Copies
1.	Defence Technical Information Center Cameron Station Alexandria, Virginia 22304-6145	2
2.	Library, Code 0142 Naval Postgraduate School Monterey, California 93943-5002	2
3.	Dr. Edward M. Wu Professor of Aeronautics, Code 67Wt Naval Postgraduate School Monterey, California 93943-5000	10
4.	Lt. Gen. D. Apostolakis Chief of the Air Force Hellenic Air Force General Staff Holargos, Athens - GREECE	1
5.	Mj. Gen. E. Psomas Deputy Chief of the Air Force Hellenic Air Force General Staff Holargos, Athens - GREECE	1
6.	Mj. Gen. A. Tziritas Technical Inspector of the Air Force Hellenic Air Force General Staff Holargos, Athens - GREECE	1
7.	Lt. Gen. N. Stapas Chief of the Tactical Forces Hellenic Tactical Air Command Larisa - GREECE	1

8.	Mj. Gen. P. Mavrakis Commander of the Air Training Command Dekelia Airfield - GREECE	1
9.	Mj. Gen G. Tsaligopoulos Commander of the Air Support Command Elefsina Airfield - GREECE	1
10.	Br. Gen. P. Golemas Commander of the 202 National State Factory Elefsina Airfield - GREECE	1
11.	Col. A. Banakos Commander of the Air Force Research & Technology Center Ano Glyfada, Athens - GREECE	1
12.	Lt. R.W. Baker 720 Baylor Avenue Bonita, California 92002	1
13.	Mj. D.M. Petridis 10 Tenedou Str. Ano Ilioupoli Athens 16342 - GREECE	5